NON-SURGICAL TISSUE ENGINEERING APPROACHES FOR SUB-FAILURE LIGAMENT AND TENDON INJURY REPAIR

By

EMMANUEL CHIEMEKA EKWUEME

A Dissertation submitted to the

Graduate School-New Brunswick

Rutgers, The State University of New Jersey

In partial fulfillment of the requirements

for the degree of

Doctor of Philosophy

Graduate Program in Biomedical Engineering

Written under the direction of

Joseph W. Freeman, PhD

and approved by

_____

_____

_____

_____

New Brunswick, New Jersey

May, 2015

Abstract of the Dissertation

NON-SURGICAL TISSUE ENGINEERING APPROACHES FOR SUB-FAILURE LIGAMENT AND TENDON INJURY REPAIR

By Emmanuel C. Ekwueme

Dissertation Director:

Joseph W. Freeman, Ph.D.

Ligaments and tendons are dense collagenous tissues that assist the body during locomotion and mechanically stabilize joints by operating primarily in tension. During sports and daily use, they often sustain sub-failure injuries such as sprains and strains. Due to a lack of sufficient tissue vascularization and a tenuous healing response after injury, healing is often lengthy and incomplete. Current non-surgical treatment is conservative and includes drug therapy (non-steroidal anti-inflammatory drugs or NSAIDs, corticosteroid injections, etc.) and rest, ice, compression, and elevation or RICE. However, the repaired tissue can be prone to chronic instability and re-injury. To overcome these limitations, we investigated the potential of a series of tissue engineering (TE) approaches to specifically address the major obstacles associated with sub-failure ligament/tendon injury repair. Proliferative therapy (or prolotherapy) is an alternative treatment for damaged connective tissues that involves serial injections of an irritant solution into the injury site to initiate a localized healing response. Prior investigations have yielded inconclusive results and studies on its molecular mechanisms are limited. In our *in vitro* model, we demonstrated that prolotherapy, most notably with the popular irritant P2G, functions at the cellular level by significantly attenuating human tenocyte metabolic activity and cell migration in addition to greatly increasing prostaglandin activity. Prostaglandins, prominent

inducers of tissue inflammation, were greatly increased at both mRNA (COX-2) and protein (PGE2) levels.

Cell therapy, more specifically, the use of multipotent human mesenchymal stromal cells (hMSC) has shown great potential to serve as a suitable cell source for tenogenic regeneration and a source of trophic mediators to aid in tissue repair. Utilizing an *in vitro* bidirectional paracrine co-culture model, we assessed the tenogenic response of the interaction between primary hMSC and tenocytes across three distinct groups of human donors. Our findings showed that cross-talk led to no increases in metabolic activity in either cell type, but instead induced strong increases in collagen protein deposition. Secretome analysis using a TGF-β reporter cell line showed strong TGF-β bioactivity during co-culture. Furthermore, gene expression analysis confirmed changes in the expression patterns of a panel of anabolic and catabolic markers known to be downstream targets of TGF-β signaling and key regulators of tendon matrix maintenance.

Finally, using a series of *in vitro* and *in vivo* experiments, we demonstrated the feasibility of utilizing high elastic modulus single-walled carbon nanohorns (CNH) as a novel therapy to modulate tendon biomechanics and cell response. Our findings revealed that CNH are capable of altering explanted ovine tendon elastic modulus without affecting the ultimate tensile strength (UTS) of the tissue. Next, cell studies showed that CNH immediately affect human tenocyte response in a manner dependent on the size of aggregates formed by CNH in solution. Lastly, functional *in vivo* evaluation using a stretch-injured rat Achilles tendon model indicated that injected CNH persist in the tissue and alter injured tendon elastic modulus most notably after 7 days of treatment, without altering UTS. In conclusion, the data presented here demonstrate the potential of three unique TE approaches for repairing sub-failure ligament/tendon injury.

Acknowledgements

The journey to the PhD is one filled with countless experiences. Throughout this journey, we learn much about the world while attempting to make a clear contribution to science. They say, "It takes a village to raise a child." My doctoral training is analogous to this proverb. In fact, my doctoral development was one heavily influenced by several people around the world. First and foremost, I extend my deepest gratitude to Dr. Joseph Freeman for his indelible guidance over the years. I began working in his laboratory as an undergraduate researcher during my junior year at Virginia Tech. I continued in his lab as a post-baccalaureate researcher for one year and then re-joined his new lab at Rutgers during my second year of graduate school. Throughout my doctoral studies, he afforded me the freedom and independence to pursue my scientific curiosities. Much thanks is due to my other committee members, Drs. Michael Dunn and Charles Gatt. Their guidance over the years has also been insurmountable. Beginning in my first year of graduate work as a rotating student in their laboratory, they have always been readily available for wonderful advice. Additionally, I extend my sincere gratitude to Dr. Debabrata Banerjee. He joined my committee as an outside member and my IGERT co-advisor. With his guidance, I was able to begin to critically explore the foreign area of stem cell biology research.

In addition to my multiple advisors in New Jersey, I had the great honor to train under two outstanding researchers overseas. My thanks to Drs. Hugo Fernandes and Daniel Saris for allowing me to conduct further research with my stem cell-tenocyte co-culture system at the University of Twente in the Netherlands. For about 6 months they, along with Corina Ghebes and Joao Crispim, allowed me the independence and support to conduct great work towards the development of this dissertation. In addition, I extend my gratitude to Allison Pekannen, and

Drs. Nichole Rylander and P. Gunnar Brolinson at Virginia Tech, their guidance and provision of several critical materials utilized for the development of this dissertation has been priceless.

I have had the wonderful opportunity to share the lab with many great scientists over the years. Mrs. Yvonne Empson, who initially started the work on this project, trained me during my first semester working with prolotherapy and nanocarbons and has also been a wonderful friend and mentor throughout this entire process. I am eternally grateful for your guidance and friendship over these past few years. To the several wonderful lab mates with whom I have worked with in many capacities; Dr. Lee Wright, Dr. Kristin Mckeon-Fischer, Dr. Tea Andric, Dr. Albert Kwansa, Valerie Walters, Ajay Menon, Richa Ranade, Nicole Keenan, Rohit Rao, Yong-Soo Lee, Mahir Mohiuddin, Chalmers Brown, Barlgum Choi, Cody Yu, Jazmin Yarborough, Jamie Jackson, Brittany Taylor, and Dan Browe. Thank you all for your help, support, and camaraderie throughout this whole process. I also thank the countless research groups, scientists, and staff in the Biomedical Engineering Department at Rutgers for their help, support, and training with various endeavors over the last few years.

Finally, I would like to express an immeasurable amount of gratitude to my family and friends. I thank my parents, who have both made tremendous sacrifices in their lives in order for me to be afforded the opportunities I have today. From the beginning, they have always made education and personal development major priorities in my life, priorities I will keep for the rest of my life. To my mother, who instilled in me at a very young age to never settle and that anything can be achieved in life with proper dedication and hard work. To my father, whose own arduous academic endeavors inspired me to pursue science and medicine. To my big brother, TJ, who inspired me at an early age to strive to become a leader in more ways than imaginable. To my baby sister Praise, whose love, kindness, and nurturing has allowed me to

maintain my dedication in many aspects. To my many friends, who have tolerated my demanding and often sporadic graduate school schedule. I love you all and thank you deeply for your love, support, understanding, and mentorship. This doctorate is as much yours as it is mine, because none of this would have been possible where it not for all of you in my life. And finally, to my Heavenly Father - the Almighty, without whom none of this would have been possible. I thank You.

Dissertation Dedication

This dissertation is dedicated to my parents, Theo and Chidi Ekwueme. It is because of who you are and the sacrifices you have made that I am who I am today.

"Character cannot be developed in ease and quiet. Only through experiences of trial and suffering can the soul be strengthened, vision cleared, ambition inspired and success achieved."

-Helen Keller

"To accomplish great things, we must not only act, but also dream; not only plan, but also believe."

-Anatole France

"Science without religion is lame; religion without science is blind."

-Albert Einstein

Prior Publications

Several portions of this work have been submitted, or are in preparation to be submitted for publication elsewhere. The following publications have been acknowledged:

- Chapter 2 in its entirety has been submitted and is currently under peer review elsewhere as a manuscript entitled:

  "Sub-failure stretch injury damage in rat Achilles tendon." **Ekwueme EC, Choi BS, Yu CF, Rao R, Mohuiddin M, Freeman JW**
- Sections of Chapter 3 are being prepared for submission for publication elsewhere as part of a manuscript entitled:

  "Proliferative therapy-induced changes in the cellular response of human tenocytes." **EC Ekwueme, Mohiuddin M, Yarborough JA, Empson YM, Paynter DM, Brolinson PG, Saris DBF, Fernandes HAM, Freeman JW**
- Chapter 4 has been submitted in its entirety and is currently undergoing peer-revision elsewhere in a manuscript entitled:

  "Cross-talk between human tenocytes and bone marrow stromal cells potentiates extracellular matrix remodeling." **Ekwueme EC, Ghebes CA, Crispim JF, Saris DBF, Fernandes HAM, Freeman JW**
- Sections of Chapter 5 are being prepared for submission for publication elsewhere as part of a manuscript entitled:

  "Single-walled carbon nanohorns modulate tendon biomechanics and tenocyte response." **Ekwueme EC, Mohiuddin M, Jackson J, Lee YS, Empson YM, Pekkanen A, Rylander MN, Fernandes HAM, Saris DBF, Freeman JW**

Table of Contents

List of Tables

List of Figures

Chapter 1. Introduction

1.1 Ligaments and Tendons (L/T)

Ligaments and tendons (L/T) are dense, collagenous connective tissues of the musculoskeletal system. They primarily serve in aiding in force translation during body locomotion. During locomotion, tendons are responsible for transferring the loads produced by muscular contraction into joint movement. Ligaments serve as mechanical stabilizers for the joints. The compositions of both tissues primarily consist of fibroblast-like cells in an extracellular matrix (ECM). The ECM of L/T is mostly composed of collagen and elastin proteins, proteoglycans, and water. In addition to the ECM composition, similarities are also evidenced in the architectural features of the tissues. Collagenous arrays of hierarchical order are packed in a rope-like manner. Furthermore, the biomechanical response of both tissues is mainly in tension. Due to their structure and composition, they have the ability to sustain high tensile loads along their longitudinal axes. However, due to their mostly avascular nature, they lack of a robust healing response after injury (2).

The collagenous nature of L/T lends to its tolerance to high biomechanical loads. Collagen, the most abundant and the key load-bearing constituent of L/T matrices, accounts for about 65 to 80% of the ligament dry weight and about 70% of the tendon dry weight (1, 3, 4). The collagen molecules are closely packed together and arranged to form the collagen fibrils. These fibrils are also closely aggregated, forming the larger collagen fibers. Next, the collagen fibers arrange further into larger fascicles and bundles, which run parallel in the direction of L/T loading (Figure 1). The collagen molecule is presented in right-handed triple helical structured chains of amino acids. These chains, known as α-chains, possess left-handed helical conformations and

are comprised of glycine, proline, and hydroxyproline. The main collagen in L/T, collagen I, is composed of two α1(I) chains and a single α2(II) chain. Each chain has its own precise amino acid sequence (Figure 1.2)(5, 6).

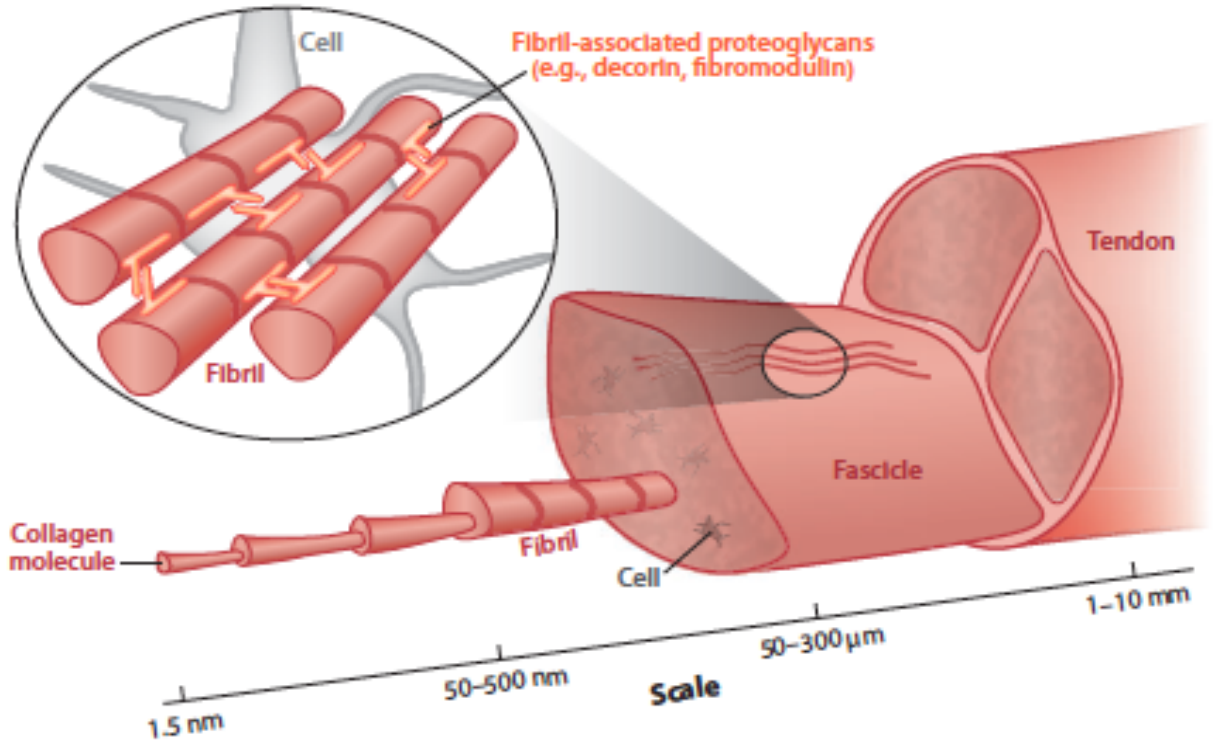

Figure 1.1 Schematic showing tendon hierarchy and length scales (1).

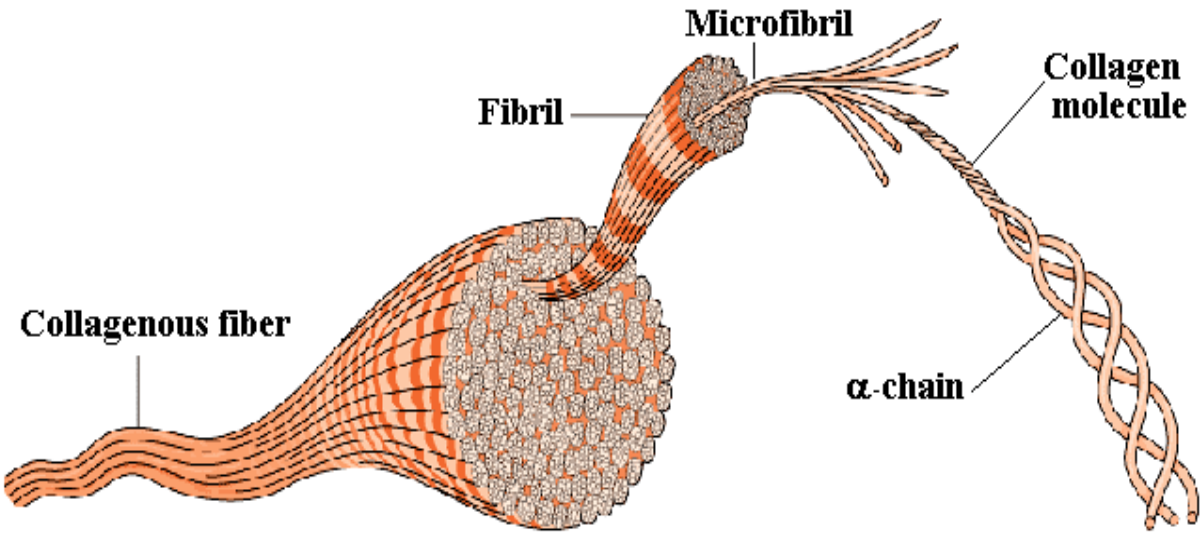

Figure 1.2 Hierarchical structure of the collagen protein (5).

1.2 Ligament and Tendon Injury, Disorder, and Healing

L/T are common sites of musculoskeletal injury. In the United States alone, annually there are over 32 million musculoskeletal injuries with about 45% of them occurring in L/T (7). L/T injury can primarily be described by some degree of damage to the mostly collagenous matrix of the tissue. There are various factors that contribute to the damage in L/T injury. More specifically, a sprain is damage to a ligament caused by an excessive loading from trauma to a joint while a strain injury is damage to a tendon as a result of overuse or trauma. The symptoms for injury include pain, stiffness, swelling, and bruising. Sprains are classified as grades I-III depending on the clinical evaluation and symptoms experienced by the patient. The descriptions for each sprain grade are summarized in Table 1.1(8, 9). A major issue with sprain injuries lies in the higher possibility of reoccurring sprain injuries, often resulting in permanently unstable joints. Previous work has shown that about 47-73% of individuals experiencing ankle sprain for

the first time will eventually suffer from reoccurring ankle sprains, leading to chronic ankle instability (10).

Table 1.1 Sprain Grade Classification and Characteristics (8, 9).

Sprain Grade	Characteristics
I	• Fibers of the ligament are stretched, perhaps partially torn • Minor tenderness and swelling • Joint does not feel unstable or give out during activity
II	• Fibers of the ligament are partially torn • Some tenderness; moderate swelling • Joint may feel unstable or give out during activity
III	• Fibers of the ligament are completely torn, or ruptured; ligament torn in two • Swelling could be minimal to severe; moderate to severe pain • Joint is unstable and gives out during certain activities

In addition to the physical damage induced by tissue trauma, genetic disorders can also lead to L/T injury. For example, one group of connective tissue disorders, known as Ehlers-Danlos Syndrome (EDS), is compounded by the defection in collagen tissue production. In EDS individuals, the final form of the various collagens and other structural proteins produced are defective due to mutations in the genes that code them. The condition results in an altered structure in the tissue and overall diminished tissue strength. Individuals with EDS often experience skin hyperextensibility, tissue fragility, and joint hypermobility. Symptoms resulting from this propensity for easy tissue damage include easy bruising and rupture, as well as frequent joint dislocations and subluxations. The condition leads to a mechanically compromised state in connective tissues and often results in chronic tissue instability in the affected individual (9, 11).

After L/T injury, the body initiates its wound healing cascade. The cascade has important sequential stages that must occur before the tissue is successfully repaired. The entire process is driven by various cell types and their release of several cellular signaling molecules. The phases of wound healing initiate with tissue inflammation, then the formation of granulation tissue, followed by a prolonged period of matrix formation and remodeling (12). Initially, injury results in notable matrix and cellular damage leading to the release of several pro-inflammatory and chemotactic signaling molecules. These signaling molecules coax the arrival of granulocytes, which then recruit monocytes and macrophages to clear debris and byproducts of tissue damage. Afterward, the macrophages release anti-inflammatory signaling molecules that attract and activate L/T progenitor cells and fibroblasts. The progenitor cells and fibroblasts differentiate and deposit new collagen at the wound site. Over time (up to several months), the newly deposited collagen eventually matures and contracts, causing the tissue to tighten (13).

1.3 L/T Injury Treatment and Repair

L/T suffer from the absence of [1] sufficient tissue vascularization and [2] a robust healing response after injury (4, 14). As a result, natural tissue healing can be lengthy and burdensome. Conventional approaches to the treatment of the acute or sub-failure type of injury are conservative. Current treatment options include drug therapy (using non-steroidal anti-inflammatory medication or NSAIDs, corticosteroid injections, etc.) and rest, ice, compression, and elevation (or RICE) with wrapping and aircasting (15, 16). For more severe cases, the use of surgical repair or replacement is often required. For the instances where surgical repair is warranted, primary repair can be achieved by reconnecting and securing the ruptured portions of the tissue with sutures, although the majority of severe cases require the total resection and replacement of the diseased or damaged tissue with graft tissue (14, 17). Although current

treatment methods have yielded clinical success in many cases, each is met with several disadvantages and shortcomings. In an attempt to circumvent the several drawback associated with current treatment options, scientists have begun to explore tissue engineering approaches to L/T repair.

1.4 Tissue Engineering (TE)

Tissue engineering (TE) has quickly become a potential option in the treatment and repair of several diseased and damaged tissues. The primary goal of TE is the integration of engineering and biological principles for the maintenance, restoration, or enhancement of tissues and organs in the body (18). TE techniques combine the singular and combinatorial use of biomaterial scaffolds, cells, drugs, small molecules, and nanoparticles to achieve this goal. In TE, cells of interest are autologously or allogeneically isolated then further expanded and propagated *ex vivo* to obtain suitable cell numbers before being implanted into the patient for tissue reparation. Irrespective of cell source and type, the TE strategy can include injection of the isolated cells directly into the target tissue or seeding them into biocompatible biomaterial constructs *in vitro* prior to implantation. The understanding behind this approach is that the implanted cells will produce the appropriate tissue-specific matrix that is necessary for cell support and tissue development. Several pre-clinical studies have demonstrated the potential of TE approaches in L/T repair using cell types including dermal fibroblasts, ligament progenitor cells, mesenchymal stem cells, and embryonic stem cells (19-22).

1.4.1 Proliferative Therapy (Prolotherapy)

Proliferative therapy, also known as prolotherapy, is an alternative treatment method used in the repair of diseased and damaged connective tissues that has been utilized since the 1930s.

Initially during the 1930s and 1940s, surgeons began exploring the use of an injection therapy as a method to stabilize loose connective tissues and joints. Believing that tissue repair was achieved via sclerosing (or scarring) or the damaged tissue, the surgeons referred to this procedure as "sclerotherapy." However, modern techniques currently utilized in clinical practice are credited to Dr. George Hackett, a physician who extensively researched sclerotherapy during the 1950s and 1960s. Dr. Hackett's work revealed that the repair mechanism of the technique was one of proliferation rather than scarring (11, 23-25). With the technique, an experienced physician injects a "proliferant" (or irritant solution) directly into the injury site of the patient to induce localized tissue inflammation, which ultimately leads to tissue reparation. Today's commonly used proliferants include phenol, sodium morrhuate (a derivative of cod liver oil), glucose, dextrose, and glycerin separately or combined. P2G, another commonly used proliferant, is a combination of phenol, glucose, and glycerin. In general, proliferants are classified by the mechanism with which they initiate tissue inflammation: irritants, osmotics, and chemotactics.

It is believed that after injection, the proliferants cause "therapeutic" trauma leading to localized cell death. This causes local tissue inflammation, initiating the body's wound healing cascade (13). It has been proposed that the proliferant treatment leads to cellular damage that triggers the release of chemotactic factors and inflammatory mediators. These factors, most notably prostaglandin, thromboxane, and leukotriene species recruit granulocytes and macrophages. This initiates the early stages of the wound healing cascade (13). In a previous study of prolotherapy, *in vivo* work showed that dextrose lead to a 47% increase in rabbit medial collateral ligaments (MCL) and a 27% strength increase in the bone-ligament junctions (26). Prolotherapy treatments have successfully been used in the clinic to treat cases of EDS in

addition to common sprains and strains (9, 11). Although studies have previously suggested possible mechanisms by which healing with this method occurs, those investigations have often led to inconsistent results and the failure to establish the specific cellular and molecular signaling mechanisms involved during prolotherapy-induced healing.

1.4.2 Mesenchymal Stem Cells (MSC)

Mesenchymal stem cells (MSC) are adult unspecialized cells that have been heavily investigated in TE applications for the repair of numerous tissues and organs. They are advantageous for TE due to their self-renewal and multipotent capabilities. With the use of appropriate stimuli, the cells can be differentiated toward a desired lineage to aid in the replacement of diseased or damaged tissues. Previous work has shown MSC to have higher proliferation rates, matrix deposition, mRNA activity of tendon related markers than other fibroblastic cell types including ligament and skin fibroblasts (20, 27, 28). Such results indicate that the promotion of MSC toward a tenogenic pathway, either before or after incorporation into the tissue, may be used as a potential tool for the enhancement of L/T repair. Furthermore, other reports have revealed that MSC begin to assume a tenogenic phenotype after exposure to soluble factors including TGF-β, BMP-12, -13, PDGF, and IGF-1 *in vitro* (21, 27, 29). In addition to serving as a potential cell source for direct differentiation, there has been much evidence suggesting that the clinical utility of MSC may also lie in their role as trophic mediators of tissue repair (30, 31).

1.4.3 Single-walled Carbon Nanohorns (CNH)

Nanocarbons are allotropes of carbon arranged in various structures and configurations. They can be presented as graphenes, carbon nanotubes, and nanohorns. These nanostructures are

utilized in biomedicine because their small size, high strength, and functional capabilities make them highly advantageous. They have recently gained popularity for their utility in next generation medical diagnostic and targeting purposes. In addition to those approaches, they have also been used to increase matrix mechanical properties in nanocomposites (32, 33). They have also been successfully utilized as biomaterials and have been shown to not have a negative effect on cellular viability, and even in some cases, aid in tissue regeneration (34, 35). More specifically, single-walled carbon nanohorns are 50-100 nm agglomerate structures of individual single-walled carbon nanotubes (Figure 1.3). The carbon nanotubes can be produced to have individual overall diameters of 2-5 nm (36, 37).

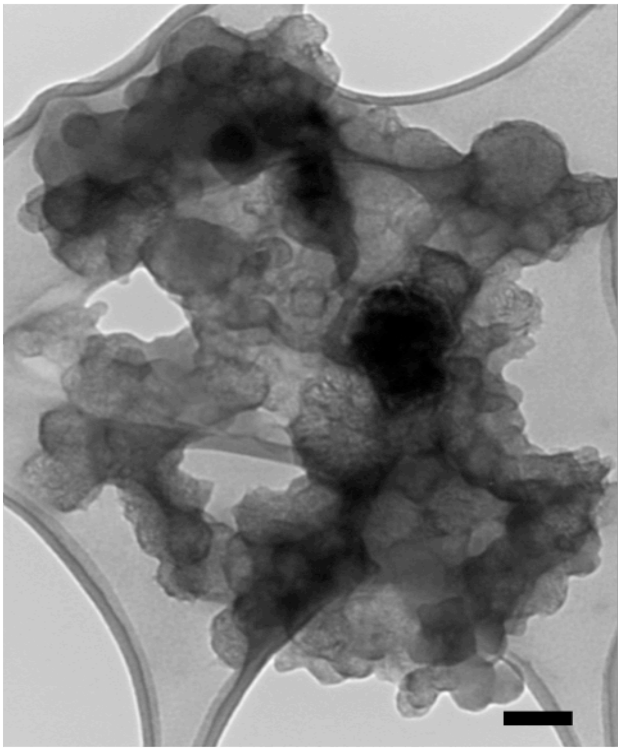

Figure 1.3 Transmission electron microscopy of CNH. Scale bar=100nm.

The diameters of CNH are on the same size scale as the ECM components in L/T matrices. This highlights their importance as potential tools for L/T repair. Their high strength and small size could be utilized to aid in stress transfer between damaged matrix fibers in grade I-II injuries in L/T. This rationale in addition to previous results have inspired the potential use of CNH in a novel modality as a biocompatible nanofiller for the mechanical reinforcement of lax connective tissue matrices.

The overall goal of this dissertation was to investigate the tenogenic healing potential of utilizing three distinct non-surgical TE techniques for the treatment of sub-failure sprain and strain injuries in L/T. To this end, we hypothesized that the incorporation of high elastic modulus nanocarbons and bone marrow-derived stromal cells to the alternative prolotherapy to create a potential customizable integrated therapy can enhance the healing potential and mechanical strength of sub-failure L/T injuries by [1] providing mechanical reinforcement of the damaged tissue and [2] inducing an increase in cellular recruitment, proliferation, and ECM deposition. Using a series of *in vitro* and *in vivo* studies, we explored the tenogenic healing potential each individual modality.

Chapter 2. Sub-failure stretch injury response in tendon matrices

Manuscript submitted to Clinical Orthopaedics and Related Research

2.1 Abstract

Sub-failure ligament and tendon injuries are of great concern to athletes and the general population. Accounting for a significant proportion of all musculoskeletal injuries per year, these injuries are a result of genetic disorder, overuse, or traumatic injury to the collagenous matrix of the tissue. The goals of this study was to design a reproducible small animal model for soft tissue sub-failure injury and investigate the biomechanical and histological response of a singular, controlled sub-failure stretch damage in rat Achilles tendon matrices. Utilizing a novel tendon stretch injury device, we showed that sub-failure stretch lead to significant changes in the elastic moduli of the toe region of the stress-strain curves of tendons. Additionally, imaging confirmed damage and disorganization of the normally aligned collagen matrix of the tendon at the tissue micro scales. Furthermore, magnetic resonance imaging and histological staining showed strong evidence of the injury at 7 days post injury *in vivo*. Additionally, biomechanical testing confirmed compromised biomechanical properties at 7 and 14 days post-injury. Results validated the clinical utility of this new *in vivo* model for the study of sub-failure injury of ligaments and tendons. Taken together, these findings provide clinically relevant information about the most common type of ligament and tendon injury.

2.2 Introduction

Sub-failure injuries such as sprains and strains account for a significant portion of musculoskeletal injuries. In the United States alone, there are over 32 million musculoskeletal injuries with approximately 45% occurring in ligaments and tendons annually (7, 38). The

injuries occur as a result of a pre-existing genetic disorder, overuse, or trauma to the mostly collagenous matrix of the tissue (1, 7, 38). This disruption of the aligned, hierarchical matrix results in compromised biomechanics during locomotion/support and leaves the tissue prone to re-injury (15, 39). Clinically, the extent of injury is divided into three main categories, grades I-III, based on the degree of damage to the collagenous matrix. Grade I injuries involve the stretching of tissue fibers with minor tenderness and swelling. Grade II injuries result in clinically detectable partial tearing of the tissue fibers with some tenderness and moderate swelling. Grade III injuries result in severe rupture or complete tearing of tissue fibers with minimal to severe swelling and pain (8, 10). These conditions are accompanied by various biological events including changes in tissue biomechanics and cellular response, decreases in collagen fiber organization, and changes in the expression patterns of several structural proteins and molecular markers (40-43).

Several sub-failure tendon and ligament injury models have been employed to study the cellular and tissue biomechanical response of sub-failure ligament and tendon injury. Previous attempts at this model have attempted to induce controllable and repeatable sub-failure damage to the tissue. For instance, Provenzano and colleagues developed a hand-held micrometer based device that stretches the medial collateral ligament (MCL) in a bowstring fashion (16, 44, 45). This resulted in a stretch-like grade II damage to the matrix of the MCL that was visible under scanning electron microscopy. Furthermore, the device induced apparent changes in the biomechanical properties of the healing MCL. Elsewhere in a study of the effect of low level laser therapy on sub-failure tendon healing, Joensen *et al* utilized a guillotine-type device to create controlled contusions in the Achilles tendons of rats (46). This model utilized a direct contact approach to creating a blunt force trauma in the tissue (47-49). This injury resulted in

histological changes after damage, but no detectable differences in biomechanical properties evidenced in the ultimate tensile strength (UTS). Fung and coworkers developed a sub-failure fatigue-loading model for rat patellar tendon (50). The model employs a custom built loading apparatus that grips the patellar tendon and induces controlled cyclic loading to mimic repetitive tissue loading and fatiguing. Results showed notable changes in tissue biomechanical properties, matrix organization, and expression patterns of several molecular markers involved in ligament and tendon maintenance that was dependent on cycles administered (50-53).

Adequate tendon and ligament sub-failure injury models must be able to create consistent, and reproducible injury in the tissue of interest. Additionally, the experimental model must possess some ability to mimic the clinical condition evidenced in sprain and strain injuries, including biomechanical, morphological, biochemical, and histological changes. Previous attempts at *in vivo* models for sub-failure injury in ligaments and tendons have encompassed several aspects of and provided useful information about the clinical condition exhibited in sprain and strain injuries but each with their respective experimental or biological limitations. The current work describes the development and characterization of a novel sub-failure stretch injury device for the investigation of sprain and strain injuries in ligaments and tendons. We utilized this novel model to study the biomechanical response of stretch injured Achilles tendons in rat cadavers and the healing of stretch injured Achilles tendons *in vivo* using a Sprague-Dawley rat model for up to 14 days.

2.3 Materials and Methods

2.3.1 Stretch Injury Device

A modified modular tendon stretch injury device was designed and developed based on the device described by Provenzano and colleagues (44). First, a 3D model was rendered using the computer aided design (CAD) program Tinkercad. Afterwards, the rendered model was 3D printed using 1.75mm acrylonitrile butadiene styrene (ABS) plastic on a Makerbot Replicator 3D Printer. Non-printed parts were obtained from the local hardware store. The device is composed of modular parts for ease of sterilization prior to use for *in vivo* experiments. In brief, the device consists of a hook attached to a spring scale and modified into a micrometer. During use, the device induces controllable and measureable transverse stretching in the mid-substance of the tendon while restraining the insertion and transition regions.

2.3.2 Injury Model

All animal experiments were conducted with approval from the Animal Care and Use Committee of Rutgers, The State University of New Jersey. The Achilles tendon was chosen because it is the largest tendon in the body and can be easily accessed in a rat model. For initial device validation studies, we utilized rat cadavers that were previously euthanized by CO_2 inhalation in other studies. For *in vivo* studies, 10 week-old Sprague-Dawley rats were obtained from Taconic Farms. Prior to surgical procedures, general anesthesia was induced and maintained with isoflurane gas. After aseptic preparation of the surgical site and administration of Marcaine as a local anesthetic, a 1-cm incision was made on the surrounding skin to expose the right Achilles tendon. The foot was then stabilized at a 90 degree angle using a brace, ensuring the same position each time the device is used. The device hook was inserted under the tendon and the foot was raised until the device gently restrained the insertion/junction points. Next, the tendon was preloaded to 2N of force by raising the micrometer to the appropriate height. The micrometer was turned in timed increments, one half turn per second, until a target

force was reached. Target forces of 10N and 20N were used for preliminary studies, while 20N was utilized for *in vivo* studies. Once the target force was reached, the micrometer was unscrewed to dissipate the force quickly and release the tendon. After performing the injury procedure, the skin above the Achilles tendon was rejoined and reinforced using sterile surgical sutures. Rats were allowed to freely roam in their cages for up to 14 days. At designated time-points, rats were euthanized. Without damaging the tendon, the muscles and surrounding tissues were carefully cut away. The tendons were immediately wrapped in phosphate-buffered solution (PBS)-soaked gauze, covered in foil, and then stored in a -20°C freezer until further testing as previously described (54, 55). For all tests, each tendon was compared to its contralateral, uninjured control.

2.3.3 Scanning Electron Microscopy (SEM)

SEM imaging was utilized to confirm damage to the tissue at the micro scale. Isolated tendons were washed and fixed with 4% paraformaldehyde solution for one hour. Afterwards, the samples were lyophilized overnight then longitudinally sliced and mounted on SEM specimen holder slides. Finally, samples were coated with 10nm of gold/palladium (Au/Pd) using a SCD 004 Sputter Coater (Blazer) before being observed under an Amray 1830I Scanning Electron Microscope.

2.3.4 Mechanical Tensile Testing

For preliminary validation tests, there were four groups of explanted tendons with a sample size of n=6; injured with 10 and 20N, and each compared to its contralateral control. For *in vivo* studies, n=4 rats were mechanically tested 7 and 14 days after injury. All samples were gently thawed in PBS at room temperature for at least 30 minutes before tensile testing. Tensile

testing was completed using a Bose EnduraTec testing machine. The transition from toe region to the linear region of the tendon was studied. The width, thickness, and gauge length of the tendon were measured before testing. The tendon was then loaded onto the machine using a custom grip set up. Samples were preloaded to 0.2N of force then strained at a displacement rate of 0.1mm/sec. The young's modulus of each sample's toe region was then calculated as previously described (56).

2.3.5 Magnetic Resonance Imaging

At 7 days post injury, n=2 rats were induced and maintained under general anesthesia with isoflurane gas. Imaging was performed using an Aspect M2 Compact High-Performance MRI. T1-weighted spoiled gradient echo sequence scans were completed with a field of view 100mm, matrix 256 x 256, TR 15 ms, TE 3.5 ms, and flip angle 30°.

2.3.6 Histological Staining

At 7 days post injury, n=2 rats were euthanized and the tendons were isolated, fixed in 4% paraformaldehyde (PFA), and sent for histological analysis. Samples were embedded in paraffin and stained with hematoxylin and eosin (H&E), Masson's trichrome, safranin-O, and Verhoeff's Von Giesen (VVG) stains (AML Labs, Rosedale, MD). Slides were imaged using an EVOS microscope.

2.3.7 Statistical Analysis

All numerical data is presented as mean±standard deviation. A one-way ANOVA with a Bonferroni's multiple comparison post-test was employed to compare various groups.

Differences were considered statistically significant for *p*-values less than 0.05, unless otherwise stated.

2.4 Results

The goal of the current work was to investigate sub-failure damage in Achilles tendon matrices. Utilizing a custom device (Figure 2.1), sub-failure stretch damage was achieved in rat Achilles tendon matrices. SEM imaging was utilized to confirm damage to the tendon mid-substance. Closer examination showed discoloration of the tissue evidenced at the site of injury (Figure 2.2). Furthermore, the SEM imaging confirmed damage at the microscopic level evidenced in the disruption of the aligned collagenous matrix that constitutes tendons and ligaments (Figure 2.3). Upon closer observation, disruptions and voids can be seen in the otherwise aligned and tight matrix after the stretch injury. Additionally, notable damage to individual collagen fibers is evident after injury.

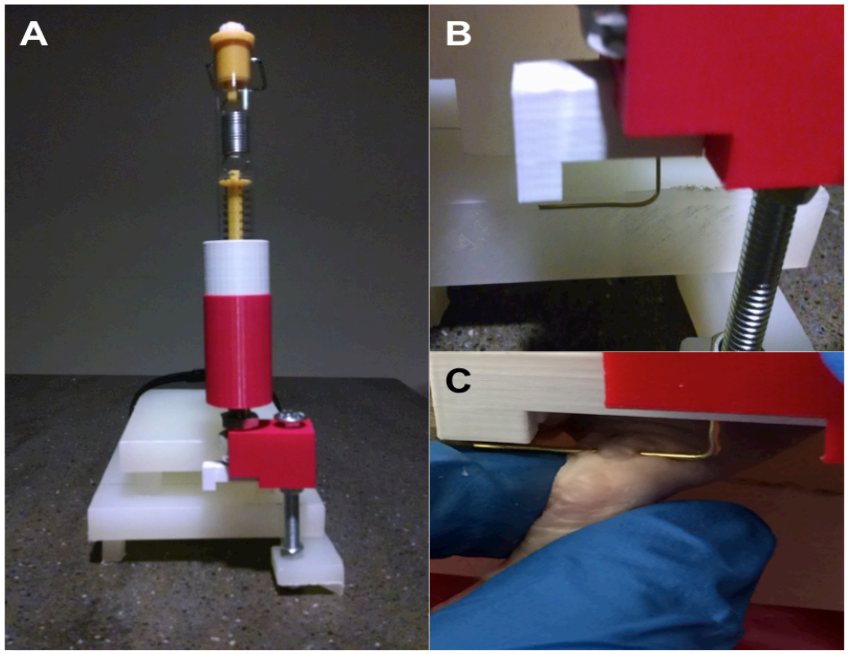

Figure 2.1 Custom built stretch device for sub-failure stretch injury of ligaments and tendons. (B) Section used to insert under tendon and stetch axially. (C) Device engaged in injuring rat cadever Achilles tendon.

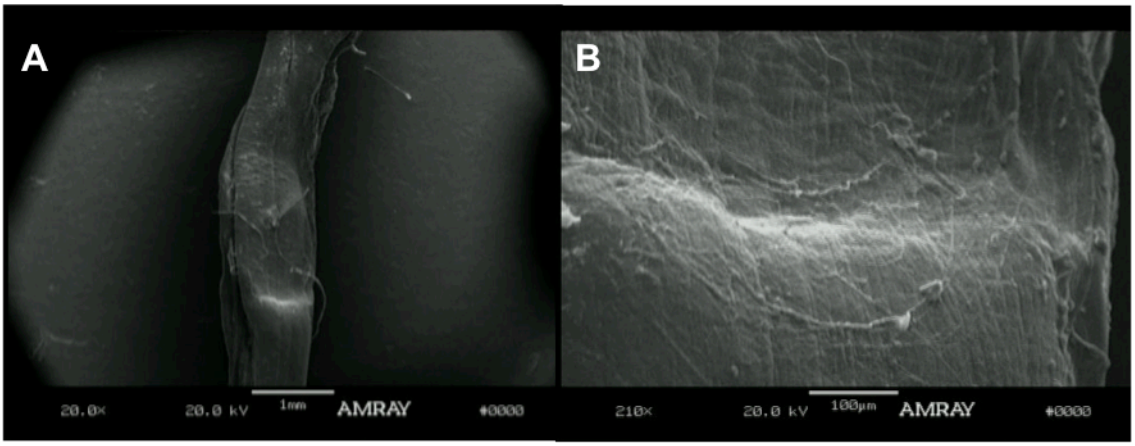

Figure 2.2 Scanning electron microscopy showing rat Achilles tendon damage. Tendon mid-substance showing discoloration of injury region (A) and detailed image showing close-up view of tissue discoloration (B).

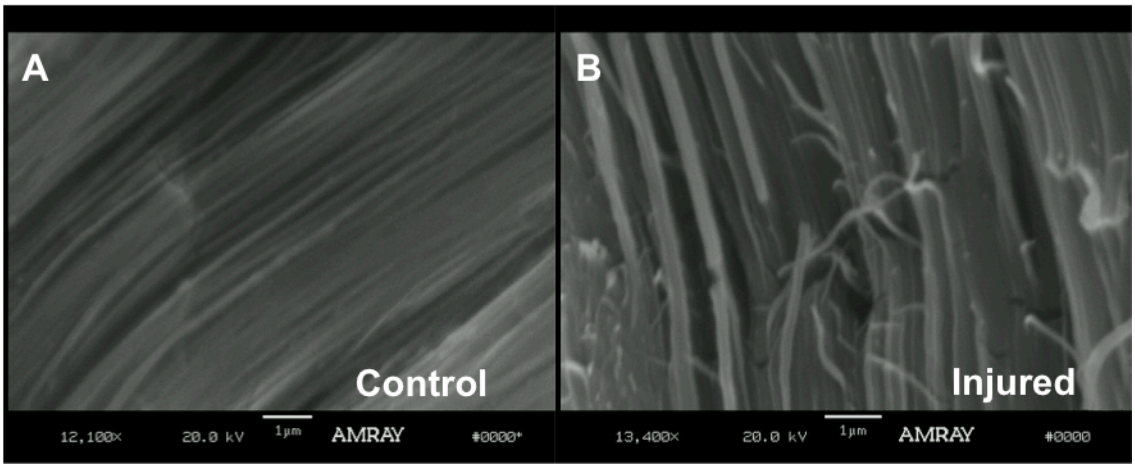

Figure 2.3 Scanning electron microscopy showing rat Achilles tendon collagen matrix disorganization. Tendon collagen fiber arrangement before (A) and after (B) sub-failure damage using the stretch injury device.

Uniaxial tensile testing with the cadaveric rat Achilles tendon model showed signficant decreases in the elastic moduli of the toe region of tendon stress-strain curves after injury with both loads tested (Figure 2.4A). Furthermore, there is a significant difference ($p<0.05$) between the 10 and 20N (26.45±10.71 vs. 43.15±14.63) groups in the percent decrease of the toe moduli of injured tendons (Figure 2.4B).

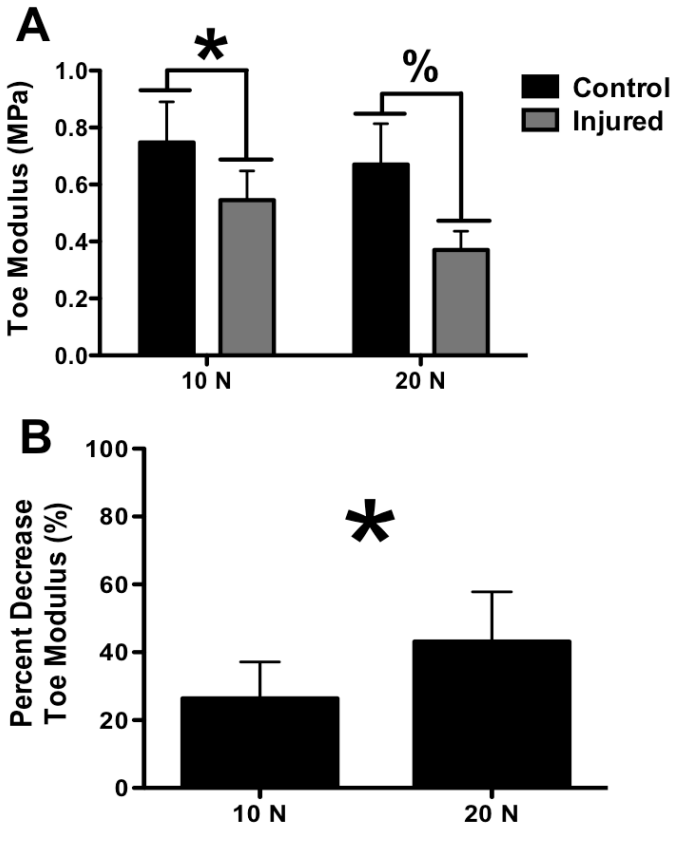

Figure 2.4 (A) Mean tensile toe region elastic modulus and (B) percent decrease of rat cadaver Achilles tendon after injury with 10 and 20N loads (*p<0.05, %p<0.01).

After completion of *in vitro* validation tests with the injury device, we proceeded to using the device to injure the Achilles tendons of rats *in vivo*. Figure 2.5 shows representative MRI scans of the rats after injury. Upon comparison with non-injured control contralateral Achilles tendon, the scans confirmed tendon damage in the injured limb at up to 7 days *in vivo.* The straight black space (indicated by the arrow) represents the uninjured control Achilles tendon connected the muscle to the joint. In the injured tendon, there is a clear disruption and disorganization of the black space present. After 7 days, the disruption in the tissue is still clearly visible in the scans.

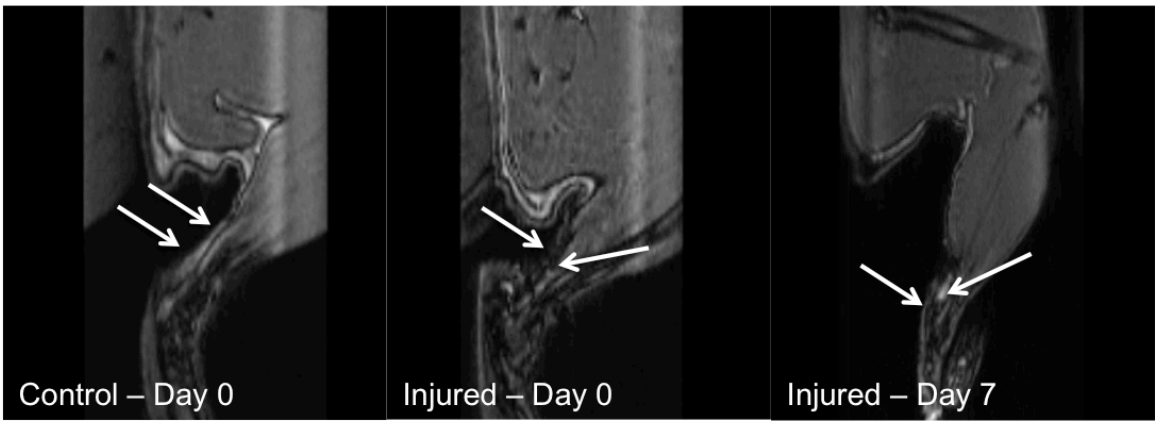

Figure 2.5 Representative magnetic resonance imaging of Sprague-Dawley rat Achilles tendon injury 7 days post injury.

Uniaxial tensile testing confirmed a significant decrease in the toe region moduli of injured tendons after 7 days (53.59±9.54%) and 14 days (44.00±5.80%) *in vivo*. Also, the testing showed that there was no significant difference between the percent change in toe region elastic modulus at 7 and 14 days post injury (Figure 2.6).

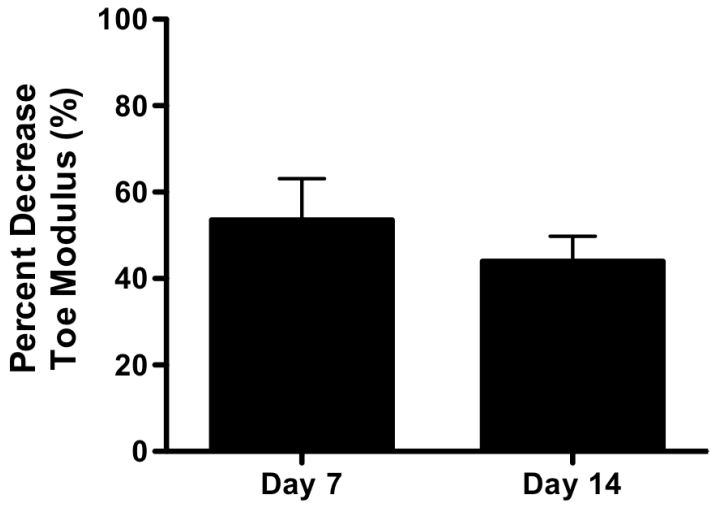

Figure 2.6 Mean percent decrease in rat Achilles tendon tensile toe region elastic modulus 7 and 14 days post injury.

Figure 2.7 demonstrates the histological staining of the tendon matrices at 7 days post injury. Results confirmed that voids in the typically tight, aligned matrix of the tendons were present 7 days after stretch injury. Moreover, a gross observation of the sections showed that the blue color of the Trichrome and brown in the VVG stains appeared to stain more intensely in the injured tendons at 7 days.

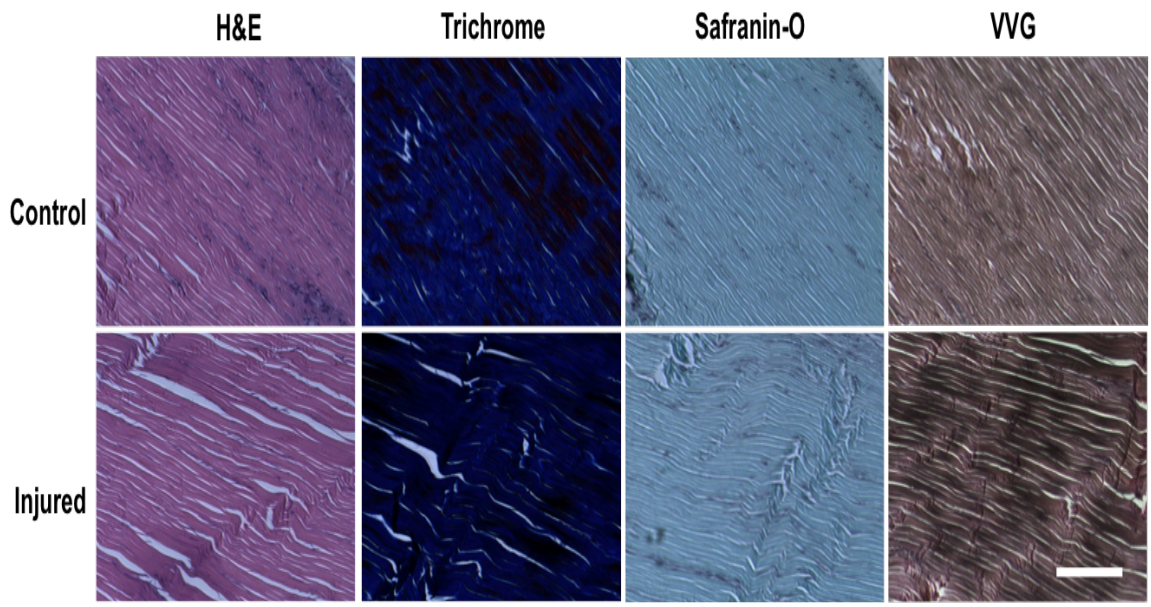

Figure 2.7 Histological staining of representative sections of rat Achilles tendon mid-substance 7 days after stretch injury. Scale bar = 400 μm

2.5 Discussion

Sprain and strain injuries are mainly characterized by the damage and disruption present in the collagenous matrix that predominantly constitutes them. We set out to investigate the biomechanical and histological response of intact Achilles tendons to injury created by a custom sub-failure stretch injury device (Figure 2.1). Validation tests using a cadaveric rat Achilles tendon model showed signs of grade II strain injury at up to 20N damage force applied to the tendon mid-substance. SEM images showed that the device could deliver consistent sub-failure damage to intact rat Achilles tendons (Figures 2.2, 2.3). The discoloration of the injury site is present after damage, confirming disruption of the matrix as a result of the stretch injury from the device.

Uniaxial tensile testing showed that both 10 and 20N loads caused significant changes in the toe moduli of the tendons (Figure 2.4A). Additionally, there was a significant difference in change in toe moduli of the tendons between the two loads (Figure 2.4B). This is notable because for ligament and tendon biomechanics, it has been reported that humans only operate within the toe region (2-4%) of the stress-strain curve (4, 22, 57). Furthermore, grade II sprains and strains which cause plastic deformation to the collagen matrix, are characterized as musculoskeletal conditions exhibiting changes in tissue biomechanics and laxity during everyday activities (8).

The device was used to study the effect of sub-failure stretch injury on intact tendon response *in vivo*. MR imaging confirmed evidence of the grade II damage in the Achilles tendons of Sprague-Dawley rats (Figure 2.5). This is significant because the grade II class of these types of injuries is described as clinically detectable disruption or disorganization of the collagenous matrix of ligaments and tendons. Furthermore, biomechanical tests showed no difference in the percent change in tensile toe modulus at 7 and 14 days after injury (Figure 2.6). Histological staining and microscopy showed the expected disorganization of the intact collagenous ECM of the tissue 7 days after injury (Figure 2.7). Interestingly, it appeared that certain colors from the Trichrome and VVG stained more intensely after injury. The blue color of the Trichrome specifically stains for the collagen in the tissue while the VVG stains for elastin. This may be evidence of the changes in expression patterns of matrix components including collagen and elastin (40-42). Further work is currently investigating this response via western blotting for protein expression and quantitative real time PCR (qPCR) for mRNA expression *in vivo*.

Limitations of the current study and the associated model include the lack of insight into the cell and biological response of the tissue in response to the sub-failure damage and subsequent healing response *in vivo*. In addition to the biomechanical and histological changes evidenced in our study, there may also be changes in the cell response and expression patterns of key molecular markers implicated in the maintenance and repair of sub-failure ligament and tendon pathologies (40-42). Furthermore, the appearance of higher intensity staining for two proteins at 7 days post-op warrants further investigation of gene and protein expression analysis using molecular biology and immunohistochemical techniques for a deeper understanding of the expression patterns of appropriate markers.

In summary, using a custom stretch injury device we investigated the biomechanical and healing response of rat Achilles tendons. Imaging confirmed a grade II sprain injury in the tendons at both the macro scale with damage to the tissue and micro scale collagen fibril network. Biomechanical testing corroborated evidence of damage with significant changes in the tensile toe moduli of Sprague-Dawley rat tendons at 7 and 14 days. Additionally, Trichrome and VVG staining suggested elevated collagen and elastin levels 7 days after injury. We have presented a novel *in vivo* model for the study of sub-failure stretch injuries in tendons. Tests performed demonstrated strong evidence supporting known signs and symptoms of grade II sprain and strain pathologies. Additional studies on the biochemical response the tissue after injury are warranted for further understanding of the injury and healing of sub-failure injuries to ligaments and tendons.

Acknowledgements

The authors gratefully acknowledge excellent technical assistance from Derek Adler in the Rutgers Molecular Imaging Center and financial support from NSF DGE 0801620 and NSF CBET 1034026.

Chapter 3. Proliferative therapy-induced changes in the cellular response of human tenocytes

Manuscript to be submitted to the American Journal of Sports Medicine

3.1 Abstract

Connective tissue healing after injury is often hampered by the lack of sufficient tissue vascularization and overall diminished intrinsic healing potential. Proliferative therapy, or prolotherapy, is a popular alternative method used in the repair and management of many connective tissue injuries and disorders. It involves the injection of a proliferant, or irritant solution, into the site of injury, which causes small-scale cell death. This therapeutic trauma is believed to initiate the body's wound healing cascade ultimately leading to tissue repair. The goal of the current work was to investigate the immediate response of two common proliferants (dextrose and P2G) on the cellular response of human tenocytes. Results showed that both solutions led to significant decreases in the metabolic activity of both primary and immortalized tenocytes with P2G having the more pronounced effect. Additionally, both solutions led to decreased cellular migration in the tenocytes. Gene expression analysis confirmed that treatment led to the up-regulation of key pro-inflammatory markers including IL-8 and COX-2 and down-regulation of the matrix marker collagen type I. Furthermore, using a reporter cell line for TGF-β, a prominent anti-inflammatory marker, we demonstrated that treatments led to decreased TGF-β bioactivity. Moreover, secretome analysis of soluble proteins using ELISA showed a trend of decreasing levels of TGF-β after proliferant treatments. Lastly, analysis showed that treatment with P2G significantly elevated levels of soluble PGE2, a prominent inducer of inflammation. Taken together, these results suggest that prolotherapy, more so with P2G, works

at the fundamental level by decreasing cellular function and eliciting a pro-inflammatory response in tendon cells.

3.2 Introduction

Ligament and tendon healing from sub-failure injury is often hampered by incomplete healing and chronic tissue instability(16, 39). Both tissues are strong collagenous structures that operate primarily in tension and are integral in body locomotion. Due to their structure, function, and composition these tissues are often regarded as mostly avascular and therefore lack robust healing capabilities (1, 56, 57). To address this, several approaches to repair have been investigated with goals of significantly decreasing healing time and increasing tissue biomechanical properties. Conventional modalities including drug therapy (NSAIDs, corticosteroid injections, etc.) and rest, ice, compression, and elevation (or RICE) have been met with their associated drawbacks (15, 16). Due to this, several alternative approaches have garnered increasing attention.

Proliferative therapy or prolotherapy is a non-invasive, alternative treatment for damaged musculoskeletal tissues (9). The treatment involves the injection of a proliferant (or irritant solution) into the damaged or lax ligament or tendon (11, 58, 59). It is hypothesized that the proliferant causes localized tissue trauma, which leads to cell death, and the release of chemotactic factors and inflammatory mediators to initiate the body's wound healing cascade. Cell death leads to the release of factors such as prostaglandins, thromboxanes, and leukotreines, which recruit cells from the initial phase of the cascade. Granulocytes and macrophages from the initial stage of inflammation release factors that attract and activate fibroblasts. These fibroblasts deposit new collagen at the wound site, which eventually matures and contracts,

causing the ligament or tendon to tighten and strengthen(13). Common proliferant choices include dextrose, phenol, glucose, glycerin, and sodium morrhuate used either alone or in combination (one common combination is P2G, which is comprised of phenol, glycerin, and glucose).

Prolotherapy has been reported to be successful in treating cases of Ehlers-Danlos Syndrome and common joint sprains and strains although investigations into the mechanisms behind the treatment's healing have yielded inconsistent results(16, 45, 58, 59). Unfortunately, very little research exists about the *in vitro* cellular response of proliferants in clinical use. Previous *in vitro* work by our group determining the effect of P2G on ECM building cells has shown that the local response to prolotherapy of resident fibroblasts and osteoblasts in the tissue may not be adequate for complete healing, making assistance from the body's wound healing cascade necessary(58). More specifically, P2G treatments can lead to recoverable cell death and collagen deposition. However, the response from treatment groups never surpassed controls, suggesting that the local response of resident cells may be insufficient for complete tissue healing *in vivo*. These initial results warranted further investigation into understanding the proliferant-induced cell response with a special focus on the immediate cascade of events (within 1 day). Considering such, it would be valuable to ascertain the hypothesized underlying molecular mechanisms leading to the prolotherapy-induced inflammatory response *in vitro*.

In this study, we investigated the effects of two common proliferant drugs, dextrose (or d-glucose) and P2G, on the cellular response to proliferative therapy. Utilizing primary human hamstring tenocytes and immortalized human Achilles tenocytes, we examined the effects of proliferant exposure on cell metabolic activity, migration, mRNA expression of markers related to tendon healing and associated inflammatory markers, and release of bioactive proteins. We

hypothesized that both proliferants will induce considerable changes in cellular response which ultimately lead to cell death and induction of inflammation *in vitro*.

3.3 Materials and Methods

3.3.1 Proliferants

Two commonly used proliferants, 50% dextrose and P2G (a combination of 2% phenol, 25% glucose, and 25% glycerin) were obtained (Buderer Drug Company, Perrysburg, OH, USA) and utilized for cellular studies.

3.3.2 Cell isolation and culture

All studies were conducted with approval from the Rutgers Environmental Health and Safety Office, the Medical Ethical Research Committee at the Utrecht Medical Center, and MST Twente. Following standard written informed consent, human hamstring tendon (hHT) samples were harvested from an adult patient undergoing anterior cruciate ligament reconstruction. After isolation, the tendons were rinsed with sterile phosphate buffered saline (PBS). Excess muscle tissue was carefully removed and the tendon was cut into smaller pieces. Next, the tendon pieces were cultured in growth medium consisting of Dulbecco's modified Eagle's medium (DMEM) (PAA Laboratories, Australia) supplemented with 10% fetal bovine serum (FBS) (Lonza, Basel, Switzerland), 1% penicillin streptomycin, and 0.2 mM ascorbic acid (Sigma Aldrich, St. Louis, MO) in order for the cells to migrate from the tissue pieces. Primary cells between passages 2 and 4 were used for experiments. Immortalized human Achilles tendon tenocytes (hAT) were a kind gift from Dr. Denitsa Docheva at the Walter Brendel Centre of Experimental Medicine at the Ludwig-Maximilian University of Munich. Both cell types were maintained in α–MEM at pH 7.6 supplemented with 1% PS and 10% FBS (Life Technologies).

3.3.3 Experimental design

Cells were seeded on tissue culture well plates at a density of $5x10^3$ cells/cm^2 plate and allowed to adhere overnight before treating with 0.024% (v/v) of P2G and dextrose. After 6, 12, and 24 hours of treatment cell populations were evaluated using assays as described below. After 24 hours, the conditioned medium was collected and stored at -80°C for further analysis of cell secretome. Both hHT and hAT were utilized for cellular metabolic activity and gene expression assays. Only hHT were used for the conditioned medium assays and only hAT were utilized for the scratch wound healing assay.

3.3.4 Cellular metabolic activity

Cell metabolic activity was evaluated using the fluorometric PrestoBlue Assay (Life Technologies). At each time-point, each well was emptied. Then, 10% PrestoBlue reagent in fresh cell culture medium was added to each well. The plates were incubated for one hour followed by measurements of fluorescence in technical duplicates at 560 nm excitation and 590 nm emission with a Tecan spectrophotometer (Mannedorf, Switzerland). Fluorescent values for treatment groups were normalized to control groups.

3.3.5 Tenocyte scratch wound healing assay

Cell migration was assessed using the standard scratch wound-healing assay. Briefly, $10x10^5$ cells/cm^2 hAT were seeded and allowed to reach confluence. A scratch was induced across the cell monolayer using a sterile 1 mL pipette tip. Afterward, culture medium was replaced with fresh medium and cell populations were treated with either P2G or dextrose. At various timepoints, the migration of cells while closing the “wound” was monitored using light microscopy. Images were analyzed using NIH Image J.

3.3.6 Real-time quantitative RT-PCR analysis (qPCR)

For qPCR studies, total RNA was extracted with the RNeasy Mini Kit (Qiagen, Valencia, CA, US) according to the vendor's protocol. Isolated RNA was normalized then converted to cDNA using the Reverse Transcription System (Promega Corporation, WI). After reverse transcription, the cDNA was combined with SYBR Green Master Mix (Life Technologies, CA) and the primers for markers of interest then subjected to qPCR. Experiments were conducted with GAPDH as the housekeeping gene. Specific primers for wound healing and pro-inflammatory markers are represented in Table 1. Samples and reagents were subjected to qPCR using the PikoReal PCR System (Thermo Fisher, St. Louis, MO).

Table 3.1 Primer Sequences and Product Sizes for Quantitative Reverse Transcription-Polymerase Chain Reaction

Gene		5' DNA sequence 3'	Product Size (bp)
Collagen I	Forward	5' GTCACCCACCGACCAAGAAACC 3'	121
	Reverse	5' AAGTCCAGGCTGTCCAGGGATG 3'	
Collagen III	Forward	5' GCCAACGTCCACACCAAATT 3'	88
	Reverse	5' AACACGCAAGGCTGTGAGACT 3'	
IL-1β	Forward	5' TCCCCAGCCCTTTGTTGA 3'	91
	Reverse	5' TTAGAACCAAATGTGGCCGTG 3'	
IL-6	Forward	5' GGCACTGGCAGAAAACAACC 3'	85
	Reverse	5' GCAAGTCTCCTCATTGAATCC 3'	
IL-8	Forward	5' CTGGCCGTGGCTCTCTTG 3'	69
	Reverse	5' CCTTGGCAAAACTGCACCTT 3'	
NFκB-1	Forward	5' ATGTATGTGAAGGCCCATCC 3	105
	Reverse	5' TTGCTGGTCCCACATAGTTG 3'	
COX-2	Commercially Available	Qiagen QT00040586	
GAPDH	Forward	5' ACAACTTTGGTATCGTGGAA '3	458
	Reverse	5' AAATTCGTTGTCATACCAGG '3	

3.3.7 TGF-β Bioactivity

We employed a TGF-β reporter cell line to screen for anti-inflammatory effects of the proliferants. Transformed mink lung cells (TMLC), a kind gift from Dr. Daniel Rifkin in the

Department of Cell Biology at New York University, are cells that have been modified to produce luciferase under activation of a TGF-β-responsive plasminogen activator inhibitor-1 (PAI-1) promoter(60, 61). TMLC were seeded in triplicate at $8x10^3/cm^2$ and allowed to attach overnight in basic DMEM. Cells were then exposed to proliferants for 16 hours. At this point, the experiment was stopped and cells were washed with PBS, lysed, and then analyzed for luciferase activity using a standard luciferin substrate kit (Promega) and luminometer (Tecan).

3.3.8 Secretome analysis

Conditioned medium collected from HT cultures were analyzed for a panel of two soluble factors. ELISA kits for total TGF-β1 (Biolegend) and PGE2 (Cayman Chemical Co.) were obtained and utilized to assess levels of soluble protein secreted by HT after treatment with proliferants. Assays were performed in technical duplicate according to manufacturer's directions and absorbance was quantified using a Molecular Devices EMax microplate reader.

3.3.9 Statistical Analysis

All quantitative data is reported as mean±standard deviation. A two way ANOVA was performed with a Bonferroni's multiple comparison post-test to compare proliferant groups. A one-way ANOVA was employed for comparison of groups in the mRNA expression experiments (GraphPad Prism Software 5.0, La Jolla, CA, USA). Unless otherwise stated, differences were reported as statistically significant for *p*-values less than 0.05.

3.4 Results

3.4.1 Cellular metabolic activity

Utilizing hHT and hAT cell lines, we explored the effect of P2G and dextrose treatments on cell metabolic activity using PrestoBlue. For all time-points, the metabolic activity of hHT populations treated with P2G was significantly lower compared to populations treated with dextrose. The metabolic activity of hHT populations reached lowest levels after 12 hours for both proliferant groups. Additionally, hAT populations exhibited lower metabolic activity when treated with P2G. Furthermore, after 24 hours hAT populations showed no signs of recovery after treatment with P2G (Figure 3.1).

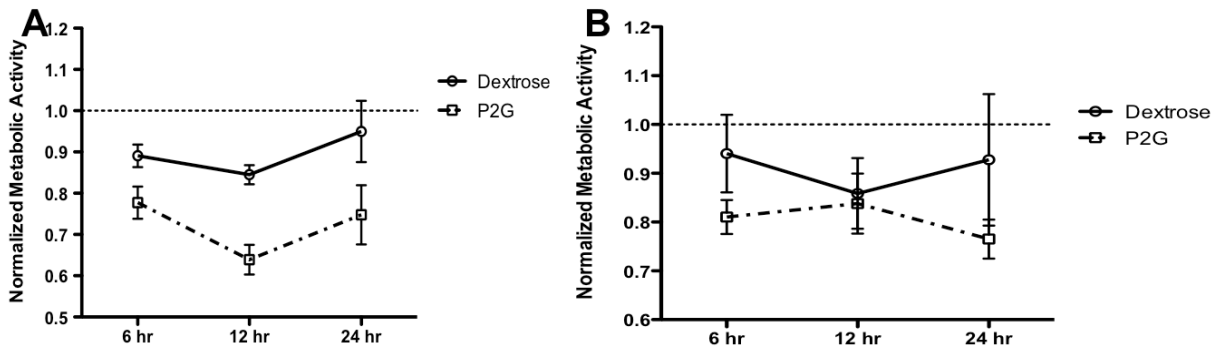

Figure 3.1 Prolotherapy induces decreased metabolic activity in tenocytes. Normalized cell metabolic activity of (A) hHT and (B) hAT during 24 hours of treatment with proliferants. Fluorescent values normalized to non-treated control populations.

3.4.2 Scratch Wound Healing Assay

The tenocyte scratch wound healing assay showed P2G to have a greater effect inhibiting cellular migration when compared to dextrose. After 24 hours, cell populations treated with dextrose began to reclose the wound. On the contrary, cells treated with P2G showed less cell migration and even experienced an increase in the size of the wound. Additionally, after 6 hours

of treatment with both proliferants, cell populations experienced significant decreases ($p<0.01$) in average cell migration rate (Figure 3.2C).

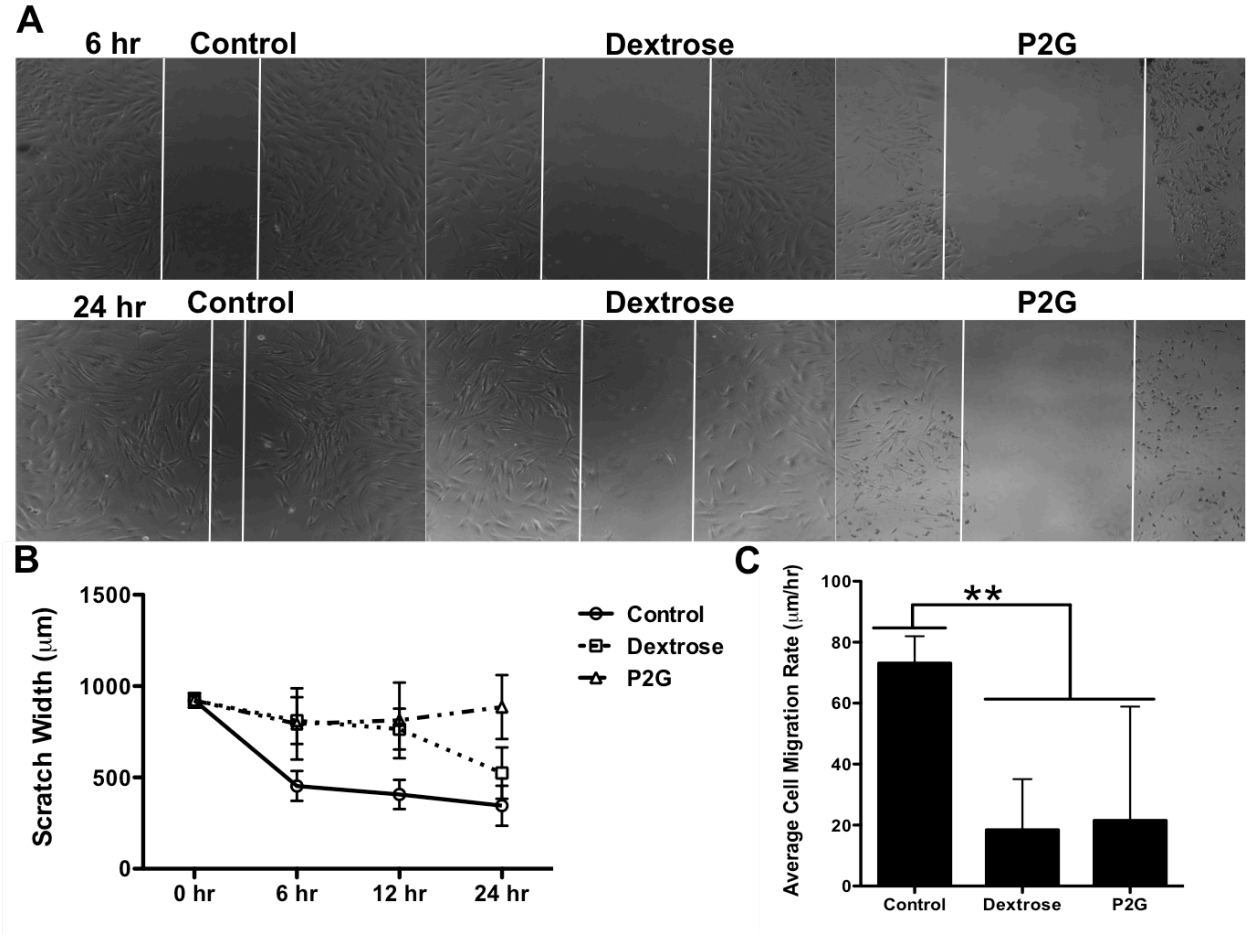

Figure 3.2 Prolotherapy decreases cellular migration in hAT. (A) Brightfield imaging of hAT during wound closure (white vertical lines) during treatment with proliferants. (B) Effect of proliferants on scratch width. (C) Effect of proliferant on average cell migration rate (**$p<0.01$).

3.4.3 mRNA Expression

After 6 hours of treatment with proliferants, hHT and hAT were evaluated for the mRNA expression of a panel of markers relative to tendon health related to wound healing. Results showed that in hHT, dextrose induced significant decreases in mRNA expression of collagen type I, IL-8, and NFκB-1. Similary, P2G treatment led to decreased transcripts of collagen type I. Furthermore, P2G treatment was found to increase the mRNA expression of COX-2 and IL-8 (Figure 3.3A). In hAT populations, dextrose caused a decrease in mRNA expression of collagen types I, III, and NFκB-1. P2G also caused decreases in the expression of collagen type I and NFκB-1. Additionally, there was an upregulation of COX-2, IL-6, and IL-8 after treatment with dextrose while P2G upregulated COX-2 and IL-8 (Figure 3.3B).

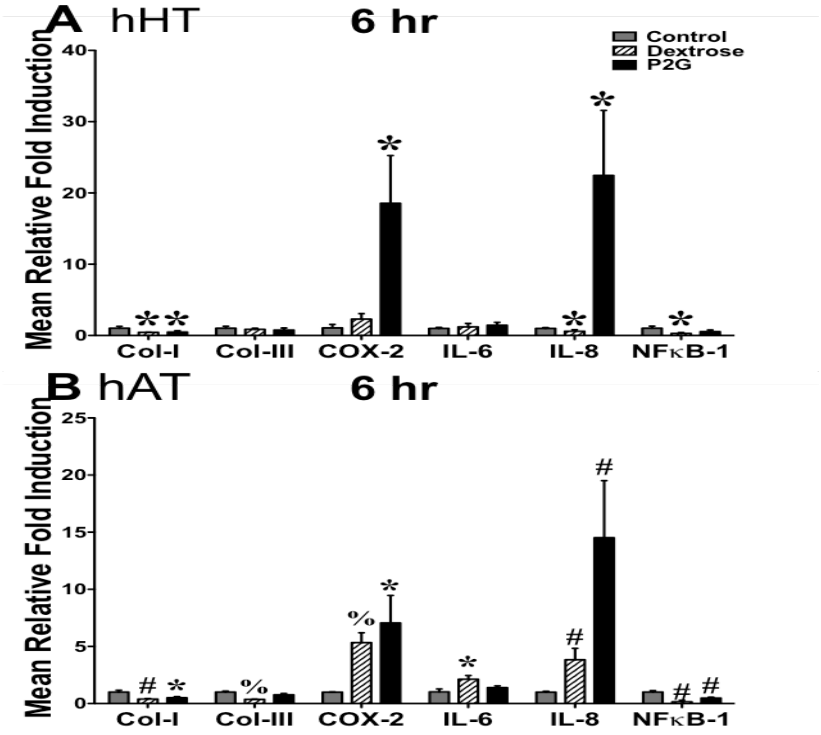

Figure 3.3 Prolotherapy induces decreased mRNA expression of growth-related markers and elevated expression of inflammatory markers. (A) hHT and (B) hAT mRNA expression after six hours of proliferant exposure (*p<0.05, #p<0.01, %p<0.001).

3.4.4 TGF-β Bioactivity

TGF-β bioactivity of the proliferants was evaluated using a TGF-β reporter cell line. After 16 hours, both proliferants induced decreased bioactivity after treatment. More specifically, P2G-treated TMLC exhibited the lowest TGF-β bioactivity in comparison to control cells and dextrose-treated populations (Figure 3.4).

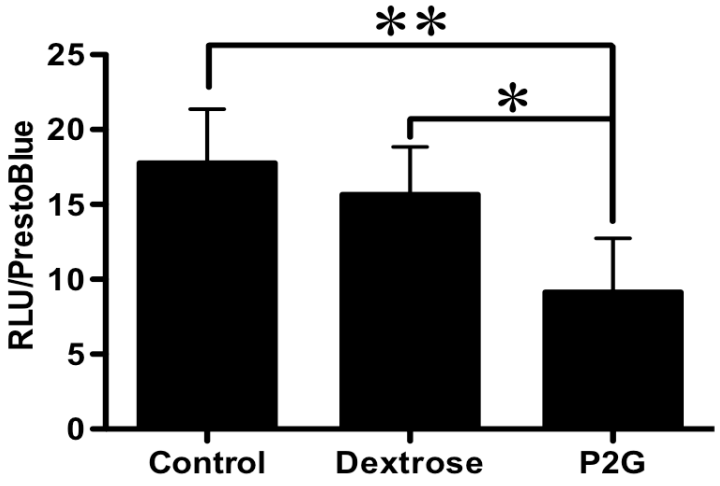

Figure 3.4 Normalized TGF-β bioactivity of TMLC after 16-hour treatment with proliferants (*p<0.05, **p<0.01).

3.4.5 Secretome Analysis

Conditioned medium was collected from proliferant-treated hHT populations after 24 hours of treatment and the samples were assessed for soluble protein concentrations of TGF-β1 and PGE2 using ELISA. After assessment of total TGF-β1 results showed a trend of decreasing

protein levels after treatment with proliferants, with P2G eliciting the lowest amount of TGFβ1 compared to the control cells (Figure 3.5A). Also, protein levels of PGE2 showed that P2G treated hHT produced significantly higher ($p<0.01$) levels of protein compared to dextrose treated and control hHT populations (Figure 3.5B).

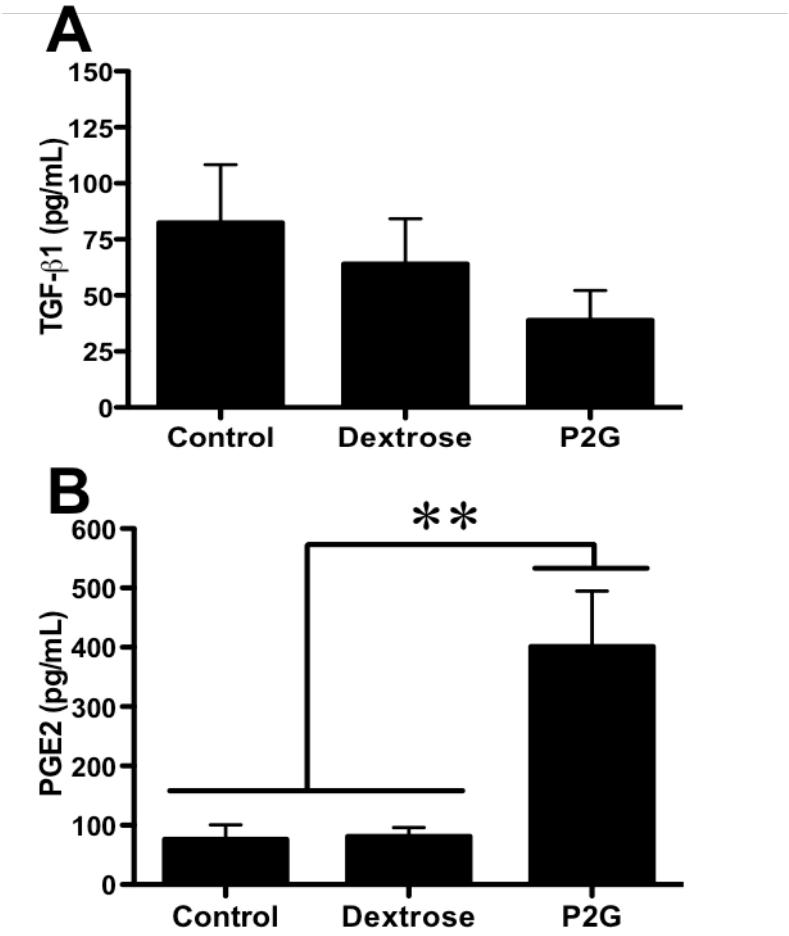

Figure 3.5 Proliferants induce elevated PGE2 secretion and decresase TGF-β1 secretion. (A) Total TGF-β1 and (B) PGE2 secretion from HT after I day of treatment with proliferants (**$p<0.01$).

3.5 Discussion

The goal of the current study was to elucidate the immediate response of prolotherapy at the cellular level by comparing the effect of two commonly used proliferant drugs, dextrose and P2G, on human tenocytes. To the best of our knowledge, this is the first study directly assessing the *in vitro* response of these two commonly administered proliferants in human tenocytes. Although various molecules have been utilized as proliferants for prolotherapy, the theory behind the modality suggests that they all should be effective in eliciting a localized inflammatory response in the target tissue. Proliferant drugs are classified into three categories: irritants, osmotics, and chemotactics. Each class is named after the suggested mechanism of action for initiating the localized inflammatory response (59, 62). Dextrose is considered an osmotic that functions via the dehydration and subsequent necrosis of cells after injection. The most active ingredient in P2G, phenol, works as an irritant which oxidizes into quinine groups leading to cellular damage. Both molecules ultimately result in cell death that initiates the body's wound healing cascade.

Previous work involving the utility of proliferant molecules *in vitro* for orthopedic applications is very limited and available studies span several different applications. Investigations involving dextrose have explored elevated levels in the study of diabetic conditions and effect on various cell responses. In a study with human mesangial cells, Clarkson and colleagues showed that elevated extracellular glucose levels led to the differential expression of 200 genes that were primarily involved in the regulation of extracellular matrix production, cell growth, and cell cytoskeletal maintenance (63). Additionally, in a study of elevated glucose levels on the effect of human renal fibroblasts, Lam and coworkers showed that connective tissue growth factor (CTGF) and insulin-like growth factor (IGF-I) were heavily implicated in glucose-

induced collagen deposition during fibrosis (64). Also, Pedersen *et al* showed that elevated phenol levels exhibited significant cytotoxicity in human colonic epithelial cells (65).

Utilizing a primary and an immortalized line of human tenocytes, we investigated the effect of the proliferants on cell metabolic activity. In agreement with the central hypothesis behind prolotherapy, both proliferants resulted in decreased cell activity levels during treatment. Results showed that P2G induced much lower cell activity than dextrose at every timepoint assesed for the hHT (Figure 3.1A). A similar trend was seen for hAT at 6 and 24 hours of treatment (Figure 3.1B). In the scratch assay wound healing model, we attempted to elucidate the effect of the proliferants on the cellular migration of hAT. Results showed that both dextrose and P2G, but most notably P2G, induced decreased cellular migration in hAT during 24 hours of treatment (Figure 3.2). Interestingly, it appeared that cell populations treated with dextrose started to show some recovery by beginning to close the gap at the 24-hour time-point. The wound healing assay is a common model to study cellular migration (66, 67). In this system, we utilized it to study the effect of the proliferants on disrupting the migratory capabilities in our cell model, hence another critical assay for effect of proliferants on cell function.

Gene expresssion analysis of both hHT and hAT at 6 hours of treatment showed that both proliferants did not increase the mRNA expression of growth and matrix-related markers including collagen types I and III. Instead, both treatments resulted in significantly decreased mRNA transcripts of both genes in hAT and only decreased collagen I mRNA in hHT. Furthermore, expression analysis of a panel of pro-inflammatory markers showed that P2G signigicantly induced elevated mRNA transcripts of COX-2 (also known as prostaglandin-endoperoxide synthase 2 or PTGS-2) and interleukin-8 or IL-8. Additionally, a similar trend was seen in hAT with P2G treatments significantly elevating COX-2 and IL-8 transcripts. Dextrose

treatments induced decreased expression of IL-8 and NFκB-1 in hHT. There was also significantly elevated mRNA expression of COX-2, IL-6, and IL-8 after dextrose treatment of hAT. These results suggest that prolotherapy with dextrose and P2G, most notably P2G, induced elevated mRNA expresssion of certain pro-inflammatory markers, especially COX-2 and IL-8.

COX-2 has been implicated in many pro-inflammatory responses seen in tendon pathology and wound repair (68, 69). Additionally, it is recognized as the precursor to and involved in the production of prostaglandin E_2 or PGE2, a potent inducer and mediator of tissue inflammation (70). Additionally, TGF-β has been implicated in the development of several muscuskeletal tissues and is a well-known anti-inflammory factor (71, 72). Utilizing a reporter cell line to screen for TGF-β bioactivity, we saw that both dextrose and P2G significantly decreased TGF-β bioactivity after 24 hours of treatment (Figure 4A). This result, in addition to results obtained from the gene expression studies, motivated the secretome analysis of conditioned medium from proliferant-treated hHT cultures. Using ELISA to measure soluble protein levels of TGF-β1 and PGE2, we saw a trend of decreaed protein levels of TGF-β1 after treatment with proliferants (3.4B). Furthermore, results showed a significant rise in PGE2 levels after treatment with P2G (Figure 3.4C). It is hypothesized that prolotherapy induces cellular death and the subsequent release of pro-inflammatory and chemotactic factors which initiate the body's wound healing cascade (13, 16, 45). Results from our experiments directly support aspects of this theory, however more work is needed to further determine the clinical effectiveness of prolotherapy.

The results from our experiments showed that human tenocytes treated with dextrose and P2G experienced considerable decreases in cellular activity. Furthermore, we showed that both proliferants, most notably P2G, lead to significantly decreased cellular migration. Moreover,

gene expression studies confirmed the up-regulation of pro-inflammatory markers COX-2 and IL-8, while the growth-related markers collagen type I was down-regulated. Screening with a reporter cell line confirmed a strong decrease in TGF-β bioactivity after treatment with both proliferants. Lastly, we showed that both proliferants led to decreases in total TGF-β1 secretion and a strong increase in PGE2 secretion after treatment with P2G. These findings support the theory behind the mechanism of prolotherapy, with P2G proving to be a more potent inducer of inflammation *in vitro*.

Acknowledgements

The authors gratefully acknowledge financial support from NSF CBET 1243144 and NSF CBET 1034026.

Chapter 4. Cross-talk between human tenocytes and bone marrow stromal cells potentiates extracellular matrix remodeling *in vitro*

Manuscript submitted to the Journal of Cellular Biochemistry

4.1 Abstract

Tendon and ligament (T/L) pathologies account for a significant portion of musculoskeletal injuries and disorders. Tissue engineering has emerged as a promising solution in the regeneration of both tissues. Specifically, the use of multipotent human mesenchymal stromal cells (hMSC) has shown great promise to serve as both a suitable cell source for tenogenic regeneration and a source of trophic factors to induce tenogenesis. Using three donor sets, we investigated the bidirectional paracrine tenogenic response between human hamstring tenocytes (HT) and bone marrow-derived hMSC. Cell metabolic assays showed that neither cell type experienced significant increases in proliferation during co-culture. Histological staining confirmed that co-culture specifically induced collagen protein levels in both cell types at varying time-points. Gene expression analysis using qPCR showed up-regulation of anabolic and catabolic markers involved in extracellular matrix maintenance for hMSC and HT. Furthermore, analysis of hMSC/HT co-culture secretome using a reporter cell line for TGF-β, a potent inducer of tenogenesis, showed high TGF-β bioactivity. Finally, we showed that the paracrine interaction of these two cell types potentiates matrix remodeling/turnover, which may be attributed to TGF-β signaling. These results have significant implications in the clinical use of hMSC for common T/L pathologies.

4.2 Introduction

Musculoskeletal injuries are a significant problem for the healthcare system. In the United States, there are approximately 32 million musculoskeletal injuries per year costing $950 billion in direct costs and lost wages with tendon and ligament (T/L) injuries accounting for about 45% of these injuries (7, 17, 73, 74). T/L are dense collagenous tissues involved in joint stability and locomotion. Ligaments are responsible for the structural support necessary to connect bones and stabilize joints, while tendons transfer the force generated from muscles into limb movement. Both tissues are composed of fibroblast cells embedded within an extracellular matrix (ECM) of collagens, elastin, and proteoglycans. They are hierarchical in architecture given that they operate primarily in tension. Injury due to trauma or genetic disorder often leads to varying degrees of change in the expression patterns of key structural proteins, tissue cellularity, disorganization of the collagen matrix, and inflammation (50, 52). Conventional methods of repair for the sub-failure (grades I, II) class of injuries include rest, ice, compression, and elevation or RICE (15), which is contingent on the innate healing ability of the tissue. In severe cases such as ruptures and avulsions (grade III), surgical reconstruction may be required (4, 14, 15, 17). However due to the lack of sufficient vascularization and poor ECM remodeling, tissue healing is often lengthy and incomplete. As a result of the associated drawbacks with current treatment options, there is a need for functional tendon healing modalities.

Tissue engineering (TE) has emerged as a promising option for tendon repair. Biomaterials and cells, used individually or in combination, have shown the potential to repair numerous T/L dysfunctions *in vitro* and *in vivo* (75-80). More specifically, the use of multipotent mesenchymal stem or stromal cells (MSC) as a cell source has proven to be a feasible modality for scaffold incorporation or direct injection. Recent *in vitro* and *in vivo* work has shown that localized MSC delivery may be beneficial for T/L repair by increasing cell

number, enhancing ECM deposition and maturation, and increasing tissue biomechanical properties after injury (20, 75, 81-83). This has led to work identifying MSC as both a suitable cell source for TE-inspired tenogenic regeneration and a potential source for the secretion of a plethora of soluble factors that mediate the healing response (30, 31, 84, 85). To this end, studies have identified several soluble factors as potential mediators in the enhancement of tenogenesis in both MSC and T/L fibroblasts (80, 86). Amongst these factors, transforming growth factor-beta or TGF-β has been widely reported to be a potent inducer of tenogenic regeneration (20, 27).

Proteins of the TGF-β superfamily are considered pleiotropic cytokines that play a prominent role during wound healing and musculoskeletal tissue development (71, 72). More specifically, during T/L development, TGF-β has been reported to be a key mediator of a panel of genes that are responsible for the anabolic and catabolic maintenance of ECM *in vitro* and *in vivo* (87, 88). Molecular changes evidenced in the altered expression of anabolic markers such as collagens and proteoglycans are known to accompany the healing of T/L (89). Additionally, changes in the expression patterns of catabolic markers such as the collagen-degrading MMP family (matrix metalloproteinases) and proteoglycan-cleaving ADAMTS family (a disintegrin and metalloproteinase with thrombospondin motifs) have also been reported (41, 89-92). The balance between the regulation and production of these markers has significant implications in the extent of matrix remodeling during regeneration (40, 41).

The objective of this study was to determine the effect of the paracrine signaling, or cross-talk, between primary human hamstring tenocytes (HT) and hMSC on the expression of T/L markers in both cell types *in vitro*. We hypothesize that the co-culture of hMSC with HT will lead to enhanced tenogenic cell function when compared to populations cultured separately.

We postulate that this exchange of soluble factors will facilitate the maintenance of ECM produced by both cell types, ultimately leading to enhanced tenogenic regeneration *in vivo*. To test this hypothesis, we employed an indirect cell co-culture model to investigate the effects of co-culture on cell metabolic activity, ECM production, and gene expression of anabolic and catabolic tenogenic markers. Additionally, we indirectly investigated TGF-β bioactivity in the secretome of each cell type and during co-culture via a TGF-β reporter bioassay. Lastly, we directly assayed for the effect of hMSC secretome on tenocyte morphology via immunostaining.

4.3 Materials and Methods

4.3.1 Tissue harvest, cell isolation, and hMSC characterization

The experimental overview summarizing the experimental design and all cell and secretome analyses conducted is presented in Figure 4.1. All experiments were conducted in accordance with recommendations and approval from the Medical Ethical Research Committee at the Utrecht Medical Center and MST Twente. Following standard written informed consent, hamstring tendon (HT) samples were harvested from 3 adult patients undergoing anterior cruciate ligament reconstruction. The tendons were isolated, rinsed with phosphate buffered saline (PBS), and excess muscle tissue was carefully removed prior to dissection and mincing into smaller pieces. Next, tendon pieces were cultured in growth medium of Dulbecco's modified Eagle's medium (PAA Laboratories, Australia) supplemented with 10% fetal bovine serum (FBS) (Lonza, Basel, Switzerland), 100 U/mL penicillin and 100 mg/mL streptomycin, and 0.2 mM ascorbic acid (Sigma Aldrich, St. Louis, MO) to allow the cells to migrate out from the tissue pieces.

Bone marrow aspirates were obtained from 3 additional adult patients following written informed consent. Donor set patient information for all patients is presented in Table 4.1. hMSC were isolated and cultured in hMSC basic medium consisting of alpha minimal essential medium (αMEM; Life Technologies, Carlsbad, CA) supplemented with 10% fetal bovine serum (FBS) (Lonza), 100 U/mL penicillin and 100 mg/mL streptomycin (Life Technologies), 2 mM L-Glutamine (Life Technologies), and 0.2 mM ascorbic acid (Sigma Aldrich), as previously described (66, 93). Phenotypical characterization of hMSC was performed as previously described (94). Briefly, $2x10^6$ mononuclear cells (MNC) from the aspirates were seeded in duplicate and allowed to attach in a T25 flask for three days. Afterwards, the bone marrow aspirate was washed away and the attached cells were cultured for a total of 14 days. The first 7 days in hMSC basic medium, then another 7 days in mineralization medium (consisting of hMSC basic medium, 1% β-glycerophosphate (βGP), and 10^{-8}M dexamethasone). After 2 weeks, the colonies were fixed using 10% formalin and stained for alkaline phosphatase (ALP) (Sigma) for 30 min and soon after with Crystal Violet staining (Sigma) for 10 min to analyze both the colony forming potential as well as the osteogenic differentiation potential of each individual colony. Images were acquired using an Epson Perfection V750 PRO scanner.

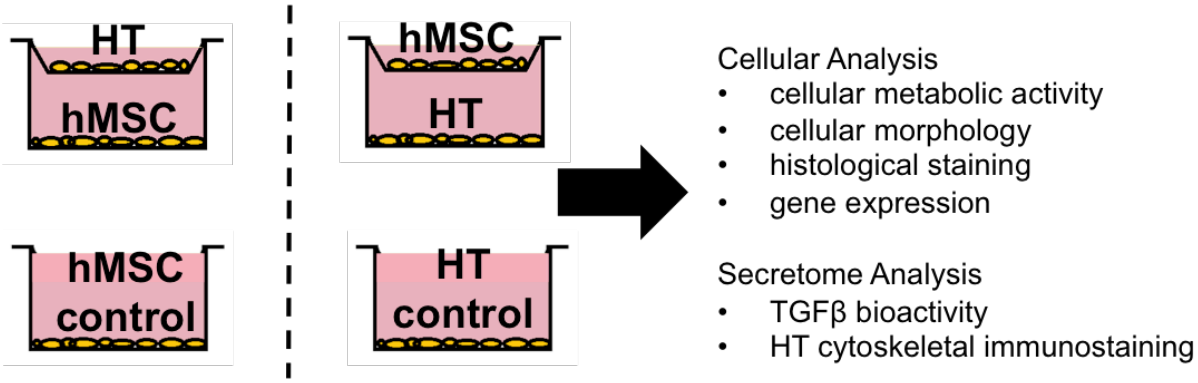

Figure 4.1 Experimental design overview schematic. Experimental design showing co-culture configuration and non co-culture control groups. Experiments were performed in biological triplicate.

Table 4.1 Donor Set Patient Information						
	Donor Set 1		Donor Set 2		Donor Set 3	
Cell Type	hMSC	HT	hMSC	HT	hMSC	HT
Gender	Female	Male	Male	Female	Male	Female
Age	67	25	72	24	52	21

4.3.2 Co-culture Condition

Cells between passage 2 and 5 were used for co-culture experiments and maintained for up to 14 days in a reduced factor medium containing 1% FBS and 1% P/S, without the addition of L-Glutamine or ascorbic acid. Indirect co-culture of hHT/hMSC was achieved using 1 μm pore sized permeable well plate inserts (Greiner Bio One, Kaysville, UT). In this system, $2.5x10^4$ HT (n=3) were seeded on the bottom of well-plates, hMSC were seeded on the permeable membrane at a 1:1 ratio and allowed to adhere overnight before placing the inserts in

the well-plates. The reverse configuration was also studied to determine the effect of co-culture on hMSC. Assays were conducted on the cells seeded on the bottom well and control groups consisted of each cell type seeded separately. After 3 days of co-culture, conditioned medium was collected for further analysis. For the first two donor sets, only half the cell culture medium was replaced 2-3 times per week to allow continuous cross-talk between cells and preserve the co-culture microenvironment. For the third donor set, culture medium was replaced with complete fresh medium after the first two time-points to further delineate the effects of preserving co-culture microenvironment on proliferation. For the first donor set, assays were conducted at 1, 3, and 7-day time-points to assess the earlier cell response between the two cell types. For the second and third donor sets, assays were conducted at 1, 3, 7, and 14-day time-points to also assess later cell responses.

4.3.3 Cellular Metabolic Activity

Cell metabolic activity (n=3) was evaluated as previously described (95) using the flurometric Presto Blue assay according to manufacturer's specifications. Briefly, at each time-point, the inserts were removed; medium aspirated and 10% (v/v) Presto Blue solution in basic medium was added. After a 1 hour-incubation the fluorescence was measured in technical duplicate using a Perkin Elmer Victor^3 1420 multilabel counter at 560 nm excitation and 590 nm emission wavelengths. Fluorescent values were normalized for no-cell blank control wells as well as the first time-point non-co-culture control group to represent proliferation over time.

4.3.4 ECM Deposition

To assess ECM deposition (n=3) at each time-point, we employed the semi-quantitative collagen/non-collagen staining assay as previously described (96, 97). In brief, medium was

discarded, cells were washed with PBS and stained using Sirius Red/Fast Green Collagen Staining Kit (Chondrex Inc. Redmond WA, USA). After performing the assay according to manufacturer's protocol, absorbance was read at 480 nm for Sirius Red and 605 nm for Fast Green with a spectrophotometer. Absorbance values for co-culture groups were normalized to control values.

4.3.5 Real-time quantitative reverse-transcription polymerase chain reaction (qPCR)

Expression of tenogenic markers in both cell types (n=3) was evaluated using qPCR as previously described (79, 98). Total RNA was isolated and purified by spin protocol using Bioke RNA II Nucleospin RNA isolation kit (Machery Nagel, Düren, Germany) according to manufacturer's protocol. Afterward, RNA concentrations were measured using a ND100 spectrophotometer (Nanodrop technologies, USA). Total RNA was normalized for all groups then reverse transcribed to obtain cDNA using iScript (BioRad, Hercules, CA, USA) according to the manufacturer's directions. The cDNA was subjected to qPCR using iQ SYBR Green Supermix (Biorad) on a Real-time PCR Detection System (BioRad). Specific primer sequences are listed in Table 4.2. Relative gene expression was calculated using the $\Delta\Delta C_T$ method, normalized to beta-2-microglobulin (B2M) as an endogenous control.

Table 4.2 Primer Sequences and Product Sizes for Quantitative Reverse Transcription-Polymerase Chain Reaction

Gene		5' DNA sequence 3'	Product Size (bp)
Collagen I	Forward	5' GTCACCCACCGACCAAGAAACC 3'	121
	Reverse	5' AAGTCCAGGCTGTCCAGGGATG 3'	
Collagen III	Forward	5' GCCAACGTCCACACCAAATT 3'	88
	Reverse	5' AACACGCAAGGCTGTGAGACT 3'	
Tenomodulin	Forward	5' TGTATTGGATCAATCCCACTCTAAT 3'	92
	Reverse	5' TTTTTCGTTGGCAGGAAAGT 3'	
Tenascin C	Forward	5' TGGGCAGATTTCACGGCTG 3'	207

	Reverse	5' TGCTCTGAGCCCGAATGTC 3'	
Aggrecan	Forward	5' AGGCAGCGTGATCCTTACC 3'	136
	Reverse	5' GGCCTCTCCAGTCTCATTCTC 3'	
TIMP-3	Forward	5' CCAGGACGCCTTCTGCAAC 3'	71
	Reverse	5' CCTCCTTTACCAGCTTCTTCCC 3'	
MMP-1	Forward	5' GGGAGATCATCGGGACAACTC 3'	72
	Reverse	5' GGGCCTGGTTGAAAAGCAT 3'	
MMP-3	Forward	5' TGGCATTCAGTCCCTCTATGG 3'	116
	Reverse	5' AGGACAAAGCAGGATCACAGTT 3'	
MMP-13	Forward	5' AAGGAGCATGGCGACTTCT 3'	72
	Reverse	5' TGGCCCAGGAGGAAAAGC 3'	
ADAMTS-4	Forward	5' CAAGGTCCCATGTGCAACGT 3'	115
	Reverse	5' CATCTGCCACCACCAGTGTCT 3'	
ADAMTS-5	Forward	5' TGGCTCACGAAATCGGACA 3'	74
	Reverse	5' GGAACCAAAGGTCTCTTCACAGA 3'	
B2M	Forward	5' GACTTGTCTTTCAGCAAGGA 3'	106
	Reverse	5' ACAAAGTCACATGGTTCACA 3'	

4.3.6 TGF-β Bioassay

Quantification of soluble-TGF-β bioactivity was determined for co-culture conditions using transformed mink lung cells (TMLC) that have been genetically modified to produce luciferase under control of the TGF-β -responsive plasminogen activator inhibitor-1 (PAI-1) promoter (60, 61). TMLC were a kind gift from Dr. Daniel Rifkin in the Department of Cell Biology at the New York University School of Medicine. TMLC ($8x10^3/cm^2$; n=3) were grown overnight before being exposed to the conditioned medium from co-culture experiments for one day. Cells cultured in 1% serum medium were utilized as basal controls. Afterwards, cells were lysed and luciferase activity was assessed by light production from a luciferin substrate (Promega) using a luminometer (Perkin Elmer).

4.3.7 Immunostaining

For cell morphology studies, all components utilized were from donor set 1. Here, HT were seeded at $5x10^5$ cells/cm^2 (n=4) on tissue culture plates and allowed to attach overnight. The next day, conditioned medium samples collected from hMSC and HT were analyzed for effect on HT for 24 hours. Control groups included basal conditions (1% FBS αMEM) and +10ng/mL TGF-β1. Afterwards, cells were washed with PBS and fixed with 4% paraformaldehyde solution. After permeabilizing with 0.1% Triton X-100/PBS and blocking with 2% BSA/PBS-Tween (0.1%), the cells were stained with Phalloidin flurophore (1:40). Afterward, the cells were washed with PBS and counterstained for DAPI. Images were obtained using a BD Pathway Bioimager.

4.3.8 Statistical Analysis

All numerical data reported as mean±standard deviation. A two-way ANOVA with a Bonferroni's multiple comparison post-hoc analysis was employed for comparing the various groups of cell populations for cell proliferation studies. A Student's t-test was employed for comparing groups in the mRNA expression studies (GraphPad Prism Software 5.0, La Jolla, CA, USA). Differences were considered statistically significant for *p*-values less than 0.05, unless otherwise stated.

4.4 Results

4.4.1 hMSC Characterization

We began by first characterizing the hMSC isolated after 14 days of expansion. Preliminary work with the hMSC used showed confirmation for self-renewal potential using a

CFU assay (Figure 4.2A) and osteogenic differentiation potential using ALP mineralization staining (Figure 4.2B).

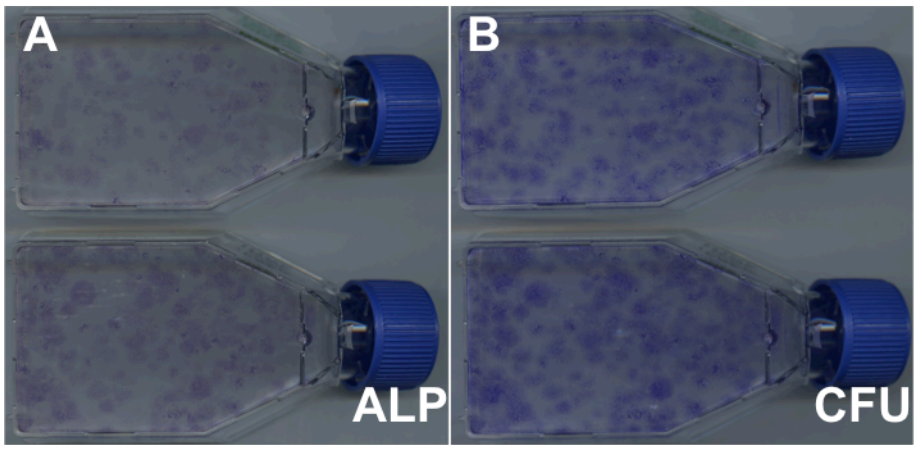

Figure 4.2 Representative images for hMSC characterization via (A) ALP staining for osteogenic mineralization potential and (B) crystal violet staining for CFU and self-renewal potential.

4.4.2 Effect of cross-talk on hMSC morphology, proliferation and ECM deposition

The goal of this study was to examine the effect of the paracrine interaction between hMSC and HT on the tenogenic cell function of both cell types. During co-culture, brightfield imaging of the hMSC after 3 days confirmed that there were no drastic differences between hMSC co-cultured with HT and control populations both in cell morphology and cell number (Figure 4.3A,B). Cell metabolic activity data obtained via the fluorometric Presto Blue assay showed that for each donor set, cell activity was never significantly increased, more so decreased, during co-culture with HT (Figure 4.3C). hMSC from donor set 2 were the only group to experience elevated proliferation after co-culture after 7 days, although not significant.

Furthermore, Sirius Red/Fast Green staining showed a significant increase in collagen to non-collagen protein ratio after 7 and 14 days in donor set 2 (Figure 4.3D).

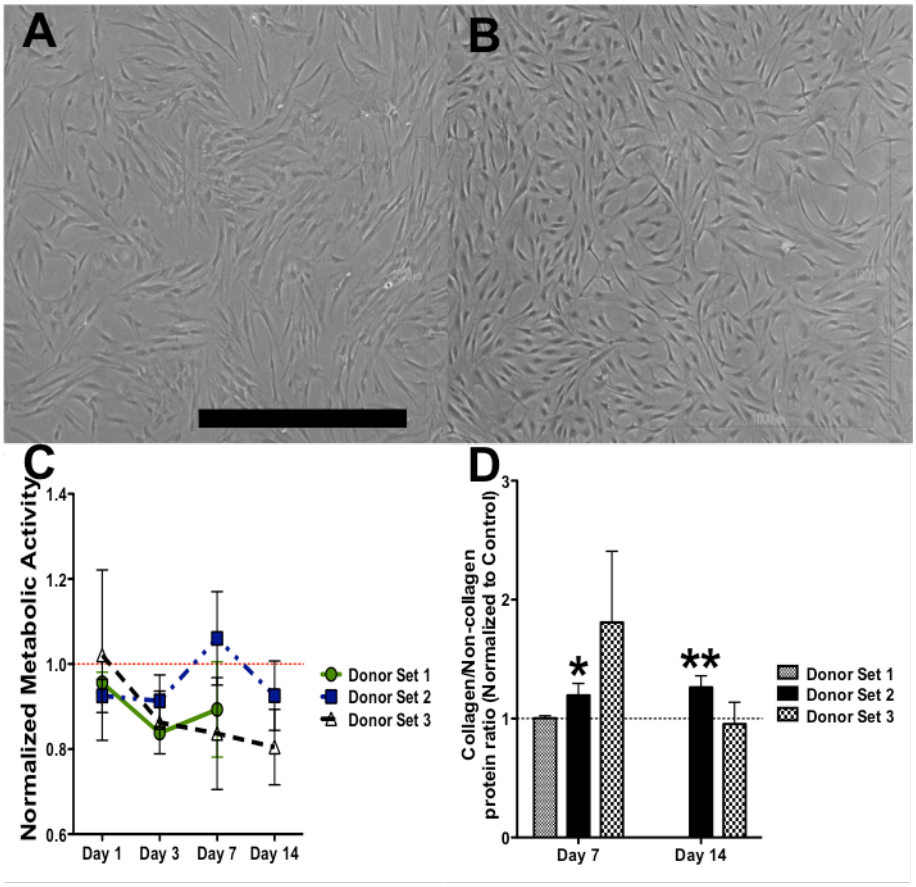

Figure 4.3 Effect of co-culture on hMSC cell function. Representative brightfield microscopy of (A) control hMSC and (B) hMSC during co-culture with HT after 3 days (scale bar = 1 mm). (C) Metabolic activity of hMSC during co-culture with HT normalized to non co-cultured control hMSC populations (dashed line at 1). (D) Sirius Red/Fast Green staining of hMSC during co-culture with HT normalized non co-cultured control hMSC populations (dashed line at 1) (*$p<0.05$, **$p<0.01$).

4.4.3 Effect of cross-talk on HT morphology, proliferation, and ECM deposition

Brightfield imaging of HT showed that after 3 days of co-culture with hMSC HT experienced no drastic differences in cell morphology or higher cell number (Figure 4.4A-B). Furthermore, cell activity data obtained via Presto Blue assay showed a general trend of decreased metabolic activity during co-culture except for the second donor set after 14 days. Additionally, there was a general trend of increasing cell activity with HT during co-culture after 3 days (Figure 4.4C). Lastly, Sirius Red/Fast Green staining showed that HT from donor sets 2 and 3 had elevated collagen to non-collagen protein levels during co-culture after 7 days. HT from donor set 3 maintained higher collagen/non-collagen levels after 14 days of co-culture with hMSC (Figure 4.4D).

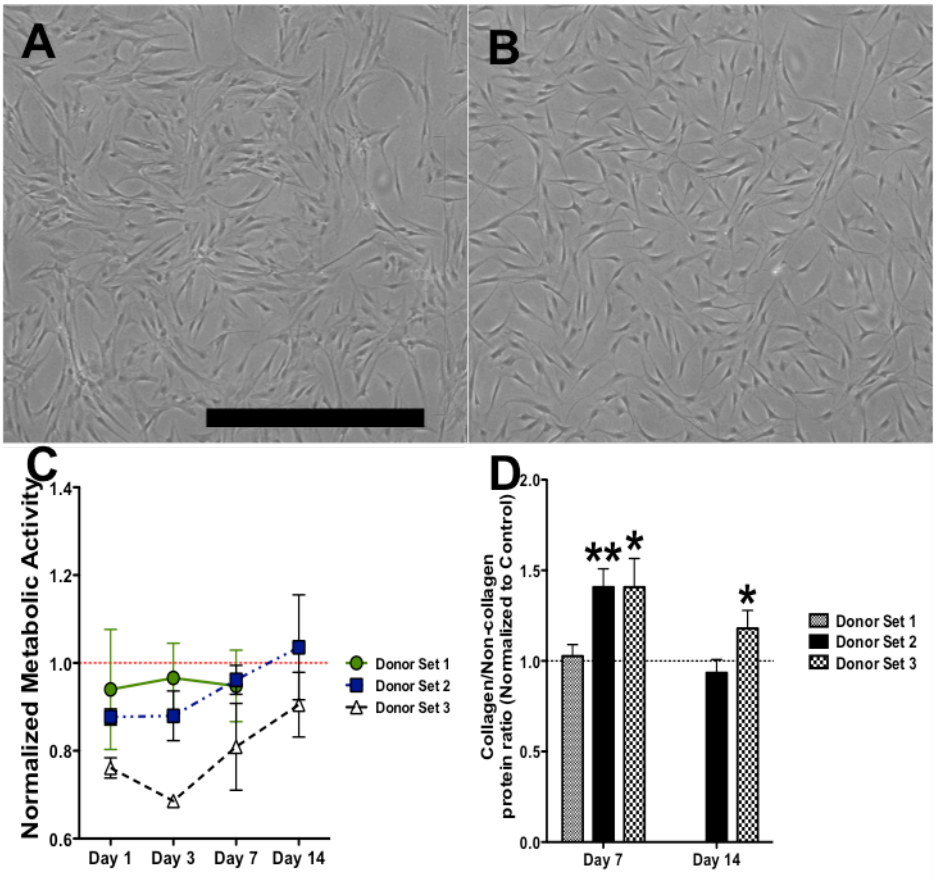

Figure 4.4 Effect of co-culture on HT cell function. Brightfield microscopy of (A) control HT and (B) HT during co-culture with hMSC after 3 days (scale bar = 1mm). (C) Metabolic activity of HT during co-culture with hMSC normalized to non co-cultured control HT populations (dashed line at 1). (D) Sirius Red/Fast Green staining of HT during co-culture with hMSC normalized to non co-cultured control HT populations (dashed line at 1) (*$p<0.05$, **$p<0.01$).

4.4.4 mRNA expression of tendon related markers

To further understand T/L matrix development during co-culture, we assessed a panel of anabolic markers that play critical roles in ECM development. Results of qPCR experiments are presented in Table 4.3. Analysis of mRNA expression of anabolic genes shows that in the first donor set, hMSC experienced significantly higher levels of Tenomodulin after co-culture at 3

and 7 days while HT exhibited up-regulation of Tenascin C during co-culture after 7 days. In the second donor set, HT experienced up-regulation of tissue inhibitor of metalloproteinase-3 (TIMP-3) during co-culture with MSC at 7 and 14 days. There was also an up-regulation of collagen type I at 14 days. In the third donor set, MSC experienced higher mRNA levels of Tenomodulin and Aggrecan during co-culture with HT at 7 and 14 days. HT exhibited up-regulation of Tenascin C and Tenomodulin after 7 and 14 days of co-culture with MSC (Table 3).

Next, we screened a panel of catabolic markers characteristic of T/L ECM development. Expression analysis of catabolic markers in the first donor set showed that MSC exhibited up-regulation of ADAMTS-5 at 7 days after co-culture with HT. In the second donor set, MSC showed up-regulation of MMP-1 and MMP-13 after 7 days of co-culture while the HT showed elevated mRNA levels of ADAMTS-4 at 7 days and all genes evaluated at 14 days after co-culture with hMSC. The third donor set showed that MSC had higher expression of ADAMTS-5 at 7 days of co-culture while HT experienced up-regulation of MMP-1 and MMP-13 after 7 days of co-culture (Table 4.3). Overall, our data indicates that in addition to affecting the expression patterns of anabolic markers, cross-talk between HT and MSC may also activate changes in the expression patterns of catabolic markers.

Table 4.3 Relative mRNA Expression of hMSC and HT during Co-culture

A. hMSC

	Donor Set 1		Donor Set 2		Donor Set 3	
Gene	Day 3	Day 7	Day 7	Day 14	Day 7	Day 14
Collagen I	1.1±0.24	1.6±0.27	1.1±0.21	0.9±0.48	1.0±0.19	0.7±0.16
Collagen III	1.7±0.66	1.4±0.49	1.0±0.17	1.5±0.32	0.9±0.12	1.0±0.32
Tenascin C	1.0±0.4	1.2±0.21	0.90±0.19	1.4±0.39	0.5±0.22	0.7±0.40

Tenomodulin	5.2±1.96*	4.9±2.0*	1.0±0.26	0.6±0.20	4.2±1.75*	2.2±0.20*
Aggrecan	1.4±0.25	2.5±0.72*	1.0±0.39	0.7±0.37	1.5±0.15*	3.8±1.13*
TIMP-3	0.9±0.21	1.5±0.38	1.4±0.22	0.8±0.32	0.8±0.05	0.9±0.16
MMP-1	1.4±0.16	1.0±0.45	2.6±0.11***	1.7±0.47	1.7±1.12	0.9±0.15
MMP-3	1.8±0.70	0.8±0.20	1.7±0.42	1.2±0.32	1.5±0.55	0.8±0.11
MMP-13	1.0±0.62	1.1±0.47	2.0±0.39*	0.5±0.34	0.8±0.14	0.8±0.14
ADAMTS-4	1.0±0.39	1.7±0.58	1.7±0.23	1.0±0.39	1.0±0.14	0.8±0.25
ADAMTS-5	1.7±0.85	3.0±1.21*	1.8±0.35*	1.1±0.39	1.6±0.29*	1.5±0.30

B. HT

	Donor Set 1		Donor Set 2		Donor Set 3	
Gene	Day 3	Day 7	Day 7	Day 14	Day 7	Day 14
Collagen I	1.19±0.25	1.39±0.52	1.33±0.44	3.95±1.49*	1.50±0.54	0.91±0.27
Collagen III	1.75±0.46	1.23±0.32	1.41±0.54	1.63±0.64*	1.51±0.08	1.07±0.64
Tenascin C	2.19±0.96	1.87±0.35*	0.95±0.41	1.89±1.18	2.09±0.84	2.05±0.35
Tenomodulin	ND	ND	ND	ND	1.39±0.90	2.80±1.52
Aggrecan	1.24±0.40	1.04±0.42	0.77±0.39	0.62±0.23	1.47±0.43	0.74±0.46
TIMP-3	1.85±1.12	0.95±0.20	2.06±0.43*	2.66±0.64*	2.27±0.82	0.74±0.30
MMP-1	0.65±0.62	1.11±0.08	1.16±0.20	3.72±0.77**	4.14±0.94*	0.61±0.30
MMP-3	1.37±0.92	1.14±0.14	1.90±0.22*	0.90±0.23	2.06±0.67	0.94±0.45
MMP-13	1.0±0.62	1.33±0.26	1.05±0.14	2.12±0.29**	3.16±0.98*	1.61±0.11
ADAMTS-4	2.53±0.94	1.43±0.21	1.61±0.19*	2.03±0.41*	2.47±1.01	0.98±0.42
ADAMTS-5	0.54±0.44	0.90±0.24	0.64±0.17	1.20±0.37	1.18±0.46	0.73±0.29

Transcript levels expressed as relative compared to non co-cultured control cell populations. Normalized to B2M (*$p<0.05$, **$p<0.01$).

4.4.5 Conditioned Medium TGF-β bioassay

Assuming that the cross-talk between the two cell types was predominantly responsible for the differences in cell response, we conducted a preliminary screen of the culture medium for soluble TGF-β bioactivity. After three days of co-culture, the conditioned medium was collected and analyzed for cell secretome effect on TGF-β bioactivity using a luciferase-producing reporter cell line. After 1 day of culture with the conditioned medium, TGF-β bioactivity was

significantly higher in MSC-conditioned medium for the first donor set (n=3). The second donor set showed higher TGF-β bioactivity in the co-culture media for both cell types when compared to MSC-conditioned medium (n=3). Lastly, the third donor set showed no significance in TGF-β bioactivity between treatment groups (Figure 4.5). Next, we used the conditioned medium from the first donor set to culture HT and analyzed the effects on cell morphology. Results showed that HT cultured in hMSC-conditioned medium appeared to be more elongated and have larger actin cytoskeletal staining when compared to other groups evaluated (Figure 4.6).

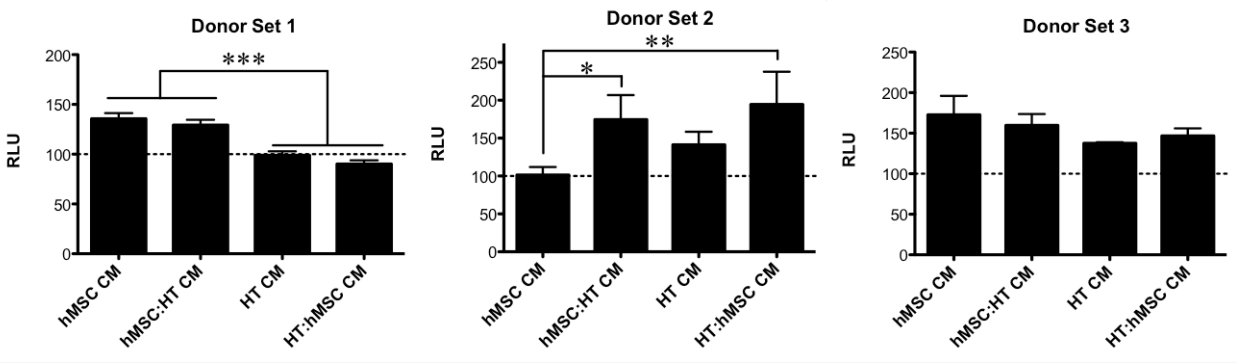

Figure 4.5 Relative TGF-β bioactivity after culture with co-culture derived conditioned medium normalized to cells cultured in basal conditions (dashed line). (*$p<0.05$, **$p<0.01$, ***$p<0.001$).

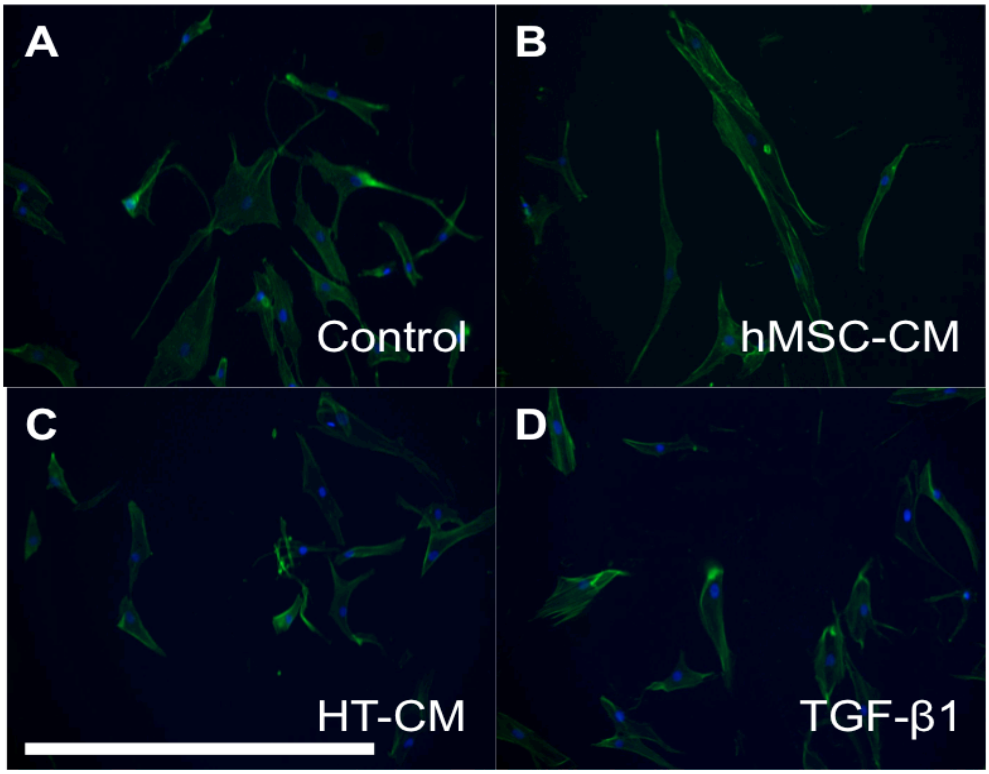

Figure 4.6 Immunofluorescent imaging of HT from donor set 1 fixed and stained for actin (green) and nuclei (blue). Cells were cultured under basal conditions (A), with hMSC-conditioned medium (B), HT-conditioned medium (C), and 10 ng/mL TGF-β1 (D) for 24 hours (scale bar = 500 μm).

4.5 Discussion

We investigated the effects of cross-talk between HT and hMSC on the cell response of both cell types. While the majority of the data sets between donors appeared consistent, these studies revealed some unexpected inter-donor variability. Previous work investigating this response between T/L cells and MSC has reported a noticeable enhancement of cell response evidenced in increased cellular proliferation, ECM deposition, and up-regulation of several tenogenic markers (80, 83, 84). Thus, we hypothesized that the indirect co-culture of the two

cell types would lead to an enhancement of tenogenic function in *both* cell types. To the best of our knowledge, this is the first study on the paracrine interaction between these two cell types across three unique sets of adult human donors. Initially, we observed differences amongst the donor sets in proliferation, ECM production, and mRNA expression. With this in mind, we aimed to consider trends common amongst donor sets.

Results from the co-culture experiments showed that there was no increase in the cell proliferation of either cell type at any time-point evaluated (Figure 4.3C, 4.4C). This observation differed from similar studies conducted with rat tissue. Luo and colleagues showed that after 3 days of co-culturing with tenocytes, rat MSC experienced elevated metabolic activity (83). Similarly, Shimode *et al* observed significant increases in cell number of Achilles tendon tenocytes after co-culture with bone marrow-derived MSC (84). To our knowledge, our present study with a human derived model, is the first to report no enhancement, and even a decrease at some time-points, in the cell activity of these co-cultured cell types. One explanation could be species difference, or more specific, could be that there was a higher total number of cells/mL of culture medium in the co-culture groups compared to the control groups (as performed by Luo and colleagues (83)). This difference in cell number could lead to a faster consumption of serum components, hindering cell proliferation.

We then analyzed the matrix produced by the cells during co-culture (Figure 4.3D, 4.4D). According to our data, in two donor sets (n=6), there was an increase in the collagen/non-collagen ratio of the ECM deposited by each cell type. The increase in collagen is a notable result because it is the most abundant protein in T/L (1, 99). Increases in the amount of collagen deposited may accelerate the functional recovery upon cell transplantation. Although we saw no enhancement in cell metabolic activity, the cross-talk between HT and hMSC may have instead

induced more matrix production in both cell types. It is also likely that there are factors, such as TGF-β, being released that may be inhibiting cell proliferation while concurrently inducing higher ECM production (71).

The expression analysis showed, for both cell types, an up-regulation of several anabolic and catabolic markers prevalent in T/L cells (Table 4.3). For the anabolic markers assessed, Tenomodulin was up-regulated in hMSC in the presence of HT for the two donors that mRNA for Tenomodulin was detected for. Tenomodulin has been described as a late stage tenogenic marker during tendon development and is often used as a marker to indicate tenogenesis (100-102). This data supports the notion that factors released from HT have the potential to induce tenogenesis in undifferentiated hMSC (21, 83). For HT, there was an observed up-regulation of markers including collagen type I and TIMP-3 in one donor set and Tenomodulin in another set. All of these markers have been well documented as tenogenic markers involved with matrix development and assembly. Markers including collagen type I, Tenomodulin, and Tenascin C are known to be directly involved in the anabolic maintenance of T/L ECM. TIMP-3 belongs to a family of proteinases that have specificity for members of the MMP family and inhibit MMP activity (21, 76). The balance or imbalance between MMPs and TIMPs strongly influences matrix remodeling (103). Therefore, this data indicates that co-culture may activate changes in the mRNA expression patterns of markers involved with the anabolic maintenance of T/L ECM.

Analysis of catabolic markers showed that hMSC co-cultured with HT experienced significant up-regulation of ADAMTS-5, MMP-1, and MMP-13. Also, HT co-cultured with hMSC experienced significant up-regulation of MMP-1, MMP-13, and ADAMTS-4. Previous *in vitro* and *in vivo* work on the ADAMTS and MMP family showed that tenocyte mechanotransduction (89, 92) and growth factors such as TGF-β, TNF-α, IL-1α, and IL-1β had

significant effects on catabolic activity (52, 90, 91). In addition to the up-regulation of anabolic markers, the co-culture induces up-regulation of several catabolic markers thus signifying increased matrix turnover and remodeling. It is possible that the matrix remodeling induced during co-culture could lead to a more mature collagen matrix and ultimately the enhancement of overall tissue biomechanics *in vivo*.

The mRNA expression data showed significant differences between control and treatment groups for several markers described above that are often referred to as TGF-β-target genes. Due to these findings, we performed a preliminary screen for TGF-β bioactivity in the secretome of the co-culture conditions using a TGF-β reporter cell line (Figure 4.5). Results showed that in direct comparison, TGF-β bioactivity was higher in the hMSC groups in the first donor set (n=3). The second donor set showed TGF-β bioactivity to be higher in the co-culture groups of both cell types. These results suggest that hMSC may be able to secrete higher amounts of TGF-β or lower amounts of inhibitors of TGF-β activity. Next, we aimed to explore the effect of hMSC secretome directly on HT cell morphology (Figure 4.6). After 24 hours of culture with conditioned medium from hMSC, HT appeared to have a more elongated morphology when compared to HT conditioned medium and soluble TGF-β1, a hallmark of tenogenic differentiation. This is notable because hMSC have recently been shown to have secretomes that are rich in both immunomodulatory and trophic factors (30, 31, 104). The soluble factors released from the hMSC may be responsible for the favorable response in cell morphology evidenced by the HT. These data suggest that cross-talk between the two cell types may synergistically potentiate an increase in TGF-β signaling for both cell types and that hMSC secretome may have favorable effects on tenocyte cellular morphology. On-going studies are

further examining this trend and identifying other active components involved during cross-talk between the two cell types.

The "training" or pre-differentiation of MSCs before transplantation has been discussed as a method of increasing their therapeutic efficacy and perhaps further control their *in vivo* response (66, 104). The results obtained in our studies suggest that the secretome of hMSC in their undifferentiated state can also be harnessed to potentiate ECM turnover in the target tissue. Also, given that a cell's microenvironment can modulate its secretome, further investigation into the effect of pre-differentiated MSC secretome on the tissue healing response is warranted. On-going studies are exploring these effects *in vitro*. Furthermore, the *in vivo* response of the paracrine interaction between these two cell types will be investigated using a small animal model. The effect of the therapy will be evaluated using biomechanical tissue testing and imaging techniques such as immunohistochemistry and magnetic resonance imaging.

In conclusion, the results from these studies suggest that the paracrine interaction between adult human tenocytes and hMSC induces changes in the cellular response of both cell types. Clearly there may be major differences between rat and human systems, considering human variation and age of injury/surgical repair. Here we show most notably that soluble factors were exchanged and were shown to stimulate higher collagen/non-collagen production by both cell types in two donor sets. Additionally, mRNA expression analysis showed strong changes in the expression patterns of prominent anabolic and catabolic markers of T/L ECM. Lastly, a preliminary screen of the individual and co-culture secretome of both cell types showed that the MSC secretome possessed higher TGF-β bioactivity. This work provides insight into the paracrine effect of the relationship between tenocytes and MSC on T/L ECM maintenance and explores TGF-β as a potential mediator of this response. We aim to use this cell model to begin

to explore possible therapeutic interventions as a method to enhance tenogenic regeneration *in vivo*.

Acknowledgements

The authors gratefully acknowledge financial support from NSF CBET 1243144 and NSF DGE 0801620, Integrative Graduate Education and Research Traineeship (IGERT) on the Integrated Science and Engineering of Stem Cells.

Chapter 5. Single-walled carbon nanohorns modulate tendon biomechanics and tenocyte cellular response

Manuscript in preparation to be submitted to Advanced Functional Materials

5.1 Abstract

Sub-failure ligament and tendon injury remains a significant burden to global healthcare. Due to tissue composition, structure, and function, healing is slow and usually incomplete. After injury, tissue biomechanics are compromised often leaving the tissue prone to re-injury. Current tissue engineering approaches have focused on the repair of severe damage (usually to failure) via the use of implantable constructs that aim to completely replace the damaged tissue. Here, we present the novel use of biocompatible single walled carbon nanohorns (CNH) in the repair of sub-failure injury in ligaments and tendons. Biomechanical tests with explanted porcine digitorum tendons showed the ability of CNH suspensions to modulate tendon biomechanics, most notably elastic moduli immediately after treatment. Next, *in vitro* tests showed that the immediate cell response of human tenocytes may be dependent on CNH aggregate size and particle endocytosis may mostly occur via clathrin-mediated mechanisms. Furthermore, prolonged *in vitro* exposure of CNH to tenocytes revealed no decrease in cell activity for up to 7 days, and no significant effect on collagen production. However, gene expression studies revealed significant down-regulation of collagen types I and III mRNA at 7 days with some recovery after 14 days of exposure. Also, *in vivo* experiments demonstrated the ability of CNH to alter stretch-injured Sprague Dawley rat Achilles tendon biomechanics and persist in the damaged extracellular matrix, most prominently at 7 days after treatment. Altogether, these

results show the feasibility and potential of the utility of CNH as a novel modality for sprain and strain injuries by directly affecting cellular response and damaged tissue biomechanics.

5.2 Introduction

Ligaments and tendons are strong connective tissues that are critical for the stability and locomotion of the body. They are also common sites of injury with over 32 million injuries totaling over 30 billion dollars annually in United States (2, 7, 73, 105). Both tissues primarily operate in tension with similar major constituents consisting of fibroblast-like cells embedded in a highly packed and aligned extracellular matrix (ECM) of collagens, elastin, and proteoglycans (1, 99). Due to their structure, composition, and function, they lack high vascularity; suggesting a reason for their inherent lack of a robust healing response after injury. Ligament and tendon pathologies are most often characterized by disruptions of the collagenous matrix that is 60-80% of the tissue dry weight (3, 42, 106). Natural repair is often hampered by lack of complete healing leaving the tissue prone to re-injury (8, 107). The repaired tissue is characterized by a disorganized matrix that leaves the tissue with inferior mechanical properties when compared to the native state (4).

Tissue engineering (TE) integrates the singular and combinatorial use of cells, scaffolds, nanoparticles, and small molecules to regenerate diseased or damaged tissues. Recently, TE has seen the emergence of investigations into alternative approaches for the repair of damaged ligaments and tendons via replacement with synthetic and composite scaffolds (108). Many TE approaches to tendon/ligament regeneration are limited by their application in the resolution of severe damage to the tissue. These injuries have extensive tearing or rupturing of the matrix, which require the complete replacement of the damaged native tissue. Although much progress

has been made with the use of TE approaches for complete ligament and tendon replacement, there is a need for alternative approaches for the functional repair of mild to moderate sub-failure injuries. Current treatment for sub-failure injuries include the use of conservative approaches such as rest, ice, compression, and elevation (or RICE) and drug therapy (with non-steroidal anti-inflammatory drugs or NSAIDs, corticosteroids, etc.) while severe cases often require surgical repair (16, 109).

Nanocarbons have been utilized in biomedicine for the creation of nanocomposite scaffolds to biomedical imaging and drug delivery (110-114). They are highly advantageous for such applications primarily due to their small size, high strength, relatively low toxicity, and functional capabilities (36, 37, 56, 115, 116). Recently we showed that damaged skin and tendon biomechanics could be modulated by treatment with high elastic modulus nanoparticles, most notably single-walled carbon nanohorns (CNH) (56). The injected CNH were able to recover the toe moduli of damaged skin and tendon matrices. Additionally, we showed that the CNH displayed no cytotoxic effects when cultured with rat patellar tendon tenocytes for up to 3 weeks *in vitro*. The goal of this current work was to further characterize the interaction of CNH with tendon matrix components. To this end, we evaluated the concentration dependent effect of CNH on intact ovine tendon biomechanics. Next, we assessed the effects of CNH aggregates on human tenocyte metabolic activity, ECM deposition and gene expression. Finally, we conducted a functional *in vivo* evaluation of CNH treatment using a stretch-injured rat Achilles tendon model.

5.3 Materials and Methods

All studies described were conducted in accordance and with approval from Rutgers Environmental Health and Safety Office, the Animal Care and Use Committee of Rutgers, The State University of New Jersey, and the Medical Ethical Research Committee at the Utrecht Medical Center.

5.3.1 CNH suspensions

CNH were a kind gift from Oak Ridge National Laboratory and synthesis was previously described by Geohegan and colleagues (117). Pluronic F-127 was purchased in solid form from Biotium, Inc. The pluronic is a commonly utilized nonionic surfactant to improve biomaterial solubility and has also been shown to be biocompatible (37). Pluronic was dissolved in deionized (DI) water to obtain a concentration of 1% (w/v). Afterward, dry CNH were weighed then added to the pluronic solution to obtain final concentrations of 0.2 and 1% (w/v). Suspensions used for *in vitro* cell studies and *in vivo* animal experiments were sterilized via autoclaving and exposure to UV light prior to use.

5.3.2 Ovine tendon mechanical tensile testing

The digitorum longus tendons of female sheep were used for the first mechanical testing model. Frozen sheep limbs were obtained from the Colorado State University Veterinary Teaching Hospital. Tendons were isolated and dissected from hind limbs, wrapped in PBS-soaked gauze, and stored at -20°C. The tendons were randomly placed into different groups. The first group consisted of intact-untreated control tendons. The next groups consisted of intact tendons treated with two concentrations (0.2% and 1% (w/v) in 1% (w/v) pluronic in DI water) of CNH injections. Another control group involved intact tendons treated with a phosphate buffered solution (PBS) sham injection to account for volumetric effects of the injections. For

mechanical testing, tendons were thawed in PBS and soaked for 30 minutes at room temperature. Next, tendon dimensions were measured using a Z-mike 1202 series laser micrometer (Beta LaserMike, Dayton, OH). Tensile testing was conducted using an Instron 4204 mechanical testing system (Instron Corp., Canton, MA). Tissue specimens were mounted using cryogenic freeze clamps (Enduratec, Eden Prairie, MN). Samples were allowed to freeze until 1 mm of tendon was visibly frozen on each end. With this setup, the gauge length was measured from one frozen end to the other. During testing, hydration was maintained using PBS. Tendons were pulled under uniaxial tension at a displacement rate of 0.1mm/sec until failure. For data analysis, the elastic modulus values were calculated from the linear regions of stress-strain curves.

5.3.3 CNH aggregate characterization

CNH aggregate sizes in cell culture medium were characterized prior to performing *in vitro* studies. Stock CNH suspensions were added to basic cell culture medium in well plates to obtain two lower concentrations (0.02 and 0.1% (w/v)) more suitable for cell studies. The medium consisted of α-MEM supplemented with 1% penicillin streptomycin (P/S) and 10% fetal bovine serum (FBS) (Life Technologies, Carlsbad, CA, USA). Afterward, well plates were imaged using a Leica DMI4000 microscope (Leica Microsystems, Inc., Buffalo Grove, IL). Aggregate sizes (n=27) in each group were quantified using NIH Image J software.

5.3.4 Cell culture and *in vitro* experimental design

After obtaining standard written informed consent, human hamstring tendon (hHT) samples were obtained from an adult patient receiving an anterior cruciate ligament reconstruction. The tendons were isolated, dissected, minced, and rinsed with phosphate buffered saline (PBS). Next, tendon pieces were cultured in a growth medium composed of

DMEM (PAA Laboratories, Austria) supplemented with 100U/mL/100µg/mL P/S, 10% FBS (Life Technologies), and 0.2mM ascorbic acid (Sigma Aldrich, St. Louis, MO). After migrating from tissue pieces, cells were collected and propagated. Primary cells between passages 2 and 4 were utilized for experiments. Immortalized human Achilles tendon tenocytes were obtained as a kind gift from Dr. Denitsa Docheva at the Walter Brendel Centre of Experimental Medicine at the Ludwig-Maximilian University of Munich. For experiments, both cell types were maintained in basic medium consisting of α-MEM supplemented with 1% P/S and 10% FBS (Life Technologies).

For *in vitro* experiments, cells were seeded (n=3) on tissue culture plates at a density of $5x10^3$ cells/cm^2 then allowed to attach overnight in an incubator at 37°C and 5% CO_2. The following day, cell culture medium was replaced and groups were treated with sterile stock CNH suspensions to obtain final concentrations of 0.02 and 0.1% (w/v). For immediate response studies, cell populations were evaluated for gene expression after 6 hours of CNH exposure. Cell populations were evaluated with the following assays at up to 14 days of culture for prolonged exposure studies. For cell feeding, only half of the culture medium was replaced with fresh medium 2-3 times a week.

5.3.5 Cellular metabolic activity

At designated timepoints, cell metabolic activity was evaluated (n=3) using PrestoBlue Assay (Life Technologies) as previously described (118). Briefly, the wells were emptied and the cells were incubated with 10% (v/v) PrestoBlue reagent in fresh basic medium and incubated for one hour. Afterward, fluorescence was measured in technical duplicate at 560nm excitation

and 590nm emission with a Tecan spectrophotometer (Mannedorf, Switzerland). Fluorescent values for experimental groups were normalized to control groups.

5.3.6 ECM Deposition

The deposition of collagenous and non-collagenous proteins by the primary tenocytes (n=3) in each group was assessed using Sirius Red/Fast Green staining as previously described (96, 119). At designated timepoints, the wells were emptied and the cell populations washed with fresh PBS. Afterward, the wells were stained using Sirius Red/Fast Green Collagen Staining Kit (Chondrex Inc., Redmond, WA) according to the manufacturer's protocol. Protein levels were quantified by measuring absorbance at 480nm for Sirius Red and 605nm for Fast Green using a Molecular Devices EMax spectrophotometer (Molecular Devices Inc., Sunnyvale, CA).

5.3.7 Real-time quantitative RT-PCR analysis (qPCR)

Gene expression for markers of the two main types of collagen (types I and III) found in tendon ECM and two proteins (clathrin and caveolin) possibly involved during cellular endocytosis of CNH aggregates was assessed using qPCR. Briefly, total RNA (n=3) was isolated from each group and purified with the RNeasy Mini Kit (Qiagen, Valencia, CA) according to the manufacturer's protocol. Isolated RNA was normalized for all groups then converted to cDNA using the Reverse Transcription System (Promega Corporation, Madison, WI). After reverse transcription, the cDNA was combined with SYBR Green PCR mastermix and primers for target genes and then polymerized using the PikoReal Real Time PCR System (Thermo Fisher Scientific Co., Waltham, MA). Specific primer sequences utilized for target

genes are presented in Table 5.1. Relative fold induction was calculated via the $\Delta\Delta C_T$ method and values were normalized with GAPDH as the endogenous control.

Table 5.1 Primer Sequences and Product Sizes for Quantitative Reverse Transcription-Polymerase Chain Reaction		
Gene		5' DNA sequence 3'
Collagen I	Forward	5' GTCACCCACCGACCAAGAAACC 3'
	Reverse	5' AAGTCCAGGCTGTCCAGGGATG 3'
Collagen III	Forward	5' GCCAACGTCCACACCAAATT 3'
	Reverse	5' AACACGCAAGGCTGTGAGACT 3'
CAV-1	Forward	5' ACAGCCCAGGGAAACCTC 3'
	Reverse	5' GATGGGAACGGTGTAGAGATG 3'
CLTC	Forward	5' GACAAAGGTGGATAAATTAGATGC 3'
	Reverse	5' TAAACAATGGGTTGTGTCTCTGTA 3'
GAPDH	Forward	5' ACAACTTTGGTATCGTGGAA '3
	Reverse	5' AAATTCGTTGTCATACCAGG '3

5.3.8 *In vivo* rat Achilles tendon stretch injury model

To assess the functional *in vivo* response of the CNH treatments, we utilized a sub-failure Achilles tendon stretch injury animal model previously developed by our group. A custom-made tendon stretch injury device was utilized to create consistent, reproducible stretch injuries in the Achilles tendons of rats. The Achilles tendon model was chosen because it is the largest tendon in the body and is also easily accessible in a small animal model. A total of 10 female Sprague-Dawley rats at 10 weeks of age were obtained from Taconic Farms (Taconic Biosciences, Hudson, NY), then housed and fed *ad libitum* for at least one week prior to beginning any experiments. Immediately before surgical procedures, general anesthesia was induced and maintained with isoflurane gas. The right hind limb of each rat was aseptically prepared and treated with Marcaine for local anesthesia. A 1-cm incision was made to expose the Achilles tendon. Afterward, the rat and its foot was stabilized with braces to ensure consistency for each procedure. Using the stretch injury device, a 2N preload was applied to the tendon mid-

substance before stretch injuring with 20N of force. Finally, after injuring, the foot was released and the skin above the tendon was apposed then reinforced with sterile surgical sutures. Animals were allowed to roam freely in cages for one week before treatments were administered. For treatments, rats were placed under anesthesia via isoflurane gas and 100 uL of sterile 0.2% (w/v) CNH suspension (n=4 per timepoint) or sterile PBS-sham (n=1) was injected into the damaged tendons. Afterwards, rats were returned to their cages and allowed to freely roam for up to 14 days post-treatment. After 7 and 14 days, rats were euthanized via CO_2 asphyxiation. The Achilles tendons from both hind limbs were carefully harvested and stored at -20°C until further testing. For all *in vivo* tests, each tendon was compared to its contralateral, uninjured control tendon.

5.3.9 Rat tendon mechanical tensile testing

Explanted rat tendons were mechanically tested using an MTS Tytron 250 mechanical testing machine (MTS Systems Corp., Eden Prairie, MN). Frozen tendon samples were allowed to thaw in PBS at room temperature for at least 30 minutes prior to testing. Measurements of sample dimensions were recorded immediately before testing. Uniaxial tensile testing was performed for each sample by using a pre-load of 0.2N of force, then stretching with a displacement rate of 0.1mm/sec until failure. For data analysis, the stress-strain curve was utilized to obtain a linear elastic modulus for each sample.

5.3.10 Histological analysis

After harvesting, tendons were fixed with 4% paraformaldehyde (PFA) overnight at 4°C prior to being sent for histological staining and analysis. Next, samples were paraffin embedded then stained with hematoxylin and eosin (H&E), Masson's trichrome, safranin-O, Verhoeff's

Von Giesen (VVG), and toluidine blue stains (AML Labs, Rosedale, MD). Histological slides were imaged using an EVOS light microscope (Life Technologies).

5.3.11 Statistical Analysis

All numerical data is presented as mean±standard deviation. A one-way ANOVA with a Bonferroni's multiple comparison post-test was utilized to compare the various groups. A two-way ANOVA with a Bonferroni's multiple comparison post-test was utilized to compare groups across several timepoints (GraphPad Prism Software 5.0, La Jolla, CA, USA). Unless otherwise stated, differences between groups were considered statistically significant for *p*-values less than 0.05.

5.4 Results

5.4.1 Porcine tendon mechanical testing

We began by assessing the effect of CNH treatments on intact ovine digit tendon mechanical properties. Results showed that CNH treatments lead to changes in the elastic moduli of treated tendons (Figure 5.1A). The elastic moduli of tendons treated with 1% (w/v) CNH was significantly higher ($p<0.05$) than tendons treated with 0.2% (w/v) CNH. Additionally, no statistically significant difference could be observed in the ultimate tensile strength (UTS) of all groups of tendons tested (Figure 5.1B), suggesting that CNH treatments were most effective in altering only the stiffness, rather than the overall strength of the target tissue.

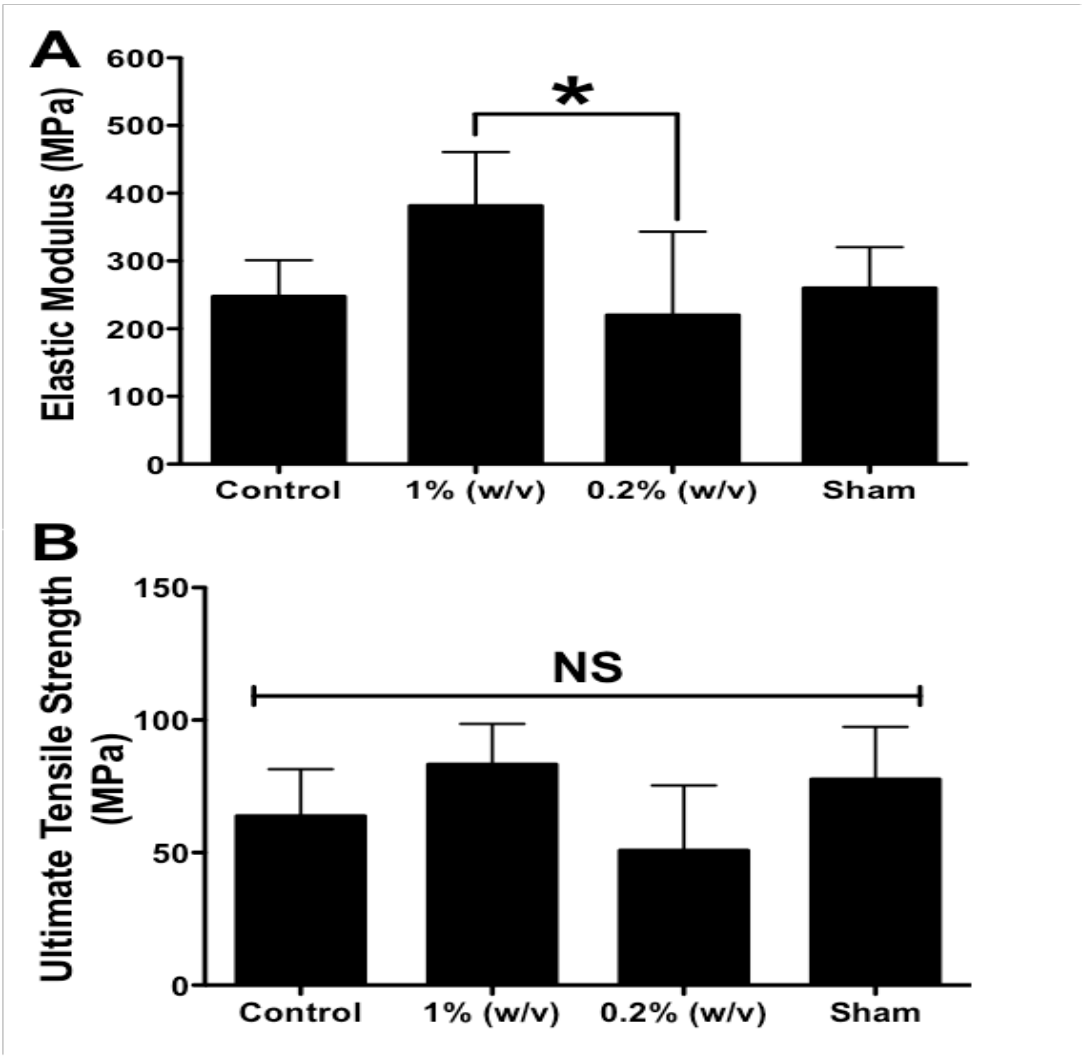

Figure 5.1 Ovine tendon biomechanics. (A) Mean elastic moduli and (B) mean ultimate tensile strength of intact porcine digit tendons after treatment with CNH and sham PBS suspensions (*$p<0.05$).

5.4.2 Immediate *in vitro* response

In addition to interacting with the tendon matrix, CNH treatments will also interact with resident cells in the tissue *in vivo*. To this end, we aimed to investigate the effect of CNH exposure on the immediate response of human tenocytes *in vitro*. First, we characterized the size of aggregates formed in basic cell culture medium by the two CNH concentrations tested (Figure

5.2). There was a significant effect of CNH concentration on aggregate size. More specifically, our measurements showed that at the higher 0.1% (w/v) concentration, CNH formed significantly larger aggregates than at the lower 0.02% (w/v) concentration (2.04±1.03 vs. 1.51±0.56 μm).

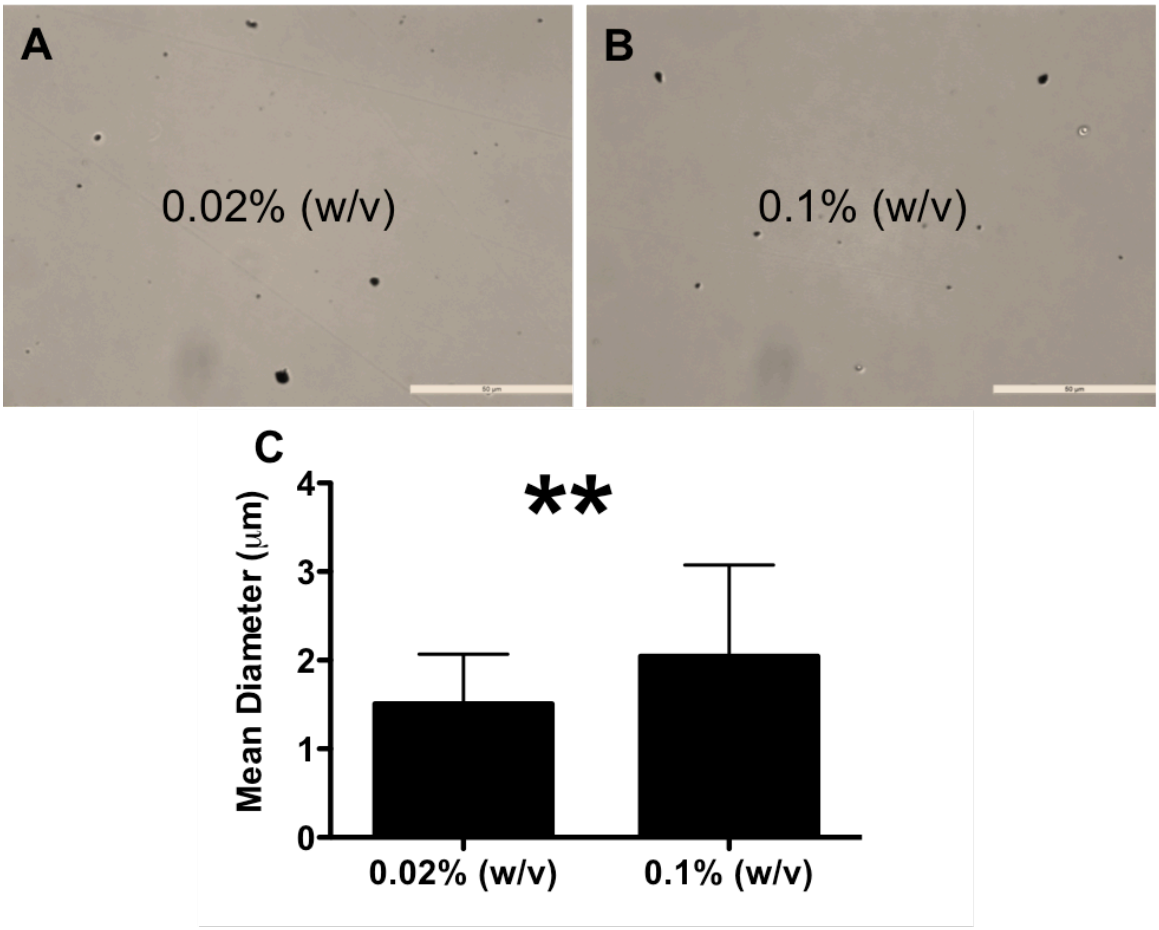

Figure 5.2 CNH aggregate size characterization. Brightfield microscopy of aggregate dispersions of (A) 0.02% (w/v) and (B) 0.1% (w/v) CNH in basic cell culture medium. (C) Mean CNH aggregate diameters in solution (**$p<0.01$).

In addition to material composition and surface chemistry, the response of cells to nanoparticle exposure is also heavily influenced by the overall size of the nanoparticles (120). Therefore, we hypothesized that the perceived differences in aggregate sizes due to CNH concentration will subsequently affect cell response. To test this hypothesis, we evaluated the immediate response of human tenocytes with qPCR after 6 hours of CNH exposure. Looking at two human tenocyte cell lines, we saw a trend of higher collagen-I mRNA expression with 0.02% (w/v) CNH in both hHT and hAT (Figure 5.3A, 3B). Furthermore, we tested for the mRNA expression of two proteins strongly implicated in two distinct mechanisms of endocytosis. Results showed that after 6 hours of CNH exposure, hAT experienced significantly higher expression of CLTC with the 0.02% (w/v) concentration. There were no apparent differences amongst all groups in the mRNA expression of CAV-1 (Figure 3C).

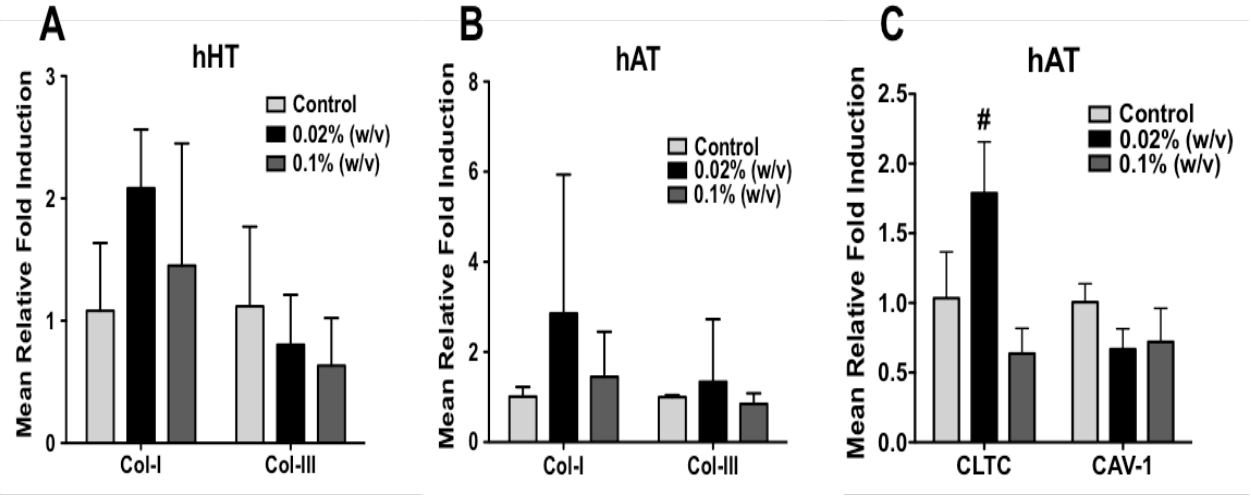

Figure 5.3 Aggregate size-dependent gene expression of human tenocytes after 6 hours of exposure to CNH suspensions. Mean collagen mRNA expression of (A) primary human hamstring tendon tenocytes and (B) immortalized human Achilles tendon tenocytes after

exposure to CNH suspensions. (C) Mean mRNA expression of clathrin heavy chain and caveolin-1 of immortalized human Achilles tendon tenocytes after exposure (#p<0.01).

5.4.3 Prolonged *in vitro* response

In addition to evaluating the immediate response of tenocytes to CNH exposure, we assessed the effect of prolonged exposure on cell response. First, we evaluated the effect of CNH exposure on the cell metabolic activity of hHT over time. Findings showed no significant effects of either CNH concentrations on cell activity until day 14. After prolonged exposure to the higher 0.1% (w/v) CNH group, hHT experienced a notable decrease (p<0.01) in cell activity by day 14 (Figure 5.4A). Additionally, ECM deposition evaluation with Sirius Red/Fast Green staining showed no strong differences between the groups evaluated over the 14-day period (Figure 5.4B).

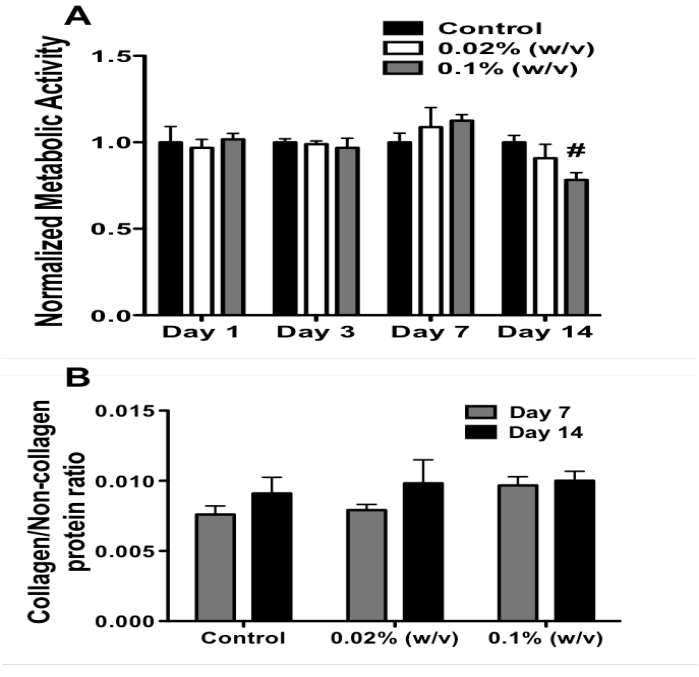

Figure 5.4 Prolonged cell response of primary human hamstring tendon tenocytes to CNH suspensions. (A) Normalized cell metabolic activity showing cytotoxic effects of CNH over 14 days *in vitro*. (B) Collagen content evaluation with Sirius Red/Fast green staining of tenocyte monolayers (#p<0.01).

Gene expression analysis of hHT during prolonged CNH exposure showed that both CNH treatment groups resulted in significantly decreased expression of both collagen types I and III after 7 days (Figure 5.5A). However, cell populations experienced some recovery of collagen-I mRNA expression after 14 days of CNH exposure with both concentrations. The 0.1% (w/v) CNH group led to a significant decrease (p<0.05) in collagen-III mRNA expression at 14 days (Figure 5.5B).

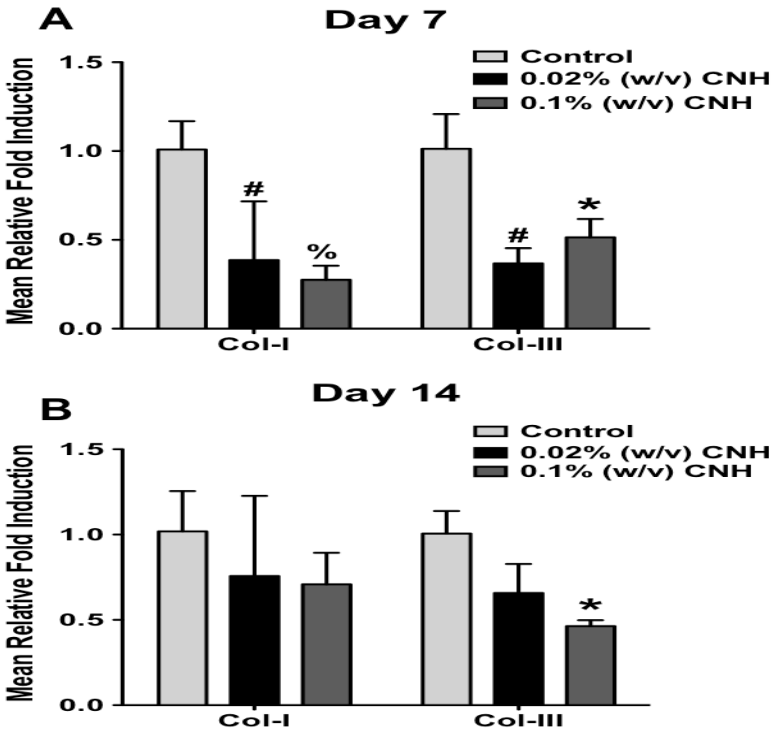

Figure 5.5 Collagen gene expression of primary tenocytes after prolonged exposure to CNH. Mean relative mRNA expression of hHT after (A) 7 and (B) 14 days of exposure to CNH suspensions (*$p<0.05$, #$p<0.01$, %$p<0.001$).

5.4.4 Functional *in vivo* response

After evaluating the *in vitro* response of CNH exposure on both tendon biomechanics and tenocyte cellular response, we next aimed to characterize the effect of CNH treatment on stretch damaged rat Achilles tendon biomechanics and ECM composition *in vivo*. With this model, we compared the effect of 0.2% (w/v) CNH and PBS sham injections on tissue response. After 7 days, there appeared to be an increase in the elastic moduli of injured tendons after treatment with CNH. Also, this perceived change is diminished after 14 days of CNH treatment (Figure 6.6A). Furthermore, there was no significant change in the UTS of damaged tendons after CNH treatment (Figure 6.6B). Figures 7 and 8 present the histological staining of isolated tendons after 7 days of treatment. The results confirmed the presence of damage in the form of noticeable voids in the tendon matrix. Additionally, the presence of CNH is evident in all of the stains.

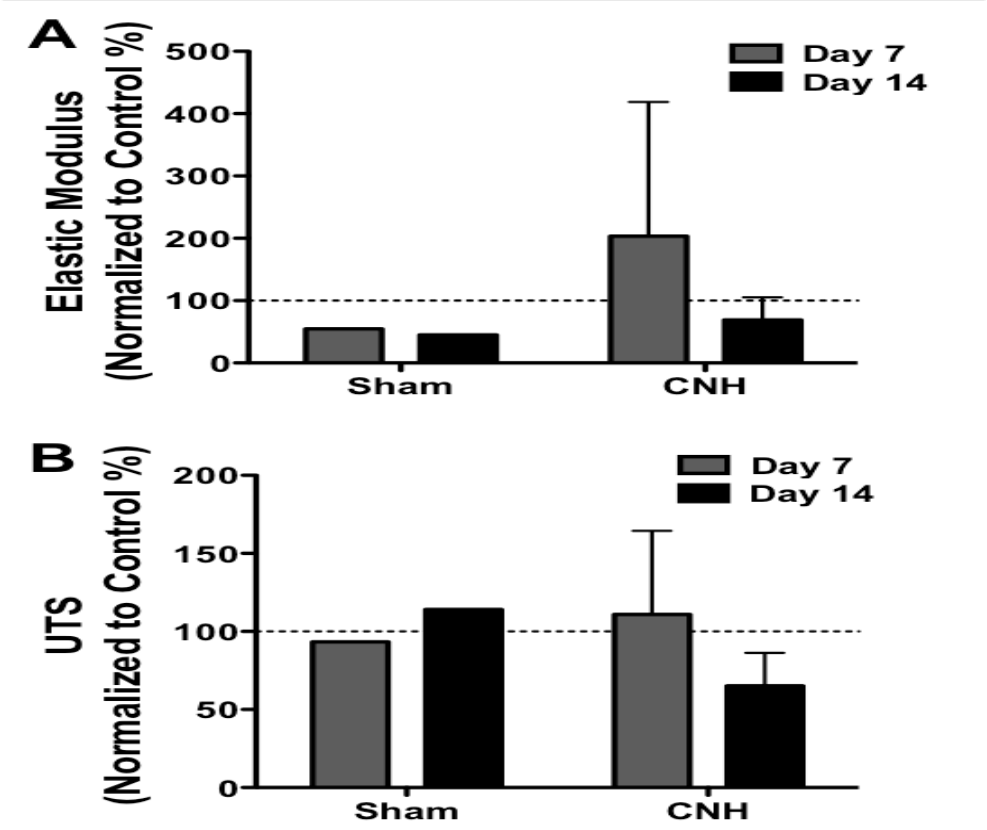

Figure 5.6 Rat Achilles tendon *in vivo* biomechanics. Mean (A) elastic moduli and (B) ultimate tensile strength of stretch-injured rat Achilles tendons normalized to uninjured contralateral control tendon values.

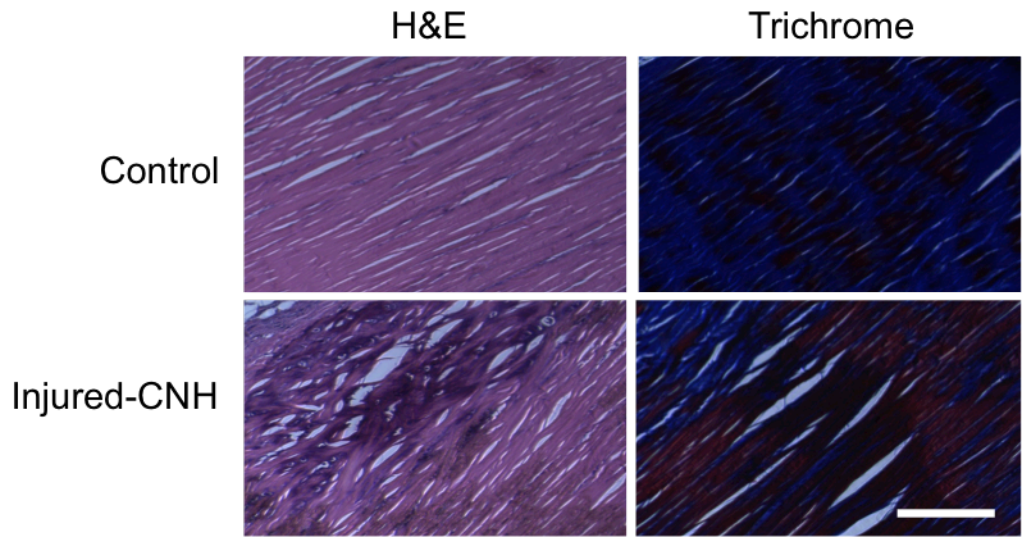

Figure 5.7 Histological staining of rat Achilles tendons. H&E and trichrome staining of uninjured control and injured-treated tendons after 7 days of CNH treatment *in vivo*. Scale bar=400μm.

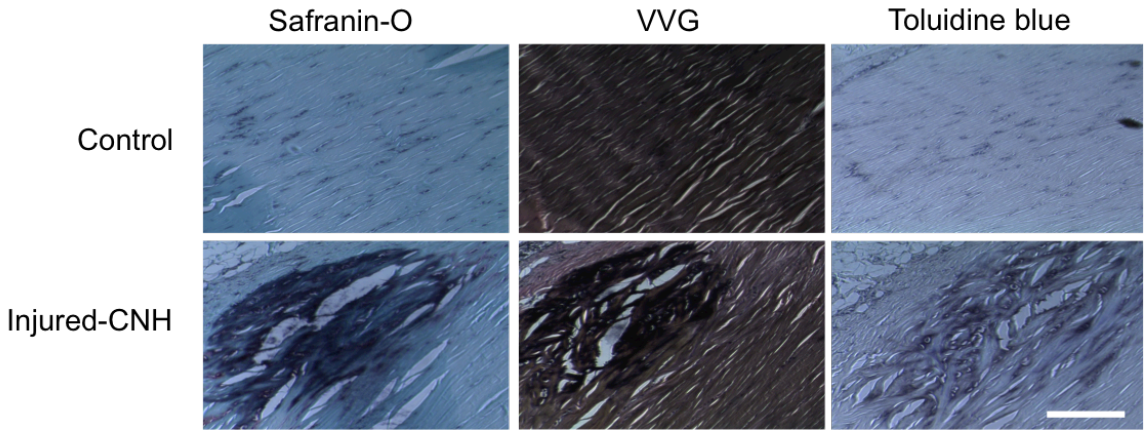

Figure 5.8 Histological staining of rat Achilles tendons. Safranin-O, Von Geisen, and toluidine blue staining of uninjured control and injured-treated tendons after 7 days of CNH treatment *in vivo*. Scale bar=400μm.

5.5 Discussion

Current efforts to repairing sub-failure ligament and tendon pathologies encompass conventional approaches utilizing drugs (such as NSAIDs and corticosteroid injections) and conservative methods such as RICE (15, 16). Treatment with these methods can often be effective at decreasing tissue inflammation and eventually recovering some of the lost tissue biomechanical properties, but they all fail to provide immediate recovery of tissue biomechanics (1, 4). Additionally, the healed tissue is mechanically inferior to the native tendon therefore leaving the tissue prone to re-injury. Utility of CNH for this purpose, allows for the immediate mechanical reinforcement of the compromised matrix after injury. Our previous work showed that likely due to their inherent high elastic moduli and shape, CNH were effective in immediately modulating stretch damaged connective tissue biomechanics. More specifically CNH treatment led to increased porcine skin and tendon toe moduli (56).

Here we hypothesized that CNH would be effective in altering (1) tendon matrix mechanical properties and (2) tenocyte cellular response. In agreement with previous results, we showed that CNH were effective in altering intact ovine tendon biomechanics. CNH treatment showed strong differences in the elastic moduli of the tendons, however there was no significant difference in the UTS of the treated tendons. This suggests that CNH treatment may be effective at modulating functional tendon biomechanics by increasing stiffness *in vivo*.

Results from the *in vitro* analysis of the cellular response of CNH exposure to human tenocytes showed that by 6 hours both cell lines experienced some concentration-dependent changes in the gene expression of collagen type I. The interaction of cells with nanoparticles initiates with the cellular uptake of the nanoparticle (121). This information, in addition to our

immediate collagen gene expression results, motivated us to screen for possible modes of CNH uptake in the tenocytes because it is well established that the uptake response of cells to nanoparticles is also size-dependent (122). Cellular uptake of nanoparticles is often accompanied by changes in the expression patterns of endocytic-related proteins such as clathrin heavy chain (CLTC) and caveolin-1 (CAV-1) (123, 124). Our results showed that hAT populations exposed to 0.02% (w/v) CNH experienced elevated mRNA expression of only CLTC. This suggests that CNH aggregates formed by the lower CNH concentration relied more on clathrin-mediated endocytosis to enter the cells. Clathrin-mediated endocytosis is a common mode of nanoparticle uptake in many cell types (125, 126). Prior work involving the effect of nanoparticle size on the mechanism of receptor- (or protein-) mediated uptake in non-phagocytic murine B16 cells showed a strong correlation of clathrin-mediated uptake with particles <200nm in size, while uptake transitioned to caveolae-mediated mechanisms for larger particles at 500nm (127). These findings, in addition to our results, support our hypothesis that the cellular response of tenocytes to CNH exposure is also partly dependent on the size of aggregates formed in solution. Interestingly, this implies that controlling CNH aggregate size could be utilized to further control cell behavior. Introducing new surface chemistries or functionalizing CNH to control aggregate size could be utilized to enhance their overall therapeutic potential.

Further characterization of cell response to CNH exposure revealed no noticeable effects on the metabolic activity of primary tenocytes until 14 days. At this point, the higher 0.1% (w/v) CNH concentration led to significantly lower metabolic activity when compared to control populations. This could signify that the tenocytes are able to tolerate a certain amount of CNH for up to 14 days before experiencing changes in viability or overall cell function. In addition, we saw no strong differences in the collagen/non-collagen ratio of CNH treated primary

tenocytes for up to 14 days. Gene expression analysis showed that both CNH concentrations led to significant down-regulation of collagen types I and III mRNA after 7 days. At 14 days, tenocytes treated with 0.02% (w/v) CNH experienced recovery of collagen type I mRNA expression while populations exposed to 0.1% (w/v) exhibited significantly lower levels of collagen-III mRNA expression than control populations. CNH functionalization can be utilized to further control cell response. Modification of CNH with specific collagen-promoting and -binding peptides, such as fibronectin may be utilized to enhance the tenogenic response of cells exposed the CNH.

We also showed, for the first time, the feasibility of utilizing CNH treatments to treat a sub-failure tendon injury *in vivo*. Compared with the PBS sham treatment group, the CNH group led to a higher increase in the elastic moduli of injured rat Achilles tendons after 7 days of treatment. Histological analysis also confirmed the presence of CNH in the injured tendon matrix at day 7. Although our current finding was not statistically significant, this warrants further investigation with a larger sample size. Additionally, by day 14 any change in the elastic moduli of the injured tendons was diminished and returned to levels comparable to controls. Also, there is no significant difference in the UTS of the injured tendons after CNH treatment at day 7 and 14. Assuming that this change in injured tendon biomechanics (most notably the elastic modulus) after CNH treatment is due to the mechanical reinforcement capabilities of CNH, this suggests that after 14 days this perceived reinforcement is diminished. This could be due to the clearing of unattached CNH over time. This will be investigated in future studies with longer timepoints and *in vivo* imaging techniques to track the biodistribution of the injected CNH suspension over time.

Results from our experiments showed that CNH could be utilized to modulate tendon biomechanics and tenocyte cell response. Moreover, we showed for the first time *in vivo* the potential of utilizing CNH to aid in the functional repair of sub-failure injury in rat Achilles tendons. Taken together, our data clearly shows the feasibility of this novel approach to treating sprain and strain injuries in ligaments and tendons.

Acknowledgements

The authors gratefully acknowledge technical assistance with the ovine tendon biomechanical testing from the Orthopedic Research Laboratory at Rutgers-Robert Wood Johnson Medical School and financial support from NSF CBET 1243144 and NSF DGE 0801620.

Chapter 6. Conclusions, future directions, and perspective

In conclusion, this dissertation explored the biomechanical and histological basis of sub-failure injury in ligaments and tendons and the potential of several non-surgical tissue engineering modalities. We showed that the cause of sprain and strain injuries lies in the evidence of compromised tissue biomechanics and matrix disruption. Using a custom stretch injury device, we induced consistent grade II strain injuries in the Achilles tendons of rats. The injury was successfully confirmed *in vivo* using magnetic resonance imaging, histological staining, and biomechanical tensile testing techniques.

Current treatment options in the management of ligament and tendon sub-failure injuries are inadequate and often rely on the limited intrinsic healing potential of the tissue. This contributes to sustained, compromised tissue biomechanics, leaving the tissue prone to re-injury. To this end, we first explored the potential of utilizing proliferative therapy in the treatment of ligament and tendon pathologies. Previous work on the efficacy of proliferative therapy for ligament and tendon repair remains limited and results have been inconclusive. We showed that the therapy, most notably with the P2G irritant, was effective in causing localized cell death and eliciting a pro-inflammatory response in human tenocytes. More specifically, treatments lead to a strong decrease in the metabolic activity of cells and led to elevated levels of prostaglandin species both at the mRNA and protein levels. Prostaglandin is a well-known pro-inflammatory factor and a potent inducer of tissue inflammation *in vitro*. Our results demonstrated *in vitro* the potential of using proliferative therapy to locally initiate the body's wound healing response. It is hypothesized that the initiated wound healing response will ultimately lead to the recruitment of new progenitor and fibroblast cells to the injury site to deposit additional ECM leading to

enhanced tissue repair. More experiments will be conducted to evaluate the *in vivo* efficacy of proliferative therapy.

Cell therapy is a commonly investigated regenerative medicine approach for ligament and tendon repair. Although several studies have shown the potential of utilizing stem and progenitor cells to facilitate the repair and development of ligament and tendon tissues, there are very few studies aimed at unraveling the effect of cell-cell communication, or cell signaling mode on tissue healing potential. In systems employing cell-seeded constructs, the seeded cells experience multiple modes of cell signaling during the process of neovascularization and new tissue formation *in vivo*. Also, other systems like those employing the direct injection of free cells or the encapsulation of suspended cells rely on one mode of cell signaling initially but then experience changes as the scaffold biodegrades and transplanted cells migrate during repair. It has been established that the secretome and transcriptome of implanted cells are heavily influenced by their microenvironment. An additional goal of this dissertation was to gain insight into the optimal mode of cell signaling required for the improved repair of sub-failure tendon and ligament pathologies.

In chapter 4 we explored the effect of paracrine signaling between primary hMSC and tenocytes on the tenogenic response of both cell types in 3 different sets of human donors. Our results showed that the paracrine interaction of the two cell types *in vitro* led to changes in the expression patterns of both anabolic and catabolic markers of tendon and ligament ECM. This response is due to the secretion and exchange of a plethora of soluble factors, most likely TGFβ, by both cell types. The observed response in this paracrine model motivates and warrants further understanding of the effects of this type of cell signaling on tissue repair *in vivo*. Also, preliminary *in vitro* work performed by our group using a juxtacrine direct co-culture model

between hMSC and tendon cells showed that direct contact between the two cell types also led to enhanced cell function evidenced by increases in metabolic activity and collagen deposition in the co-culture groups (Figure 6.1). Those results, in addition to our findings in chapter 4, inspired the need for further in-depth studies on cell signaling during co-culture between the two cell types. To this end, we developed a human tenocyte collagen reporter cell line (discussed in Appendix A-1) for implementation into our studies. With the reporter cells, we can directly examine the effect of both modes of cell signaling on the response of the tenocytes. Future studies will attempt to determine which mode of cell signaling and specific candidate signaling molecules are most dominant at various timepoints during MSC-mediated tenogenesis.

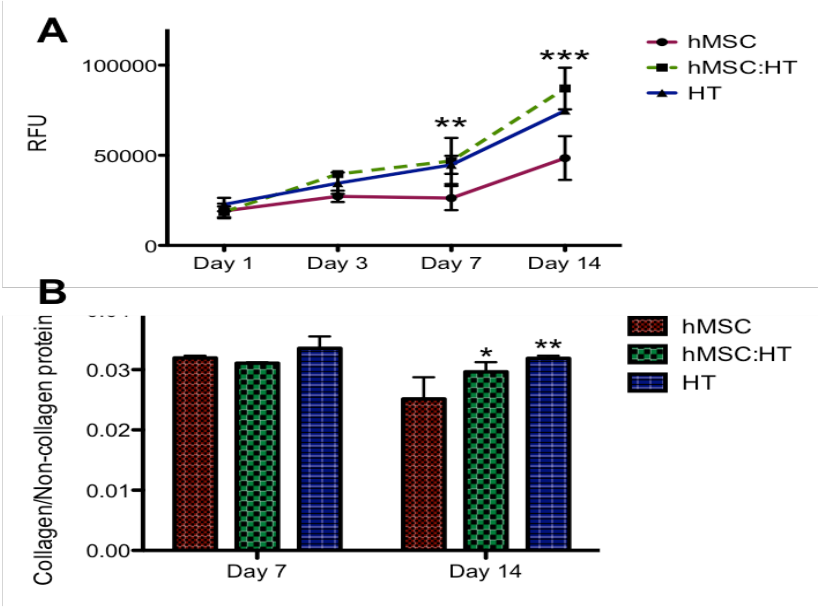

Figure 6.1 Cellular response primary hMSC and HT in direct co-culture. (A) PrestoBlue cell metabolic activity of co-cultures. (B) Sirius red/fast green assessment of protein deposition during co-culture.

Chapter 5 examined the potential of the novel utility of CNH to treat sub-failure injury in tendons. We confirmed that CNH treatments were able to modulate ovine tendon biomechanics, altering the elastic moduli of treated tendons *in vitro*. Additionally, we showed that CNH are tolerated by tenocytes for up to 14 days *in vitro* and that cell response is likely dependent on the size of CNH aggregates formed in solution. Finally, using our sub-failure rat Achilles tendon *in vivo* model, we showed that injected CNH were able to persist in the tissue and increase damaged tendon biomechanics, especially after 7 days of treatment. Moreover, our results substantiated the potential utility of the CNH as a potentially suitable modality for sub-failure ligament and tendon injuries. Additional studies are needed to further understand CNH biodistribution after treatment. More animal studies will be performed with fluorescently-tagged CNH to track the *in vivo* location of injected CNH suspensions over time (Figure 6.2).

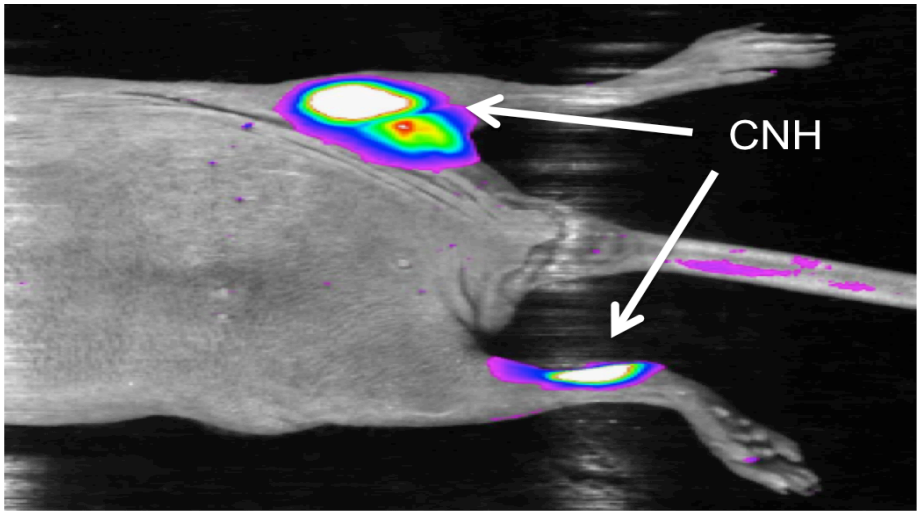

Figure 6.2 Fluorescent imaging of a nude mouse cadaver injected with CNH-GFP suspensions.

Our studies have shown the potential of several non-surgical approaches to aid in the enhanced repair of sub-failure injuries in ligaments and tendons. Each of the approaches examined primarily addresses one of the two main obstacles (compromised tissue biomechanics

and deficient bioactivity) to improving sub-failure ligament and tendon injury repair. There is great potential in these modalities for improving and contributing to the fields of orthopedics and tissue engineering. Further *in vitro* and *in vivo* studies are necessary in order to better understand the effects of the therapies at the cell and tissue levels. Additionally, the combination of several of the therapies could be utilized as a customizable hybrid treatment method to strategically address specific aspects of sub-failure ligament and tendon injury and repair over time.

Appendix A. Development and characterization of a human tenocyte collagen-I reporter cell line

A.1 Abstract

Genetic reporter systems are specialized tools used in tissue engineering and molecular biology to study the gene expression and regulation of biological processes. In this work, we developed a dual promoter reporter system for collagen type I activity in human Achilles tenocytes. In this lentiviral system, luciferase activity is driven by the activation of a collagen-Iα1 promoter in addition to the constitutive expression of green fluorescent protein (GFP) for cell tracking purposes. We confirmed the successful transduction of immortalized human Achilles tendon tenocytes using fluorescent imaging for GFP. We then validated the reporting capabilities of the cell line with a standard luciferase assay and qPCR for collagen activity. The new cell line can be utilized as a tool to study tenogenic responses for *in vitro* and *in vivo* tissue engineering applications.

A.2 Introduction

Tendons and ligaments are dense collagenous tissues of the musculoskeletal system that are critical in providing locomotion and stability for the body. They have very similar structure, composition, and function. In addition, they are both arranged in an aligned hierarchical architecture that allows for the efficient transfer and bearing of large loads required for the body's stability and locomotion (1, 4, 99). Due to the high incidence of tendon and ligament injuries and the many disadvantages associated with current treatment options, they have become an intense area of interest for tissue engineering (TE) (85, 108). TE involves the singular and combinatorial use of biomaterial scaffolds, cells, small molecules, and nanoparticles with the

ultimate goal of repairing diseased and damaged tissues (73, 105). The past few decades have seen the emergence and growth of several new approaches to solving complex biological problems. More specifically, TE has motivated a serious effort to develop specialized systems that could serve as potential *in vivo* therapies or *in vitro* models to understand tissue development and disease progression.

Collagen constitutes the majority of total protein present in ligaments and tendons. The high mechanical strength of the tissue is primarily due to their tight hierarchical architecture and high collagen content (57). Due to this, many TE approaches to ligament and tendon repair aim to assess collagen expression and production as a hallmark of positive tenogenesis *in vitro* an *in vivo*. There is a general understanding that the induction of increased or enhanced collagen bioactivity in the system will lead to a stronger, more functional repaired tissue *in vivo*.

Genetic reporter systems are common tools utilized in molecular biology to aid in the study of gene expression and regulation in cells and tissues of interest (128, 129). The systems serve as indicators of specific biological activities. Systems generally involve the use of a target gene to "promote" or drive the expression of a "reporter" protein. Afterward, the level of genetic activity of a target gene is measured by an assay for the reporter protein. Ideally, the chosen reporter protein is a foreign protein that is otherwise undetectable or missing from the genome of the cell or tissue of interest. Previous TE approaches have successfully utilized genetic reporter cell lines as models for tissue development, injury, and disease progression (66, 128, 130). A major advantage of these systems includes the ease of implementation for high throughput screening assays of candidate biomaterials and small molecules. Although several reporter systems have been developed and utilized for different musculoskeletal processes, there is a need

for a specialized reporter system that can easily be applied in the study of human tenogenesis for TE applications.

In this manuscript we describe the development and characterization of a novel human Achilles tenocyte reporter cell line to monitor the expression of collagen-Iα1. Using a recently developed a second-generation dual lenti-viral vector that both produces luciferase (*luc*) under activation of a collagen-Iα1 promoter and constitutively expresses green fluorescent protein (GFP), we transduced immortalized human Achilles tendon tenocytes. The resultant reporter tenocytes were confirmed for successful transduction via fluorescent imaging and *luc* production.

A.3 Materials and methods

A.3.1 Cell culture

All procedures were performed in accordance with and approval from the Rutgers University Environmental Health and Safety Office and the Medical Ethical Research Committee at the Utrecht Medical Center.

Immortalized human Achilles tendon tenocytes (hAT) were obtained as a kind gift from Dr. Denitsa Docheva at the Walter Brendel Centre of Experimental Medicine at the Ludwig-Maximilian University of Munich. hAT were maintained in basic medium consisting of α-MEM supplemented with 10% fetal bovine serious (FBS) and 1% penicillin/streptomycin (P/S) (Life Technologies, Carlsbad, CA). Osteogenic differentiation medium utilized for validation experiments consisted of α-MEM supplemented with 10% FBS, 1% P/S, 0.1M L-ascorbic acid-2-phosphate (ASAP), 0.01 M dexamethasone, and 0.02% β-glycerophosphate.

A.3.2 Lentiviral production

The dual-promoter reporter construct pLV-Col2.3-tk/luc-mnd-GFP was obtained as a kind gift from Dr. Zhenghong Lee in the Department of Biomedical Engineering at Case Western Reserve University. The construct, shown in Figure 1, is a second generation, self-inactivating lentiviral vector with tk/luc expression driven by the Col1α1(2.3) promoter and green fluorescent protein (GFP) expression driven by the constitutively active MND promoter (130).

Figure A.1 Schematic showing relative positions of promoters and reporters (130).

Active reporter gene viral particles were produced by packaging the construct with helper plasmids (psPAX2, pMD2.G, and pCEP4-TAT) and transfecting HEK 293T helper cells as previously described (128, 130). After confirmation of successful transfection, viral supernatants produced by helper cells were collected and further concentrated using ultracentrifugation techniques.

A.3.3 hAT transduction

To generate the reporter cell line, we seeded hAT in 6-well plates at a density of $2X10^4$ cells/cm^2. After allowing the cells to attached overnight, we incubated cultures with active LV-Col2.3-tk/luc-mnd-GFP viral particles at a 1:20 ratio in viral transduction medium. Viral transduction medium consisted of basic medium without FBS supplementation. After incubating for 16 hours, the medium was replaced with fresh medium to allow the cells to recover for 1 day.

Transduction was performed in two rounds before allowing cultures to reach confluence in fresh basic medium. After successful transduction was confirmed via fluorescent imaging, cells were further sub-cultured to obtain more cells with medium changes 2-3 times per week. Finally, the population of transduced cells was further enriched using fluorescence activated cell sorting (FACS) for GFP-positive cells at the Rutgers University Flow Cytometry/Cell Sorting and Confocal Microscopy Core Facility. Afterward, the final product was the new reporter cell line hAT-pCOL.

A.3.4 *In vitro* validation

To confirm the ability of the cells to successfully report collagen expression activity, we seeded hAT-pCOL at a density of $1x10^4$ and $3x10^4$ cells/cm^2 in well plates and allowed them to attach overnight. The next day, we cultured the cells with basic medium, basic medium supplemented with 10 ng/mL of TGF-β1, basic medium supplemented with 0.2 mM ASAP, or osteogenic differentiation medium for 7 days. Afterward, groups were washed with sterile PBS then assessed for *luc* activity and collagen mRNA expression as described below.

A.3.5 Collagen bioassay

Luciferase activity as a result of collagen expression was assessed using a standard luciferase assay (Promega, Madison, WI) according to manufacturer protocols. After washing with PBS, cells were lysed then subjected to a freeze-thaw cycle to further enhance lysis. Afterward, lysates were combined with the luciferin substrate and light production was quantified using a luminometer (Tecan, Mannedorf, Switzerland).

Prior to cell lysis, groups were first evaluated for metabolic activity using the fluorometric PrestoBlue assay (Life Technologies). Briefly, cells were incubated with 10%

PrestoBlue solution in basic medium for 1 hour and then fluorescence was assessed using a spectrophotometer (Tecan). Final bioactivity results are represented as *luc* activity values normalized to metabolic fluorescent values.

A.3.6 Real-time quantitative RT-PCR analysis (qPCR)

The expression of collagen type I mRNA was evaluated using qPCR. Total RNA was extracted and purified using the RNeasy Mini Kit (Qiagen, Valencia, CA) according to manufacturer's directions. Purified RNA was normalized and then reverse transcribed to produce cDNA using the High Capacity cDNA Reverse Transcription Kit (Life Technologies). qPCR was performed using the SYBR Green PCR mastermix (Life Technologies), cDNA, and primers for human colIα1; sense 5'-GTCACCCACCGACCAAGAAACC and anti-sense 5'-AAGTCCAGGCTGTCCAGGGATG, and human GAPDH; sense 5'-ACAACTTTGGTATCGTGGAA and anti-sense 5'-AAATTCGTTGTCATACCAGG. Relative gene expression was determined using the $\Delta\Delta C_T$ method and normalized to GAPDH as an endogenous control.

A.3.6 Statistical analysis

All quantitative data is reported as mean±standard deviation. A one-way ANOVA with Bonferroni's multiple comparisons post-hoc test was utilized in the comparison of multiple groups during validation experiments. A student t-test was employed for comparison of groups in the qPCR experiments (GraphPad Prism Software 5.0, La Jolla, CA). Unless otherwise mentioned, results were considered statistically significant for *p*-values less than 0.05.

A.4 Results

Immortalized hAT cells were genetically modified to become collagen activity reporter cells. Successful transduction was confirmed using fluorescent imaging for GFP. Figure 2 shows images of hAT-pCOL after cell sorting. The final merged image (Figure A.2C) presents confirmation that all cells present after sorting were positive for GFP, thus signifying a homogeneous population of hAT-pCOL reporter cells.

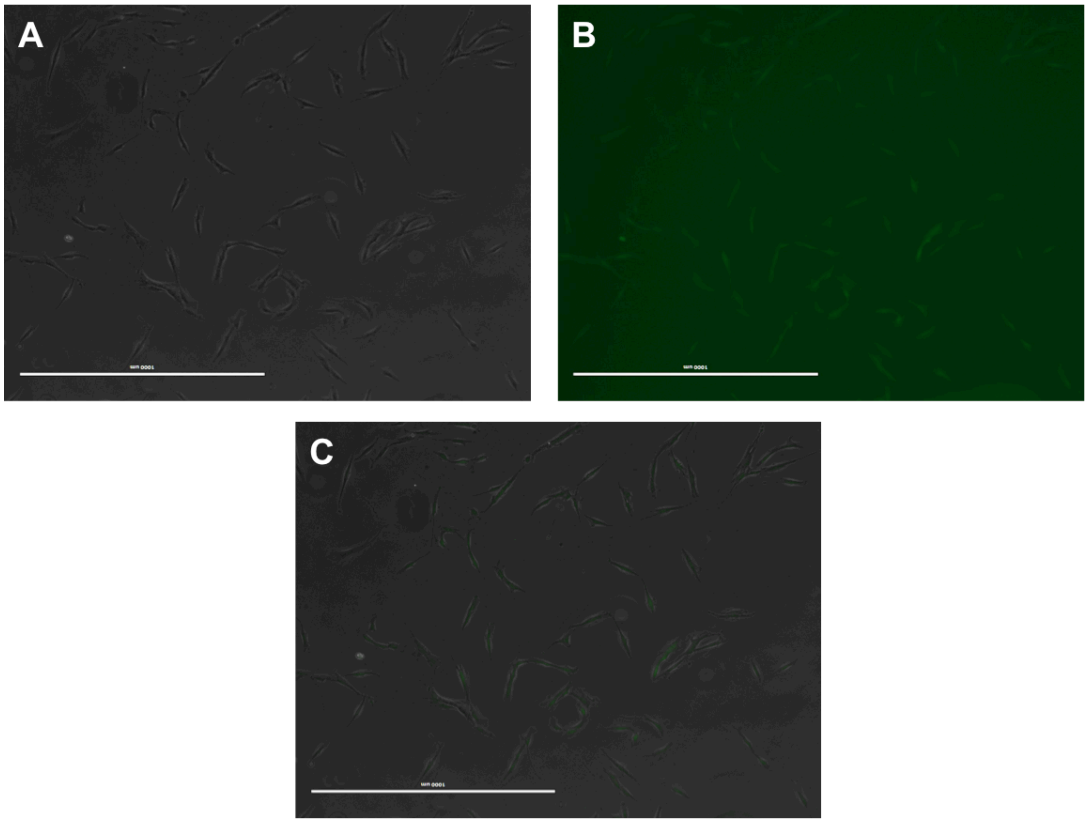

Figure A.2 Visual confirmation of successful viral transduction. (A) Brightfield imaging of purified hAT after enrichment of successfully transduced populations. (B) Enriched hAT viewed under fluorescent microcopy for confirmation of GFP expression. (C) Merged image showing enriched population of hAT-pCOL cell populations. Scale bars=1mm.

We conducted *in vitro* validation experiments to confirm the ability of hAT-pCOL to successfully report collagen expression activity. Starting with cells seeded at two different concentrations (Figure A.3), we cultured hAT-pCOL for 7 days under 4 different conditions. Afterwards, we assessed the cells for collagen bioactivity via a luciferase assay. Results showed that hAT-pCOL cultured with the osteogenic differentiation medium had the highest collagen bioactivity (Figure A.4). Cells cultured with ASAP were the second highest. Additionally, there appeared to be no significant difference in collagen bioactivity between the two initial cell densities for any conditions tested.

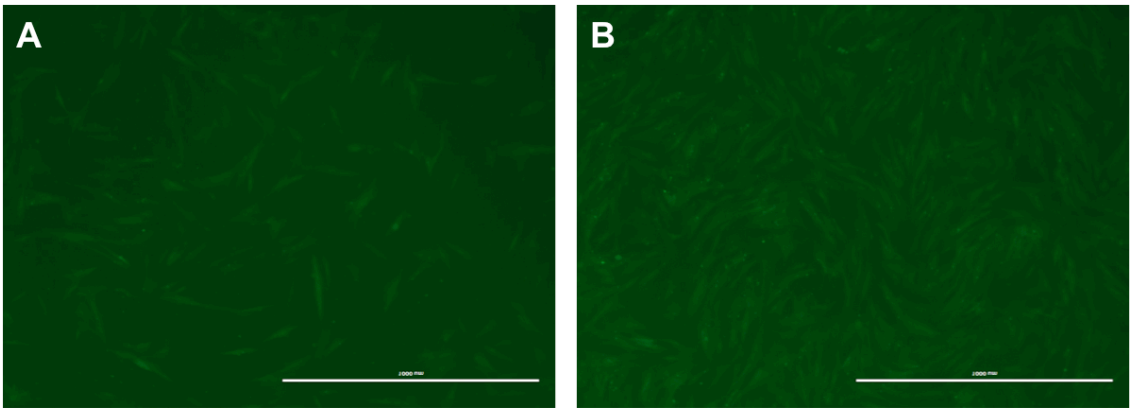

Figure A.3 Fluorescent imaging of hAT-pCOL cells seeded at (A) $1x10^4$ and (B) $3x10^4$ cells/cm^2. Scale bars=1mm.

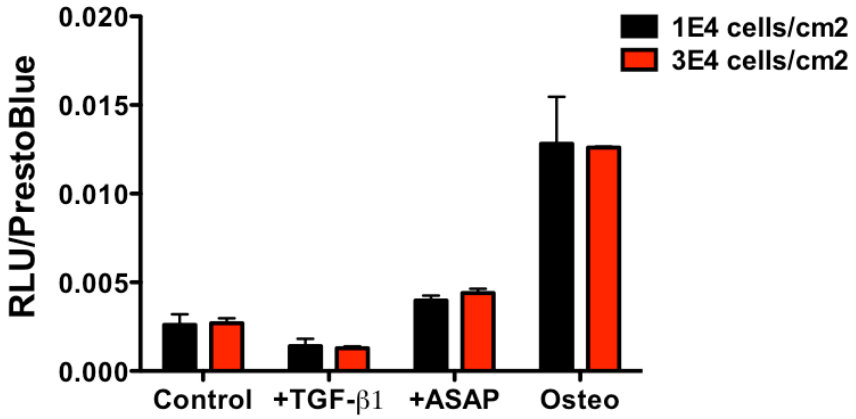

Figure A.4 Collagen bioactivity of hAT-pCOL after 7 days of culture under different medium conditions.

Gene expression analysis of hAT-pCOL was performed with qPCR after culturing under basal and osteogenic conditions. Results showed that culture with osteogenic differentiation medium led to a significantly higher expression ($p<0.01$) of collagen-I mRNA after 7 days.

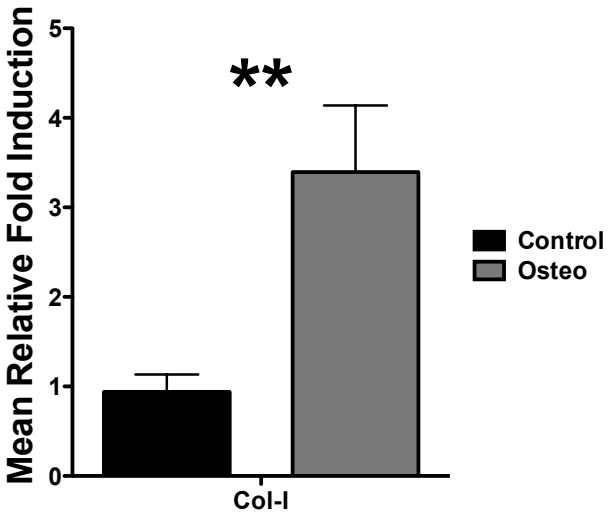

Figure A.5 Mean relative expression of collagen-I mRNA in hAT-pCOL after 7 days of culture in basic and osteogenic differentiation medium (**$p<0.01$).

A.5 Discussion

Corn and colleagues recently developed a dual promoter reporter system to track and monitor the osteogenic differentiation of transplanted hMSC in a murine model of segmental bone defects. Utilizing bioluminescent imaging, they confirmed the ability of the system to provide useful information about the location and activation of collagen expression of the cells in a hydrogel (130). We aimed to employ that system in the development of a specialized genetic reporter cell line capable of reporting on the collagen activity of human tenocytes. The reporter cells can be utilized as a tool to study the tenogenic potential of a wide array biomaterials. Similarly, they can also be utilized to study the effects of various culture conditions in inducing tenogenesis *in vitro* and *in vivo*.

Our results showed the successful generation of human tenocyte reporter cells capable of reporting collagen bioactivity. Validation tests using several culture conditions showed the osteogenic differentiation medium to be most effective amongst all conditions at facilitating higher mRNA expression of collagen-I. This result was expected because the active components of the osteogenic medium formulation are well known to be effective in encouraging a strong deposition of ECM in stem cells. Additionally, the ASAP alone is also known to be a potent inducer of strong ECM deposition (131). Considering the fact that tendon cells are responsible for the deposition and formation of the collagenous tendon matrix, it was expected that both conditions would be capable of inducing strong collagen expression. Finally, gene expression analysis with qPCR showed that the osteogenic differentiation medium also led to a strong upregulation of collagen-I mRNA, in agreement with the luciferase activity results.

The validation tests conducted with our system utilized soluble cues to assess regulation of collagen expression in the tenocytes. Although initial results were positive in demonstrating the effectiveness of our system, further testing is necessary to fully confirm the utility of system for other TE ligament and tendon approaches. The use of physical cues in validating the collagen bioactivity reporting capabilities of the cells would be helpful. Many TE approaches utilize some combination of biomaterials to engineer a scaffold for the regeneration of ligaments and tendons. The hAT-pCOL can potentially be utilized as a cell source to study cell seeding, spreading, alignment, and differentiation in the scaffolds (via simultaneous measurement of *luc* activity and the constitutive expression of GFP) *in vitro* and *in vivo*. Future studies will utilize the cells for biomaterial characterization tests as well the study of effect of cell signaling mode (paracrine vs. juxtacrine) on tenogenesis during mesenchymal stem cell-mediated tendon and ligament repair.

In conclusion, we have successfully developed a human tenocyte cell line capable of reporting collagen expression levels as a result of cell culture conditions. Using fluorescent imaging, we confirmed successful viral transduction of tenocytes with the constitutive expression of GFP in the final reporter cell line. Finally, using standard assays for quantification of luciferase activity and gene expression analysis, we confirmed the efficacy of the cells to report collagen bioactivity *in vitro*.

References

1. Voleti PB, Buckley MR, Soslowsky LJ. Tendon healing: repair and regeneration. Annu Rev Biomed Eng. 2012;14:47-71. Epub 2012/07/20. doi: 10.1146/annurev-bioeng-071811-150122. PubMed PMID: 22809137.

2. Laurencin CT, Freeman JW. Ligament tissue engineering: an evolutionary materials science approach. Biomaterials. 2005;26(36):7530-6. PubMed PMID: 16045982.

3. Amiel D, Billings E, Akeson WH. Ligament structure, chemistry, and physiology. In: Daniel D, Akeson WH, O'Connor J, editors. Knee ligaments: structures, function, injury and repair. New York: Raven Press; 1990. p. 77–91.

4. Sharma P, Maffulli N. Tendon injury and tendinopathy: healing and repair. J Bone Joint Surg Am. 2005;87(1):187-202. Epub 2005/01/07. doi: 10.2106/JBJS.D.01850. PubMed PMID: 15634833.

5. Becker W, Kleinsmith L, Hardin J. The World of the Cell. San Francisco: Benjamin/Cummings Publishing; 2003.

6. Freeman JW, Silver FH. Elastic energy storage in unmineralized and mineralized extracellular matrices (ECMs): a comparison between molecular modeling and experimental measurements. Journal of theoretical biology. 2004;229(3):371-81. Epub 2004/07/06. doi: 10.1016/j.jtbi.2004.04.018. PubMed PMID: 15234204.

7. Rothrauff BB, Tuan RS. Cellular therapy in bone-tendon interface regeneration. Organogenesis. 2014;10(1):13-28. Epub 2013/12/12. doi: 10.4161/org.27404. PubMed PMID: 24326955; PubMed Central PMCID: PMC4049890.

8. Beynnon B, Renstrom P. A prospective, randomized clinical investigation of the treatment of first-time ankle sprains. The American Journal of Sports Medicine. 2006;34(9):1401-12.

9. Linetsky FS, Botwin K, Gorfine L, Jay G, Raphael M, Mikulinsksy A, Parris W, Pollak S, Ray A, Saberski L, Taraschi P, Torres F, Trescot A. Regenerative Injection Therapy (RIT): Effectiveness and Appropriate Usage. The Pain Clinic Magazine. 2002:38-45.

10. Brown C, Padua D. Individuals with mechanical ankle instability exhibit different motion patterns than those with functional ankle instability and ankle sprain copers. Clin Biomech. 2008;23:822-31.

11. Hackett G. Ligament & Tendon Relaxation (Skeletal Disability) - Treated by Prolotherapy, (Fibro-osseous Proliferation). 3rd ed. ed. Springfield, IL: Charles C. Thomas; 1958.

12. Clark R. Cutaneous tissue repair: basic biologic considerations. Journal of the American Academy of Dermatology. 1985;13:701-25.

13. Banks A. A rationale for prolotherapy. Journal of Orthopaedic Medicine. 1991;13(3).

14. James R, Kesturu G, Balian G, Chhabra A. Tendon: biology, biomechanics, repair, growth factors, and evolving treatment options. J Hand Surg Am. 2008;33(1):102-12.

15. Lynch S, Renstrom P. Treatment of acute lateral ankle ligament rupture in the athlete. Conservative versus surgical treatment. Sports Medicine. 1999;27(1):61-71.

16. Jensen KT, Rabago DP, Best TM, Patterson JJ, Vanderby R, Jr. Early inflammatory response of knee ligaments to prolotherapy in a rat model. J Orthop Res. 2008;26(6):816-23. Epub 2008/02/02. doi: 10.1002/jor.20600. PubMed PMID: 18240327; PubMed Central PMCID: PMC2755507.

17. Vunjak-Novakovic G, Altman G, Horan R, Kaplan D. Tissue Engineering of Ligaments. Annu Rev Biomed Eng. 2004;6:131-56.

18. Griffith L, Naughton G. Tissue engineering--current challenges and expanding opportunities. Science. 2002;5557:1009-14.

19. Young M. Stem cell applications in tendon disorders: a clinical perspective. Stem Cells Int. 2012;2012:637836. Epub 2012/03/27. doi: 10.1155/2012/637836. PubMed PMID: 22448174; PubMed Central PMCID: PMC3289928.

20. Lui P, Rui Y, Ni M, Chan K. Tenogenic differentiation of stem cells for tendon repair-what is the current evidence? Journal of Tissue Engineering and Regenerative Medicine. 2011:1-20.

21. Lee IC, Wang JH, Lee YT, Young TH. The differentiation of mesenchymal stem cells by mechanical stress or/and co-culture system. Biochem Biophys Res Commun. 2007;352(1):147-52. Epub 2006/11/17. doi: 10.1016/j.bbrc.2006.10.170. PubMed PMID: 17107659.

22. Freeman J, Walters V, Kwansa A. Ligaments, biomaterials, and tissue engineering opportunities. In: Hollinger J, editor. An Introduction to Biomaterials, Second Edition: Taylor & Francis; 2011.

23. Linetsky FS, Manchikanti L. Regenerative injection therapy for axial pain. Techniques in Regional Anesthetia & Pain Management. 2005;9:40-9.

24. Linetsky FS, Mikulinsksy A, Gorfine L. Regenerative Injection Therapy, History of Applications in Pain Management Part I 1930's-1950's. The Pain Clinic. 2000.

25. Linetsky FS, Saberski L, Miguel R, Snyder A. Regenerative Injection Therapy, History of Applications in Pain Management Part II 1960's-1980's. The Pain Clinic. 2001.

26. Liu Y, Tipton C, Matthes R, Bedford T, Maynard J, Welmer H. An in situ study of the influence of a sclerosing solution in rabbit medial collateral ligaments and its junction strength. . Connective Tissue Research. 1983;11:95-102.

27. Gafni Y, Turgeman G, Liebergal M, Pelled G, Gazit Z, Gazit D. Stem cells as vehicles for orthopedic gene therapy. Gene Therapy. 2004;11:417-28.

28. Fan H, Liu H, Toh S, Goh J. Enhanced differentiation of mesenchymal stem cells co-cultured with ligament fibroblasts on gelatin/silk fibroin hybrid scaffold. Biomaterials. 2008;29:1017-27.

29. Zhang L, Tran N, Chen HQ, Kahn CJ, Marchal S, Groubatch F, Wang X. Time-related changes in expression of collagen types I and III and of tenascin-C in rat bone mesenchymal stem cells under co-culture with ligament fibroblasts or uniaxial stretching. Cell Tissue Res. 2008;332(1):101-9. Epub 2008/01/16. doi: 10.1007/s00441-007-0564-6. PubMed PMID: 18196274.

30. Baraniak P, McDevitt T. Stem cell paracrine actions and tissue regeneration. Regen Med. 2010;5(1):121-43.

31. Caplan AI, Dennis JE. Mesenchymal stem cells as trophic mediators. Journal of cellular biochemistry. 2006;98(5):1076-84. Epub 2006/04/19. doi: 10.1002/jcb.20886. PubMed PMID: 16619257.

32. Cadek M, Coleman J, Ryan K, Nicolosi G, Bister G, Fonseca A, Nagy J, Szostak K, Beguin F, Blau W. Reinforcement of Polymers with Carbon Nanotubes: The Role of Nanotube Surface Area. Nano Letters. 2004;4(2):353-56.

33. Bhattacharyya S, Salvetat J, Saboungi M. Reinforcement of semicrystalline polymers with collagen-modified single walled carbon nanotubes. Applied Physics Letters. 2006;88(233119). doi: 10.1063/1.2209187.

34. Sitharaman B, Shi X, Walboomers X, Liao H, Cuijpers V, Wilson L, Mikos A, Jansen J. In vivo biocompatibility of ultra-short single-walled carbon nanotube/biodegradable polymer nanocomposites for bone tissue engineering. Bone. 2008;43(2):362-70.

35. Dubin R, Callegari G, Kohn J, Neimark A. Carbon nanotube fibers are compatible with mammalian cells and neurons. IEEE transactions on nanobioscience. 2008;7(1):11-4.

36. Nakamura M, Tahara Y, Ikehara Y. Single-walled carbon nanohorns as drug carriers: adsorption of prednisolone and anti-inflammatory effects on arthritis. Nanotechnology. 2011;22:1-8.

37. Whitney J, Sarkar S, Zhang J, Do T, Young T, Manson M, Campbell T, Puretzky A, Rouleau C, Moore K, Goehegan D, Rylander C, Dorn H, Rylander M. Single Walled Carbon Nanohorns as Photothermal Cancer Agents. Lasers in Surgery and Medicine. 2011;43:43-51. doi: 10.1002/lsm..21025.

38. Butler DL, Juncosa-Melvin N, Boivin GP, Galloway MT, Shearn JT, Gooch C, Awad H. Functional tissue engineering for tendon repair: A multidisciplinary strategy using mesenchymal stem cells, bioscaffolds, and mechanical stimulation. Journal of orthopaedic research : official publication of the Orthopaedic Research Society. 2008;26(1):1-9. Epub 2007/08/07. doi: 10.1002/jor.20456. PubMed PMID: 17676628.

39. Provenzano PP, Alejandro-Osorio AL, Valhmu WB, Jensen KT, Vanderby R, Jr. Intrinsic fibroblast-mediated remodeling of damaged collagenous matrices in vivo. Matrix biology :

journal of the International Society for Matrix Biology. 2005;23(8):543-55. Epub 2005/02/08. doi: 10.1016/j.matbio.2004.09.008. PubMed PMID: 15694131.

40. Smith MM, Sakurai G, Smith SM, Young AA, Melrose J, Stewart CM, Appleyard RC, Peterson JL, Gillies RM, Dart AJ, Sonnabend DH, Little CB. Modulation of aggrecan and ADAMTS expression in ovine tendinopathy induced by altered strain. Arthritis and rheumatism. 2008;58(4):1055-66. Epub 2008/04/03. doi: 10.1002/art.23388. PubMed PMID: 18383380.

41. Jones GC, Corps AN, Pennington CJ, Clark IM, Edwards DR, Bradley MM, Hazleman BL, Riley GP. Expression profiling of metalloproteinases and tissue inhibitors of metalloproteinases in normal and degenerate human achilles tendon. Arthritis and rheumatism. 2006;54(3):832-42. Epub 2006/03/02. doi: 10.1002/art.21672. PubMed PMID: 16508964.

42. Provenzano P, Heisey D, Hayashi K, Lakes R, Vanderby R. Subfailure damage in ligament: a structural cellular evaluation. J Appl Physiol. 2002;92:362-71.

43. Glazebrook MA, Wright JR, Jr., Langman M, Stanish WD, Lee JM. Histological analysis of achilles tendons in an overuse rat model. J Orthop Res. 2008;26(6):840-6. Epub 2008/01/10. doi: 10.1002/jor.20546. PubMed PMID: 18183626.

44. PP P, K H, DN K, MD M, R V. Healing of subfailure ligament injury: comparison between immature and mature ligaments in a rat model. Journal of Orthopedic Research. 2002;20:975-83.

45. Jensen K, Rabago D, Best T, Patterson J, Vanderby R. Response of knee ligaments to prolotherapy in a rat injury model. The American Journal of Sports Medicine. 2008;36(7):1347-57.

46. Joensen J, Gjerdet NR, Hummelsund S, Iversen V, Lopes-Martins RA, Bjordal JM. An experimental study of low-level laser therapy in rat Achilles tendon injury. Lasers in medical

science. 2012;27(1):103-11. Epub 2011/05/07. doi: 10.1007/s10103-011-0925-y. PubMed PMID: 21547473; PubMed Central PMCID: PMC3254871.

47. AC S, G B, P G, PU K, NA P, BG B, D F. Effect of In-Ga-Al-P diode laser irradiation on angiogenesis in partial ruptures of Achilles tendon in rats. Photmed Laser Surg. 2005;23(5):470-75.

48. LI F, JL M, K V, AJ M, CG Z, O L, NP M, J G-G. Low-level laser therapy (LLLT) prevents oxidative stress and reduces fibrosis in rat traumatized Achilles tendon. Lasers Surg Med. 2005;37(4):293-300.

49. FS O, CE P, NA P, RE L, PS B, EB G, LM F. Effect of low level laser therapy (830 nm) with different therapy reginmes on the process of tissue repair in partial lesion calcaneus tendon. Lasers Surg Med. 2009;41(4):271-6.

50. Fung DT, Wang VM, Andarawis-Puri N, Basta-Pljakic J, Li Y, Laudier DM, Sun HB, Jepsen KJ, Schaffler MB, Flatow EL. Early response to tendon fatigue damage accumulation in a novel in vivo model. J Biomech. 2010;43(2):274-9. Epub 2009/11/27. doi: 10.1016/j.jbiomech.2009.08.039. PubMed PMID: 19939387; PubMed Central PMCID: PMC3366582.

51. Sun HB, Andarawis-Puri N, Li Y, Fung DT, Lee JY, Wang VM, Basta-Pljakic J, Leong DJ, Sereysky JB, Ros SJ, Klug RA, Braman J, Schaffler MB, Jepsen KJ, Flatow EL. Cycle-dependent matrix remodeling gene expression response in fatigue-loaded rat patellar tendons. J Orthop Res. 2010;28(10):1380-6. Epub 2010/09/15. doi: 10.1002/jor.21132. PubMed PMID: 20839322.

52. Sun HB, Li Y, Fung DT, Majeska RJ, Schaffler MB, Flatow EL. Coordinate regulation of IL-1beta and MMP-13 in rat tendons following subrupture fatigue damage. Clinical orthopaedics

and related research. 2008;466(7):1555-61. Epub 2008/05/13. doi: 10.1007/s11999-008-0278-4. PubMed PMID: 18470577; PubMed Central PMCID: PMC2505236.

53. Andarawis-Puri N, Flatow E. Tendon fatigue in response to mechanical loading. J Musculoskelet Neuronal Interact. 2011;11(2):106-14.

54. Seto A, Gatt C, Dunn M. Radioprotection of Tendon Tissue via Crosslinking and Free Radical Scavenging. Clinical Orthopedics and Related Research. 2008;466(8):1788-95.

55. Seto A, Gatt CJ, Jr., Dunn MG. Improved tendon radioprotection by combined cross-linking and free radical scavenging. Clinical orthopaedics and related research. 2009;467(11):2994-3001. Epub 2009/06/23. doi: 10.1007/s11999-009-0934-3. PubMed PMID: 19543778; PubMed Central PMCID: PMC2758987.

56. Empson YM, Ekwueme EC, Hong JK, Paynter DM, Kwansa AL, Brown C, Pekkanen AM, Roman M, Rylander NM, Brolinson GP, Freeman JW. High elastic modulus nanoparticles: a novel tool for subfailure connective tissue matrix damage. Translational research : the journal of laboratory and clinical medicine. 2014;164(3):244-57. Epub 2014/06/14. doi: 10.1016/j.trsl.2014.05.004. PubMed PMID: 24924347.

57. Kwansa A, Empson Y, Ekwueme E, Walters V, Freeman J, Laurencin C. Novel matrix based anterior cruciate ligament (ACL) regeneration. Soft Matter. 2010;6:5016-25.

58. Freeman J, Empson Y, Ekwueme E, Paynter D, Brolinson P. Effect of prolotherapy on cellular proliferation and collagen deposition in MC3T3-E1 and patellar tendon fibroblast populations. Translational Research. 2011;158:132-9.

59. Rabago D, Slattengren A, Zgierska A. Prolotherapy in primary care practice. Prim Care. 2010;37(1):65-80. Epub 2010/03/02. doi: 10.1016/j.pop.2009.09.013. PubMed PMID: 20188998; PubMed Central PMCID: PMC2831229.

60. Abe M, Harpel J, Metz C, Nunes I, Loskutoff D, Rifkin D. An assay for transforming growth factor-beta using cells transfected with a plasminogen activator inhibitor-1 promoter-luciferase construct. Analytical Biochemistry. 1994;216:276-84.

61. Wipff PJ, Rifkin DB, Meister JJ, Hinz B. Myofibroblast contraction activates latent TGF-beta1 from the extracellular matrix. The Journal of cell biology. 2007;179(6):1311-23. Epub 2007/12/19. doi: 10.1083/jcb.200704042. PubMed PMID: 18086923; PubMed Central PMCID: PMC2140013.

62. Nair LS. Prolotherapy for tissue repair. Translational research : the journal of laboratory and clinical medicine. 2011;158(3):129-31. Epub 2011/08/27. doi: 10.1016/j.trsl.2011.05.001. PubMed PMID: 21867977.

63. Clarkson MR, Murphy M, Gupta S, Lambe T, Mackenzie HS, Godson C, Martin F, Brady HR. High glucose-altered gene expression in mesangial cells. Actin-regulatory protein gene expression is triggered by oxidative stress and cytoskeletal disassembly. J Biol Chem. 2002;277(12):9707-12. Epub 2002/01/11. doi: 10.1074/jbc.M109172200. PubMed PMID: 11784718.

64. Lam S, van der Geest R, Verhagen N, van Nieuwenhoven F, Blom I, Aten J, Goldschmeding R, Daha M, van Kooten C. Connective tissue growth factor and IGF-1 are produced by human renal fibroblasts and cooperate in the induction of collagen production by high glucose. Diabetes. 2003;52:2975-83.

65. Pedersen G, Brynskov J, Saermark T. Phenol toxicity and conjugation in human colonic epithelial cells. Scand J Gastroenterol. 2002;37(1):74-9.

66. Doorn J, Fernandes HA, Le BQ, van de Peppel J, van Leeuwen JP, De Vries MR, Aref Z, Quax PH, Myklebost O, Saris DB, van Blitterswijk CA, de Boer J. A small molecule approach to

engineering vascularized tissue. Biomaterials. 2013;34(12):3053-63. Epub 2013/02/02. doi: 10.1016/j.biomaterials.2012.12.037. PubMed PMID: 23369216.

67. Liang CC, Park AY, Guan JL. In vitro scratch assay: a convenient and inexpensive method for analysis of cell migration in vitro. Nature protocols. 2007;2(2):329-33. Epub 2007/04/05. doi: 10.1038/nprot.2007.30. PubMed PMID: 17406593.

68. Legerlotz K, Jones ER, Screen HR, Riley GP. Increased expression of IL-6 family members in tendon pathology. Rheumatology. 2012;51(7):1161-5. Epub 2012/02/18. doi: 10.1093/rheumatology/kes002. PubMed PMID: 22337942; PubMed Central PMCID: PMC3380247.

69. Wang JHC, Jia F, Yang G, Yang S, Campbell BH, Stone D, Woo SLY. Cyclic Mechanical Stretching of Human Tendon Fibroblasts Increases the Production of Prostaglandin E 2 and Levels of Cyclooxygenase Expression: A Novel In Vitro Model Study. Connective Tissue Research. 2003;44(3-4):128-33. doi: 10.1080/03008200390223909.

70. Cilli F, Khan M, Fu F, Wang J. Prostaglandin E2 affects proliferation and collagen synthesis by human patellar tendon fibroblasts. Clin J Sport Med. 2004;14:232-6.

71. Leask A, Abraham DJ. TGF-beta signaling and the fibrotic response. Faseb J. 2004;18(7):816-27. Epub 2004/05/01. doi: 10.1096/fj.03-1273rev. PubMed PMID: 15117886.

72. Schiller M, Javelaud D, Mauviel A. TGF-beta-induced SMAD signaling and gene regulation: consequences for extracellular matrix remodeling and wound healing. Journal of dermatological science. 2004;35(2):83-92. Epub 2004/07/22. doi: 10.1016/j.jdermsci.2003.12.006. PubMed PMID: 15265520.

73. Butler DL, Juncosa-Melvin N, Boivin GP, Galloway MT, Shearn JT, Gooch C, Awad H. Functional tissue engineering for tendon repair: A multidisciplinary strategy using mesenchymal

stem cells, bioscaffolds, and mechanical stimulation. J Orthop Res. 2008;26(1):1-9. Epub 2007/08/07. doi: 10.1002/jor.20456. PubMed PMID: 17676628.

74. MW H, A Z, LJ S. The role of animal models in tendon research. Bone Joint Res. 2014;3:193-202.

75. Watanabe N, Woo S, Papageorgiou C, Celechovsky C, Takai S. Fate of Donor Bone Marrow Cells in Medial Collateral Ligament After Simulated Autologous Transplantation. Microscopy Research and Technique. 2002;58:39-44.

76. Liu H, Fan H, Toh SL, Goh JC. A comparison of rabbit mesenchymal stem cells and anterior cruciate ligament fibroblasts responses on combined silk scaffolds. Biomaterials. 2008;29(10):1443-53. Epub 2007/12/25. doi: 10.1016/j.biomaterials.2007.11.023. PubMed PMID: 18155134.

77. Ge Z, Goh J, Lee E. Selection of Cell Source for Ligament Tissue Engineering. Cell Transplantation. 2005;14:573-83.

78. Smith RK, Werling NJ, Dakin SG, Alam R, Goodship AE, Dudhia J. Beneficial effects of autologous bone marrow-derived mesenchymal stem cells in naturally occurring tendinopathy. PLoS One. 2013;8(9):e75697. Epub 2013/10/03. doi: 10.1371/journal.pone.0075697. PubMed PMID: 24086616; PubMed Central PMCID: PMC3783421.

79. Canseco J, Kojima K, Penvose A, Ross J, Obokata H, Gomoll A, Vacanti C. Effect on Ligament Marker Expression by Direct-Contact Co-culture of Mesenchymal Stem Cells and Anterior Cruciate Ligament Cells. Tissue Engineering: Part A. 2012;18(23-24):2549-58.

80. Schneider PR, Buhrmann C, Mobasheri A, Matis U, Shakibaei M. Three-dimensional high-density co-culture with primary tenocytes induces tenogenic differentiation in mesenchymal

stem cells. J Orthop Res. 2011;29(9):1351-60. doi: 10.1002/jor.21400. PubMed PMID: 21437969.

81. Awad H, Butler D, Boivin G, Smith F, Malaviya P, Huibregtse B, Caplan A. Autologous mesenchymal stem cell-mediated repair of tendon. Tissue Eng. 1999;5(3):267-77.

82. Lee J, Zhou Z, Taub P, Ramcharan M, Li Y, Akinbiyi T, Maharam E, Leong D, Laudier D, Ruike T, Torina P, Zaidi M, Majeska R, Schaffier M, Flatow E, Sun H. BMP-12 treatment of adult mesenchymal stem cells in vitro augments tendon-like tissue formation and defect repair in vivo. PLoS One. 2011;6(3).

83. Luo Q, Song G, Song Y, Xu B, Qin J, Shi Y. Indirect co-culture with tenocytes promotes proliferation and mRNA expression of tendon/ligament related genes in rat bone marrow mesenchymal stem cells. Cytotechnology. 2009;61:1-10.

84. Shimode K, Iwasaki N, Majima T, Funakoshi T, Sawaguchi N, Onodera T, Minami A. Bone marrow stromal cells act as feeder cells for tendon fibroblasts through soluble factors. Tissue Eng. 2007;13(2):333-41. doi: 10.1089/ten.2006.0079. PubMed PMID: 17518567.

85. Van Eijk F, Saris D, Riesle J, Willems W, Van Blitterswijk C, Verbout A, Dhert W. Tissue engineering of ligaments: a comparison of

bone marrow stromal cells, anterior cruciate ligament, and skin

fibroblasts as cell source. Tissue Engineering. 2004;10:893-903.

86. Schnabel LV, Mohammed HO, Miller BJ, McDermott WG, Jacobson MS, Santangelo KS, Fortier LA. Platelet rich plasma (PRP) enhances anabolic gene expression patterns in flexor digitorum superficialis tendons. J Orthop Res. 2007;25(2):230-40. doi: 10.1002/jor.20278. PubMed PMID: 17106885.

87. J M. TGF-beta Signal Transduction. Annu Rev Biochem. 1998;67:753-91.

88. Li L, Klim JR, Derda R, Courtney AH, Kiessling LL. Spatial control of cell fate using synthetic surfaces to potentiate TGF-beta signaling. Proceedings of the National Academy of Sciences of the United States of America. 2011;108(29):11745-50. doi: 10.1073/pnas.1101454108. PubMed PMID: 21719709; PubMed Central PMCID: PMC3141980.

89. Kuo CK, Tuan RS. Mechanoactive tenogenic differentiation of human mesenchymal stem cells. Tissue Eng Part A. 2008;14(10):1615-27. doi: 10.1089/ten.tea.2006.0415. PubMed PMID: 18759661.

90. Corps AN, Jones GC, Harrall RL, Curry VA, Hazleman BL, Riley GP. The regulation of aggrecanase ADAMTS-4 expression in human Achilles tendon and tendon-derived cells. Matrix biology : journal of the International Society for Matrix Biology. 2008;27(5):393-401. doi: 10.1016/j.matbio.2008.02.002. PubMed PMID: 18387286; PubMed Central PMCID: PMC2443387.

91. Wylie JD, Ho JC, Singh S, McCulloch DR, Apte SS. Adamts5 (aggrecanase-2) is widely expressed in the mouse musculoskeletal system and is induced in specific regions of knee joint explants by inflammatory cytokines. J Orthop Res. 2012;30(2):226-33. doi: 10.1002/jor.21508. PubMed PMID: 21800360.

92. Maeda E, Sugimoto M, Ohashi T. Cytoskeletal tension modulates MMP-1 gene expression from tenocytes on micropillar substrates. J Biomech. 2013;46(5):991-7. doi: 10.1016/j.jbiomech.2012.11.056. PubMed PMID: 23415423.

93. Fernandes H, Mentink A, Bank R, Stroop R, van Blitterswijk C, de Boer J. Endogenous Collagen Influences Differentiation of Human Multipotent Mesenchymal Stromal Cells. Tissue Engineering Part A. 2010;16(5):1693-702.

94. Gothard D, Dawson JI, Oreffo RO. Assessing the potential of colony morphology for dissecting the CFU-F population from human bone marrow stromal cells. Cell Tissue Res. 2013;352(2):237-47. Epub 2013/02/12. doi: 10.1007/s00441-013-1564-3. PubMed PMID: 23397425.

95. Zilony N, Tzur-Balter A, Segal E, Shefi O. Bombarding cancer: biolistic delivery of therapeutics using porous Si carriers. Scientific reports. 2013;3:2499. doi: 10.1038/srep02499. PubMed PMID: 23975675; PubMed Central PMCID: PMC3752615.

96. Tomikawa K, Yamamoto T, Shiomi N, Shimoe M, Hongo S, Yamashiro K, Yamaguchi T, Maeda H, Takashiba S. Smad2 decelerates re-epithelialization during gingival wound healing. Journal of dental research. 2012;91(8):764-70. Epub 2012/06/16. doi: 10.1177/0022034512451449. PubMed PMID: 22699208.

97. Kwan KH, Yeung KW, Liu X, Wong KK, Shum HC, Lam YW, Cheng SH, Cheung KM, To MK. Silver nanoparticles alter proteoglycan expression in the promotion of tendon repair. Nanomedicine. 2013. Epub 2013/12/18. doi: 10.1016/j.nano.2013.11.015. PubMed PMID: 24333594.

98. Kim K, Dean D, AG M, Fisher J. The Effect of Initial Cell Seeding Density on Early Osteogenic Signal Expression of Rat Bone Marrow Stromal Cells Cultured on Crosslinked Poly(propylene fumarate) Disks. Biomacromolecules. 2009;10(7):1810-17.

99. Ekwueme E, Kwansa A, Sharif K, El-Amin S, Freeman J. Recent Advancements in Ligament Replacement. Recent Patents on Biomedical Engineering. 2011;4.

100. Docheva D, Padula D, Popov C, Weishaupt P, Pragert M, Miosge N, Hickel R, Bocker W, Clausen-Schaumann H, Schieker M. Establishment of Immortalized Periodontal Ligament

Progenitor Cell Line and Its Behavioural Analysis on Smooth and Rough Titanium Surfaces. Europen Cells and Materials. 2010;19:228-41.

101. Docheva D, Hunziker EB, Fassler R, Brandau O. Tenomodulin is necessary for tenocyte proliferation and tendon maturation. Molecular and cellular biology. 2005;25(2):699-705. doi: 10.1128/MCB.25.2.699-705.2005. PubMed PMID: 15632070; PubMed Central PMCID: PMC543433.

102. Shukunami C, Takimoto A, Oro M, Hiraki Y. Scleraxis positively regulates the expression of tenomodulin, a differentiation marker of tenocytes. Developmental biology. 2006;298(1):234-47. doi: 10.1016/j.ydbio.2006.06.036. PubMed PMID: 16876153.

103. Attia M, Huet E, Gossard C, Menashi S, Tassoni MC, Martelly I. Early events of overused supraspinatus tendons involve matrix metalloproteinases and EMMPRIN/CD147 in the absence of inflammation. Am J Sports Med. 2013;41(4):908-17. doi: 10.1177/0363546512473817. PubMed PMID: 23404084.

104. Barminko J, Kim JH, Otsuka S, Gray A, Schloss R, Grumet M, Yarmush ML. Encapsulated mesenchymal stromal cells for in vivo transplantation. Biotechnol Bioeng. 2011;108(11):2747-58. Epub 2011/06/10. doi: 10.1002/bit.23233. PubMed PMID: 21656712; PubMed Central PMCID: PMC3178737.

105. Breidenbach AP, Gilday SD, Lalley AL, Dyment NA, Gooch C, Shearn JT, Butler DL. Functional tissue engineering of tendon: Establishing biological success criteria for improving tendon repair. J Biomech. 2014;47(9):1941-8. Epub 2013/11/10. doi: 10.1016/j.jbiomech.2013.10.023. PubMed PMID: 24200342; PubMed Central PMCID: PMC3995907.

106. Murray M. Current Status and Potential of Primary ACL Repair. Clin Sports Med. 2009;28:51-61.

107. Soroceanu A, Sidhwa F, Aarabi S, Kaufman A, Glazebrook M. Surgical versus nonsurgical treatment of acute Achilles tendon rupture: a meta-analysis of randomized trials. J Bone Joint Surg Am. 2012;94(23):2136-43. Epub 2012/12/12. doi: 10.2106/JBJS.K.00917. PubMed PMID: 23224384; PubMed Central PMCID: PMC3509775.

108. Leong NL, Petrigliano FA, McAllister DR. Current tissue engineering strategies in anterior cruciate ligament reconstruction. J Biomed Mater Res A. 2014;102(5):1614-24. Epub 2013/06/06. doi: 10.1002/jbm.a.34820. PubMed PMID: 23737190.

109. Lynch S, Renstrom P. Conservative versus surgical treatment. Sports Med. 1999;27:61-71.

110. Shearer CJ, Cherevan A, Eder D. Application and future challenges of functional nanocarbon hybrids. Advanced materials. 2014;26(15):2295-318. Epub 2014/03/29. doi: 10.1002/adma.201305254. PubMed PMID: 24677386.

111. Swierczewska M, Choi KY, Mertz EL, Huang X, Zhang F, Zhu L, Yoon HY, Park JH, Bhirde A, Lee S, Chen X. A facile, one-step nanocarbon functionalization for biomedical applications. Nano Lett. 2012;12(7):3613-20. Epub 2012/06/15. doi: 10.1021/nl301309g. PubMed PMID: 22694219; PubMed Central PMCID: PMC3405986.

112. Meng L, Zhang X, Lu Q, Fei Z, Dyson PJ. Single walled carbon nanotubes as drug delivery vehicles: targeting doxorubicin to tumors. Biomaterials. 2012;33(6):1689-98. Epub 2011/12/06. doi: 10.1016/j.biomaterials.2011.11.004. PubMed PMID: 22137127.

113. McKeon-Fischer KD, Rossmeisl JH, Whittington AR, Freeman JW. In vivo skeletal muscle biocompatibility of composite, coaxial electrospun, and microfibrous scaffolds. Tissue

engineering Part A. 2014;20(13-14):1961-70. Epub 2014/01/30. doi: 10.1089/ten.TEA.2013.0283. PubMed PMID: 24471815; PubMed Central PMCID: PMC4086678.

114. Deeken CR, Cozad MJ, Bachman SL, Ramshaw BJ, Grant SA. Characterization of bionanocomposite scaffolds comprised of amine-functionalized single-walled carbon nanotubes crosslinked to an acellular porcine tendon. J Biomed Mater Res A. 2011;96(3):584-94. Epub 2011/01/22. doi: 10.1002/jbm.a.33014. PubMed PMID: 21254390.

115. Tahara Y, Nakamura M, Yang M, Zhang M, Iijima S, Yudasaka M. Lysosomal membrane destabilization induced by high accumulation of single-walled carbon nanohorns in murine macrophage RAW 264.7. Biomaterials. 2012;33(9):2762-9. Epub 2012/01/03. doi: 10.1016/j.biomaterials.2011.12.023. PubMed PMID: 22209643.

116. Miyawaki J, Yudasaka M, Azami T, Kubo Y, Iijima S. Toxicity of Single-Walled Carbon Nanohorns. ACS Nano. 2008;2(2):213-26.

117. Geohegan D, Puretzky A, Ivanov I, Eres G, Liu Z, Styers-Barnett D, Hu H, Zhao B, Cui H, Rouleau C, Jesse S, Britt P, Christen H, Xiao K, Fleming P, Meldrum A. Laser-based synthesis, diagnostics, and control of single-walled carbon nanotubes and nanohorns for composites and biological nanovectors. Photon Based Nanoscience and Nanobiotechnology. 2006;239:205-23.

118. Sonnaert M, Papantoniou I, Luyten FP, Schrooten J. Quantitative validation of the Presto Blue metabolic assay for on-line monitoring of cell proliferation in a 3D perfusion bioreactor system. Tissue engineering Part C, Methods. 2014. Epub 2014/10/23. doi: 10.1089/ten.TEC.2014.0255. PubMed PMID: 25336207.

119. Kwan KH, Yeung KW, Liu X, Wong KK, Shum HC, Lam YW, Cheng SH, Cheung KM, To MK. Silver nanoparticles alter proteoglycan expression in the promotion of tendon repair. Nanomedicine. 2014;10(7):1375-83. Epub 2013/12/18. doi: 10.1016/j.nano.2013.11.015. PubMed PMID: 24333594.

120. Albanese A, Tang PS, Chan WC. The effect of nanoparticle size, shape, and surface chemistry on biological systems. Annu Rev Biomed Eng. 2012;14:1-16. Epub 2012/04/25. doi: 10.1146/annurev-bioeng-071811-150124. PubMed PMID: 22524388.

121. Holt B, Dahl K, Islam M. Cells Take up and Recover from Protein-stabilized Single-wall Carbon Nanotubes with Two Distinct Rates. ACS Nano. 2012;6(4):3481-90.

122. Zhang M, Zhou X, Iijima S, Yudasaka M. Small-sized Carbon Nanohorns Enabling Cellular Uptake Control. Small. 2012;8(16):2524-31.

123. Rastogi V, Yadav P, Bhattacharya SS, Mishra AK, Verma N, Verma A, Pandit JK. Carbon nanotubes: an emerging drug carrier for targeting cancer cells. Journal of drug delivery. 2014;2014:670815. Epub 2014/05/30. doi: 10.1155/2014/670815. PubMed PMID: 24872894; PubMed Central PMCID: PMC4020363.

124. Harvey J, Dong L, Kim K, Hayden J, Wang J. Uptake of Single-Walled Carbon Nanotubes Conjugated with DNA by Microvascular Endothelial Cells. Journal of Nanotechnology. 2012;2012:1-7. doi: 10.1155/2012/196189.

125. Wu X, Zhao X, Baylor L, Kaushal S, Eisenberg E, Greene LE. Clathrin exchange during clathrin-mediated endocytosis. The Journal of cell biology. 2001;155(2):291-300. Epub 2001/10/18. doi: 10.1083/jcb.200104085. PubMed PMID: 11604424; PubMed Central PMCID: PMC2198830.

126. Doyon JB, Zeitler B, Cheng J, Cheng AT, Cherone JM, Santiago Y, Lee AH, Vo TD, Doyon Y, Miller JC, Paschon DE, Zhang L, Rebar EJ, Gregory PD, Urnov FD, Drubin DG. Rapid and efficient clathrin-mediated endocytosis revealed in genome-edited mammalian cells. Nature cell biology. 2011;13(3):331-7. Epub 2011/02/08. doi: 10.1038/ncb2175. PubMed PMID: 21297641; PubMed Central PMCID: PMC4113319.

127. Rejman J, Oberle V, Zuhorn I, Hoekstra D. Size-dependent internalization of particles via the pathways of clathrin- and caveolae-mediated endocytosis. Biochem J. 2004;377:155-69.

128. Lathuilière A, Bohrmann B, Kopetzki E, Schweitzer C, Jacobsen H, Moniatte M, Aebischer P, Schneider BL. Genetic engineering of cell lines using lentiviral vectors to achieve antibody secretion following encapsulated implantation. Biomaterials. 2014;35(2):792-802. doi: 10.1016/j.biomaterials.2013.10.026.

129. Lathuiliere A, Cosson S, Lutolf MP, Schneider BL, Aebischer P. A high-capacity cell macroencapsulation system supporting the long-term survival of genetically engineered allogeneic cells. Biomaterials. 2014;35(2):779-91. Epub 2013/10/10. doi: 10.1016/j.biomaterials.2013.09.071. PubMed PMID: 24103654.

130. Corn DJ, Kim Y, Krebs MD, Mounts T, Molter J, Gerson S, Alsberg E, Dennis JE, Lee Z. Imaging early stage osteogenic differentiation of mesenchymal stem cells. J Orthop Res. 2013;31(6):871-9. Epub 2013/02/27. doi: 10.1002/jor.22328. PubMed PMID: 23440976.

131. Fernandes H, Mentink A, Bank R, Stoop R, van Blitterswijk C, de Boer J. Endogenous Collagen Influences Differentiation of Human Multipotent Mesenchymal Stromal Cells. Tissue Engineering Part A. 2010;16(5):1693-702.